GEOTHERMAL ENERGY RFI

WORK OVERVIEW

SITE REPORTS

CHOCOLATE MOUNTAINS AERIAL GUNNERY RANGE,

IMPERIAL VALLEY,

CALIFORNIA

Geothermal Energy Resource Investigations, Chocolate Mountains Aerial Gunnery Range, Imperial Valley, California

Steve Alm[1], S. Bjornstad[1], M. Lazaro[1], A. Sabin[1], D. Meade[1], J. Shoffner[2], W. C. Huang[1], J. Unruh[3], M. Strane[3], H. Ross[4]

[1]Geothermal Programs Office, U.S. Navy China Lake Naval Weapons Center, Ridgecrest, CA, USA
[2]Colorado School of Mines, Department of Geology and Geological Engineering, Golden, CO
[3]William Lettis & Associates, Walnut Creek, CA
[4]Energy and Geosciences Institute, University of Utah, Salt Lake City, UT

Keywords

Chocolate Mountains, geothermal, exploration, magnetics, gravity, LiDAR, temperature gradient

ABSTRACT

The US Navy's Geothermal Program Office (GPO), has conducted geothermal exploration in the Chocolate Mountains Aerial Gunnery Range (CMAGR) since the mid-1970s. At this time, the focus of the GPO had been on the area to the east of the Hot Mineral Spa KGRA, Glamis and areas within the Chocolate Mountains themselves. Using potential field geophysics, mercury surveys and geologic mapping to identify potential anomalies related to recent hydrothermal activity. After a brief hiatus starting in the early 2000s the past two years has seen an accelerated exploration schedule focusing on the potential extension of nearby geothermal fields and the discovery of new resources. One potential occurrence scenario being an East Mesa-type sedimentary hosted geothermal resource beneath the broad alluvial slope within the boundaries of the CMAGR. We have established three exploration areas, generally termed Hot Mineral Spa/Camp Billy Machen, East Niland and Glamis, with exploration efforts currently focused on the Hot Mineral Spa/Camp Billy Machen area. Recent exploration includes a high resolution aerial LiDAR survey flown over the project areas, securing over 177,000 square kilometers of <30cm accuracy digital elevation data. LiDAR data were analyzed to characterize the active tectonic environment, and identify Holocene structures, which are common conduits for upwelling geothermal fluids. Gravity and ground-based magnetics surveys were conducted during the summer of 2008. This data was acquired to aid in the identification of structures without fair surface expression, obscured by recent deposition. Shallow temperature gradient drilling began at the CMAGR in January of 2010. 13 temperature gradient holes were completed to a depth of 500' below ground surface. Sites were selected based on the compilation of previous exploration and resulting data is being integrated into the most recent geologic model. This model will form the basis for the selection of a deeper (2000'-4000') temperature gradient drilling campaign at the CMAGR in 2011.

Introduction

The Chocolate Mountain Aerial Gunnery Range (GMAGR) is a military air and ground training range situated along the eastern margin of the Salton Sea in southern California. The range is managed by the Marine Corps Air Station, Yuma, AZ. Due to the utilization of live ordnance, access to this area is extremely limited. As such, speculation concerning geothermal potential is largely limited to projecting geologic structures and trends from the adjacent areas, including the Salton Trough, into this region.

Figure 1. CMAGR Location Map.

The US Navy Geothermal Program Office (GPO) has conducted exploration activities within GMAGR off and on beginning in 1976, when Dr James Whelan did reconnaissance mapping and sampling of hydrothermal alteration zones in the Salvation Pass region. This work was followed in the late-1970s and early '80s with several soil mercury surveys encompassing most of the Range. In this same period the USGS drilled three heat flow holes with CMAGR – HOTS, BEAL and GSLN – showing temperature gradients of up to 5.6°F/100ft.

Exploration efforts continued throughout the 1980s as the GPO conducted several ground-based gravity and magnetics surveys and participated in the drilling of one test hole northeast of Niland at the Camp Billy Machen Special Warfare Desert Training Facility. Also in the early 1980s, the geothermal industry showed interest in the geothermal potential of the northwest corner of the CMAGR, submitting lease applications on greater than 12 square miles. These applications were rejected citing conflict with the established mission of the Range lands. Exploration continued through the 1990's with the analysis of water wells drilled for military support, however the wells were fairly shallow and produced minimal data. Access to the ranges was revoked in the early 2000s due to an increased focus on mission security. Access was reinstated in 2008 following the issuance of a directive from the Commandant, United States Marine Corps, in support of the development of geothermal resources on Marine Corps installations.

Geologic Setting of Chocolate Mountains

The Chocolate Mountains constitute 60 miles of northwest trending Mesozoic granitic rocks that unconformably overlie the pre-Cenozoic Pelona-Orocopia Schist (Crowell, 1975). Mesozoic granites are intruded and overlain by Triassic and younger Mesozoic rhyodacitic to rhyolitic plug domes, lava flows, volcaniclastic deposits, and locally thick poorly welded and welded rhyolite ignimbrite (Crowe, 1978). Following Mesozoic convergence and subduction, the crust in southern California and southern Arizona was strongly attenuated by east-west extension in late Oligocene to Miocene time. In the Chocolate Mountains, this extension was accommodated primarily by slip on north- to northwest striking normal faults, and accompanied by silicic volcanism with subordinate eruptions of andesite (Crowe, 1978).

Rifting and sea-floor spreading in the Gulf of California has been propagating northward since late Miocene time into northwestern Mexico and southern California to form landward spreading centers analogous to the oceanic spreading centers found in the Sea of Cortez.

These onshore spreading centers terminate in the Salton Trough, specifically at the Brawley Seismic Zone, where the plate boundary transitions to the pure transform nature of the San Andreas system. Large amounts of dextral slip along this system have cut and displaced basement units of the Chocolate Mountains northward; equivalent rocks are found about 160 to 240 km north on the west side of the San Andreas Fault (Ehlig, 1981; Jacobson et al., 1996).

As rifting continues in the Salton trough new crust is generated, mafic intrusions rise form the mantle and produce high heat flow that metamorphoses the sedimentary rocks to shallow depths. These centers of magmatism in the Salton Trough are directly related with well known geothermal resource areas having reservoir temperatures of more than 150ºC.

Geophysical Exploration

In the summer of 2008 gravity and magnetic data were acquired in the Hot Mineral Spa/Camp Billy Machen exploration area along the western pediment of the Chocolate Mountains. The gravity survey consisted of 390 stations at ~1300 foot spacings over a 56 square mile area along the northwest border of the CMAGR. Figure 4 displays a structural geology interpretation superimposed on the Bouguer Gravity contours that represent the observed data to tenths (0.1) or hundredths (0.01) of a mGal. Potential faults are interpreted as density contrasts and similar to the gravity highs and lows (annotated with H and L) are estimated positions indicated by the contours. The structures are mapped as being continuous in areas with closely spaced stations and dashed where a density contrast is less well-defined or less certain. Correctly locating structures with respect to the gravity anomaly or expression is complex and the interpretation of position of a buried density contrast is rapidly complicated by the presence of non-vertical density contrasts, gradual or multiple density contrasts, dipping surfaces, varying depths, and multiple bodies (density contrasts). (Ross, H.P., 2009)

A comparison with regional geology shows that essentially all gravity stations were located on younger or older Quaternary alluvium (Qal) or windblown sand, south and west of hills comprised of Tertiary volcanic and intrusive rocks, and agglomerates. Thus all "structures" are beneath younger Qal cover. Major structures trend northwest (N35W to N55W) in the Tertiary outcrop and is shown by only one major interpreted fault, down to the NE, in the

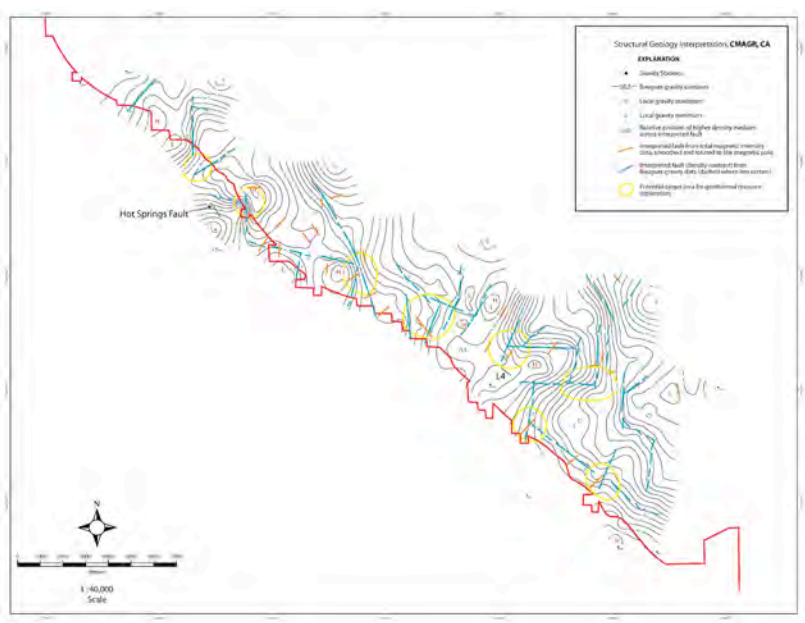

Figure 2. Structural geology interpretation based on gravity and magnetic data with potential exploration targets identified.

southernmost part of the gravity survey. Several other "structures trend N20W to N70W, but these are generally less well-defined. This anticipated major NW structural trend is disturbed (cut across) by numerous N, NE, and almost east-west structures, many of which are well-defined by gradients of 1-4 mGal and 1.5 to 3 km length. The certainty of location and type of cross-cutting features is limited by the narrow NE dimension of the survey. The general impression, however, is one of complex Tertiary volcanic and intrusive units, cut by numerous N and NE trending structures, beneath alluvial cover (Figure 2).

Total field magnetic data was acquired with a scintrex proton magnetometer system at 200 ft intervals along 22 profiles 0.2 to 7 km in length throughout the gravity survey area. The data displayed a relatively small range of magnetic variation with the majority of contour map values ranging from 47,700 to 47,850 nT, with generally low-amplitude variations. Four areas show anomalies of 100 to 150 nT, and one anomaly has an amplitude of perhaps 200-250 nT. Structural picks based on magnetic data shown in orange on Figure 4 correspond fairly closely with gravity picks in 15 locations, but orientation of the magnetic picks are generally unknown and are shown as normal to the recording profile.

These areas of agreement as a structural pick could add support to the gravity structural picks but there are some uncertainties with the data that would be improved by more sampling and some reprocessing. As it is light areas are shown on Figure 4 as potential target areas for more detailed geothermal exploration. These areas are selected mainly on the probable intersection of structures (faults) interpreted from gravity data, with minor support from magnetic picks. The rationale for the relation to geothermal targets relates to well-fractured areas at structural intersections as favorable sites for thermal fluid up-flow zones. Any correspondence of these areas with elevated ground temperatures, indications of recent faulting from LiDAR data or photography, or other geologic projections, could elevate the priority of these "raw" geothermal target areas.

Geological Exploration

High resolution LiDAR (light detection and ranging) data were acquired in late fall of 2008 over the CMAGR exploration areas. For the purposes of this project the primary application is Airborne Laser Swath Mapping (ALSM), in which the LiDAR Technology is used to gather topographic data over a specified land area and used to create a Digital Elevation Model (DEM) with a resolution of approximately 1m in the horizontal direction and 10 cm in the vertical, or better (Unruh, 2008). ALSM integrated with a GIS program can produce artificially illuminated hillshades and slope intensity maps used to identify subtle linear features, i.e. faults scarps, faceted hillsides, vegetation lineaments, and low relief slope inflections. Active or young structures within the western piedmont of the Chocolate Mountains are likely conduits for potential hydrothermal fluids near the surface. This technique greatly reduces the amount of time required to identify subtle tectonic features in large depositional environments and increases the probability of discovering these features that could easily go unnoticed.

LiDAR data for the western CMAGR were analyzed by Jeffrey Unruh and Michael Strane of Fugro-William Lettis & Associates in conjunction with other geospatial data such as gravity and magnetic data and aerial photography (as digital orthophoto quarter quadrangles). Geomorphic lineaments were identified based on alignments of slope breaks, drainage deflections, drainage confluences, and gravel bar terminations. Lineaments also were locally defined by vegetation alignments. In some cases, lineaments were identified as apparent alignments of slope inflections in the gradient (slope) maps. For the purposes of field review, the lineaments were organized into twelve spatially associated groups. The grouping of lineaments primarily was developed for ease of discussion with CMAGR in arranging field access. Unless specified otherwise, no genetic or tectonic association is implied by inclusion of one lineament with another in a particular group (Unruh, 2008).

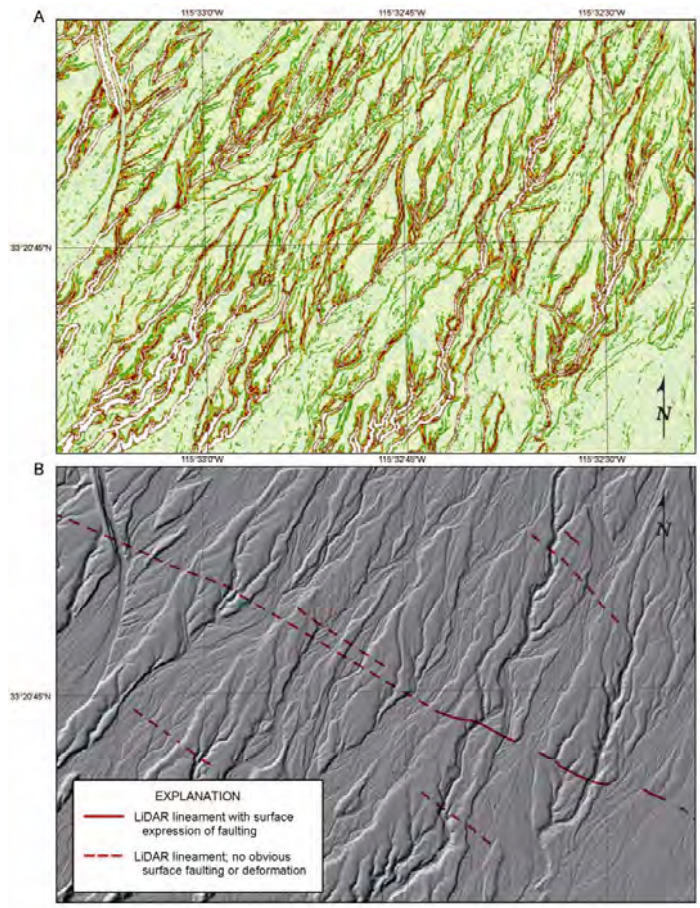

Figure 3. Detail of Central Reach of Lineament 4: (A) Slope Map, (B) Annotated hillshade map depicting northwest striking graben structure.

Of the twelve lineament groups only one, lineament 4 (Figure 3), was confirmed to have late Quaternary surface faulting and all others were determined to be of a non-tectonic nature. Lineament 4 is a northwest striking, southwest dipping structure that has 0.5 kilometer of well-defined surface expression and is rough;y traced out in both directions for a total of ~6.5 kilometers. Field surveys indicated that the scarp is about 40 (Figure 4) centimeters high in the central, well-expressed section. Observations in the field revealed a second Northeast facing, 25 centimeter scarp displacing a similar alluvial fan deposit, which makes a

200 meter wide graben structure. The younger washes that incise the older alluvial fans up to 1.5 meters have no scarps on trend with the graben structure. This suggests that the surface rupturing occurred during the late Quaternary and is post-dated by recent deposition. Based on the empirical relations among earthquake parameters determined by Wells and Coppersmith (1994) and the 40 centimeter scarp we can determine that in the case of a single event the earthquake would have been Mw 6.6 with a 22 kilometer surface rupture length and Mw 6.2 with a 12 kilometer surface rupture in the case of two similar events. This suggests the surface rupture length to be much greater than the observed rupture length and since the lineament dies out across similar deposits to the northwest it is likely that lineament 4 continues along strike to the southeast but is not observed on the surface due to recent sedimentation post-dating the last event.

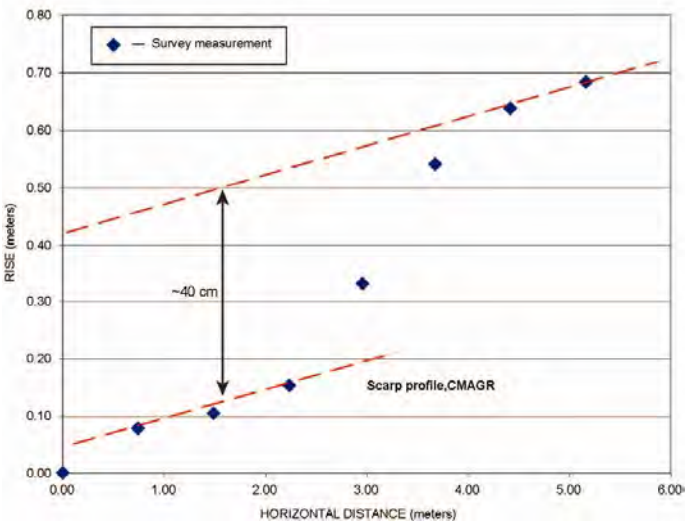

Figure 4. Field Slope data and profile of southwest dipping main fault scarp along lineament 4.

Shallow Temperature Gradient Drilling

A shallow temperature gradient drilling program, consisting of thirteen 500-foot deep slimholes, was initiated in the Hot Mineral Spa/Camp Billy Machen exploration area. Sites were targeted using the combination of geophysical/electrical anomalies and active Holocene structures discussed above. Through the months of January-March 2010 Dan's Pump and Water Well Drilling, a small business from Livermore, Ca, worked through the flashflood season of Imperial Valley to construct the temperature gradient holes (TGH). Although lost circulation was an issue on several occasions, no holes were lost before the logging phase of the project and only one hole was not completed to the target depth. Typical TGH construction consisted of setting a 50' surface conductor and drilling a 6 inch open-hole with standard mud-rotary equipment to 500 feet. Each TGH was completed with either nominal 3 inch internal diameter coupled PVC or threaded steel tubing. The type of tubing used was dependent on the mud return temperatures measured during drilling. The typical upward limit for continuous use of PVC pipe is 60°C however return temperatures are not always a good indication of the actual downhole temperatures so 46°C was the cut-off to switch to the more expensive steel completion method.

Lithologies were recorded at 10 foot intervals with a fist sized chip sample collected in a cloth bag when possible. Lithology was predominantly clays, silts, sands, and gravels. Quartz was the primary sand and silt component. Local igneous and metamorphic rock fragments dominated the heavier grained sands and gravels. Grain size generally increased with proximity to the range front of the Chocolate Mountains.

Temperature logging was conducted several times during the desired 90 day equilibration phase. Logging of temperature profiles was completed with a 100-W platinum resistance temperature device (RTD) with a 1s response time. Logging was completed going downhole and the probe was frequently calibrated using ice baths and boiling water during the project. These data require further processing to identify potential issues with equilibration time such as potential temperature disturbances by lost circulation zones and thermal rebound history. One of the most important steps in the continued evaluation of this project will be the further analysis of chip samples to define relationships between temperature spikes and lithology variations. This may assist in identifying potential high temperature lateral flow in zones of high permeability.

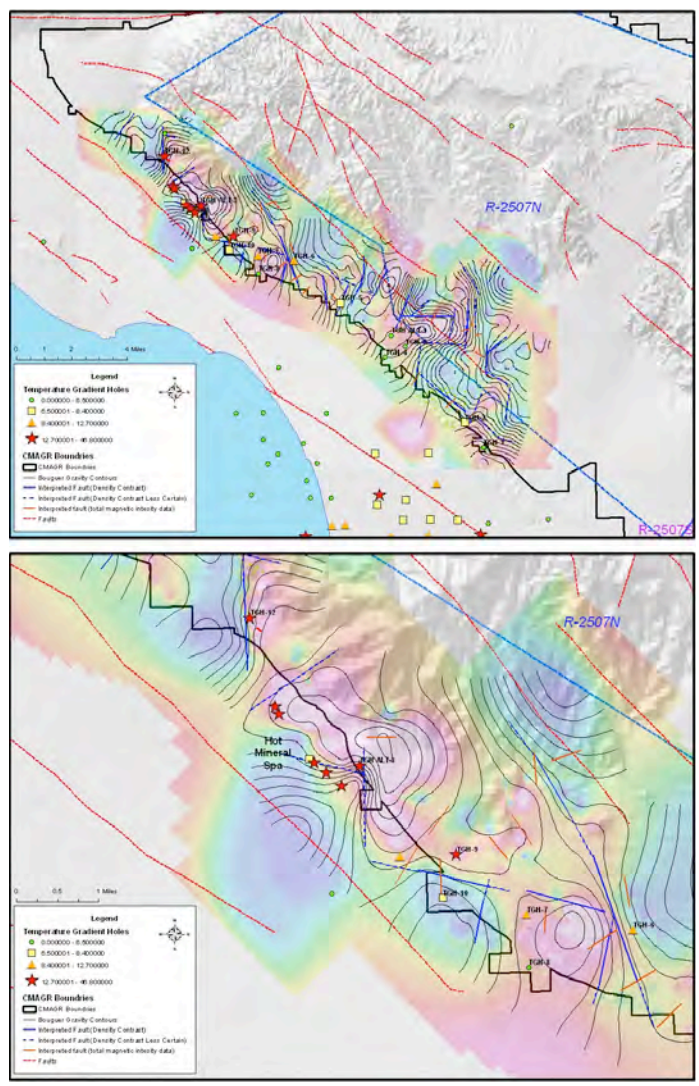

Figure 5. Location maps of recent and historic TGH drilling sites.

Temperature gradients calculated from these thirteen test holes ranged from 9.6 to 42.7 °C/100m, similar to gradients from wells at Hot Mineral Spa (Figure 5). Bottom hole temperatures (at ~500 feet) range from 37 to 62.8 °C.

Previous drilling in areas near Hot Mineral Spa and Frink Springs show elevated temperatures and most models describe the Hot Springs Fault as the outflow origin. The geochemistry of wells in and around CMAGR is predominantly sodium-chloride waters with locally abundant calcium, bicarbonate, and sulfate. As a result, these waters do not form a distinct cluster on the Piper diagram. The lack of a clustered pattern is attributed to the broad geographic spread of available data points. SiO_2-chalcedony geothermometers yield temperatures of 46-87ºC for available samples near the western margin of CMAGR. Thermal waters from the Hot Mineral Spa area emerge from springs, artesian wells, and are produced from shallow aquifers at temperatures ranging from 54-80ºC. Although the springs and producing zones are spatially associated with the Hot Springs Fault, the fault itself may not be the only structure responsible for the geothermal resource. A cross section of the northwestern Chocolate Mountains piedmont with borehole constraints on subsurface structural and stratigraphic relations indicates that a blind or buried fault east of the Hot Springs Fault displaces the crystalline basement about 260 m down to the west (Figure 6). In contrast, vertical displacement of the basement across the Hot Spring Fault is only a few tens of meters. These data suggest that rather than a single fault, the Hot Springs Fault may actually be a zone of faulting up to several hundred meters wide. Reservoir temperatures for thermal waters along the Hot Springs Fault derived from Na-K-Ca geothermometry are estimated to be about 99°C (this and the following data from Hunter, 1998). Temperature gradients from measurements in shallow wells range from about 46.3°C/100m in the crystalline basement rocks, and 72.7°C/100m in the sedimentary cover. From the inferred reservoir temperatures and geothermal gradients, Hunter (1998) estimated that the waters probably were heated at depths of 1.1 to 1.7 km. Hunter (1998) argued that the fluids were heated in a deep (bedrock?) reservoir and migrated upward along the Hot Springs Fault to charge the shallow Holocene aquifer adjacent to the range front. Stable isotope analysis of fluids from several springs and wells in the Hot Mineral Spa Geothermal Area indicates that they share a common meteoric origin, and suggests that regional recharge occurred under a cooler, wetter climate than present. To date, however, reliable 14C dates have not been obtained from the fluids to determine if the waters date back to the Pleistocene (Hunter, 1998).

Hunter summarizes that thermal waters from the Hot Mineral Spa Geothermal Area primarily occur in an approximately 40-m-thick aquifer of Holocene sands and gravels encountered at depths of about 20 to 130 m on the eastern side of the fault (Qal unit on Figure 6). A confining layer of clay and mudstone overlies the producing aquifer. Chemical analyses indicate that the total dissolved solids in the waters ranges from about 2100 to 3800 mg/L. As of 1998, 23 wells had been drilled into the producing zone, of which 14 are used for production. The aquifer produces about 4000 acre-ft of thermal water per year (Hunter, 1998). This interpretation suggests that the anomalous temperatures encountered were a result of outflow from a 100m band of faulting associated with the Hot Springs Fault. However this band may be wider than previously thought, with the primary outflow zone occurring in a series of buried normal or dip-slip faults closer to the range front. Stepping to the SE, temperature gradients recorded in the Niland region were typically less than 15°C/100m. Although the gradients were low, temperature readings were anomalously high (e.g., 52°C), compared to average regional groundwater temperatures of 24.5°C. Even though a shallow resource is very unlikely determining the outflow source and reservoir characteristics therein still remain an exploration goal of the GPO.

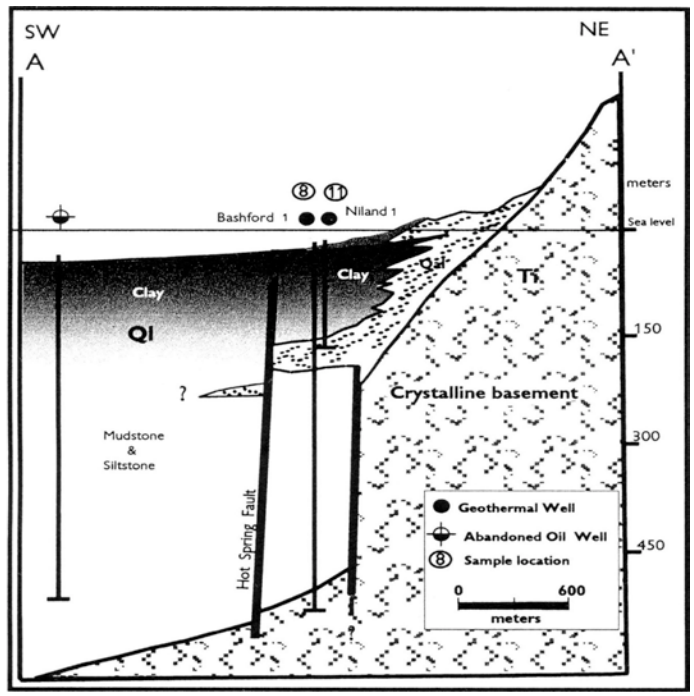

Figure 6. Geologic Cross Section Adjacent to the Hot Spring Fault (Hunter, 1998).

Conclusion

CMAGR's associations with the Salton Trough, Hot Mineral Spa, Glamis KGRA, and the limited amount of access that has been granted to its ranges make it an interesting place for exploration. We have the unique opportunity to apply our exploration model to an area that has had relatively little research done compared to its surrounding and is right on the periphery of one of the most active geothermal regions in the United States. Exploration efforts to date have been positive and have produced sufficient evidence for us to continue to refine and characterize potential drilling targets.

Future projects at CMAGR include 1) geologic mapping and sampling, 2) gravity and magnetic surveys, expanding on the current dataset and working into new areas like Glamis, 3) SP surveys in areas of geothermal interest, 4) possibly some 2D seismic lines to further interpret the structural geology beneath young alluvial deposits, and 4) more temperature gradient drilling. As work is completed in the separate exploration areas and encouraging data is received the GPO will move ahead with a deep slim-hole drilling campaign to characterize the potential resource.

Acknowledgements

We would like to thank Yuma MCAS Commanding Officer Colonel Mark A. Werth, United States Marine Corps, and Camp Billy Machen Officer in Charge Senior Chief John Salguero, US Navy for granting access and making the safety of our colleagues and co-workers a top priority. We would also like to thanks our contractors for helping utilize potential geothermal resources on DoD controlled lands.

References

Anderson, G., Agnew, D.C., and Johnson, H.O., 2003, Salton Trough Regional Deformation Estimated from Combined Trilateration and Survey-Mode GPS Data: Bulletin of the Seismological Society of America, Vol. 93, No. 6, pp. 2402–2414

Crowell, J.C., 1975, Geologic sketch of the Orocopia Mountains, southeastern California, *in* Crowell, J.C., ed., San Andreas fault, a guide to the San Andreas fault from Mexico to the Carrizo Plain: California Division of Mines and Geology Special Report 118, p. 99–110.

Crowell, J.C., 1981, An outline of the tectonic history of southeastern California, *in* Ernst, W.G., ed., The geotectonic development of California; Rubey Volume 1: Englewood Cliffs, New Jersey, Prentice-Hall, p. 583–600.

Ehlig, P.L., 1981, Origin and tectonic history of the basement terrane of the San Gabriel Mountains, central Transverse Ranges, *in* Ernst, W. G., ed., The geotectonic development of California; Rubey Volume 1: Englewood Cliffs, New Jersey, Prentice-Hall, p. 253–283.

Fuis, G.S., Mooney, W.D., Healy, J.H., McMechan, G.A., and Lutter, W.J., 1984, A seismic refraction survey of the Imperial Valley Region, California: Journal of Geophysical Research, v. 89, p. 1165–1189, doi: 10.1029/JB089iB02p01165.

Hunter, C.C., 1998, An investigation of the Hot Mineral Spa geothermal resource area, Riverside and Imperial Counties, California, in Lindsay L., and Hample, W.G., eds., Geology and Geothermal Resources of the Imperial and Mexicali Valleys: San Diego Association of Geologists, Annual Field Trip Guidebook, p. 93-108.

Grove, M., Jacobson, C.E., Barth, A.P., Vucic, A., 2003, Temporal and spatial trends of the late Cretaceous-early Tertiary underplating of Pelona and related schist beneath southern California and southwestern Arizona, Geological Society of America, Special Paper 374, p. 381-406

Jacobson, C.E., Oyarzabal, F.R., and Haxel, G.B., 1996, Subduction and exhumation of the Pelona- Orocopia-Rand schists, southern California: Geology, v. 24, p. 547–550.

Jacobson, C.E., Grove, M., Vucic, A., and Pedrick, J.N., 2005, Exhumation of the Orocopia Schist and associated rocks of southeastern California: Relative roles of erosion, synsubduction tectonic denudation, and middle Cenozoic extension, *in* Cloos, M., Carlson, W.D., Gilbert, M.C., Liou, J.G., and Sorensen, S.S., eds., Convergent margin terranes and associated regions—A tribute to W.G. Ernst: In Press: Geologic Society of America Special Paper.

Oyarzabal, F. R., C. E. Jacobson, and G. B. Haxel, 1997, Extensional reactivation of the Chocolate Mountains subduction thrust in the Gavilan Hills of southeastern California, *Tectonics*, *16*(4), 650–661.

Ross, H. P., 2009, Structural Geology Interpretation of Gravity Data, Chocolate Mountains Aerial Gunnery Range, final technical report submitted to the US Navy Geothermal Program Office, Contract No. N68936-08-P-0283.

Stephenson, D.B., and Girty, G.H., 2006, Constraining the Source of the Orocopia Schist, SE California: A comparative study of the major and trace element chemistry of Cretaceous sandstones deposited in forearc settings in Girty, G.H., and Cooper, J., eds., Using Stratigraphy, Sedimentology, and Geochemistry to Unravel the Geologic History of the Southwestern Cordillera: A Volume in Honor of Patrick L. Abbott, Pacific Section, Society of Economic Paleontologists and Mineralogists, Book 101, p.77-96.

Unruh, J., Strane, M., 2008, Interim Results of Neotectonic Reconnaissance, CMAGR, technical report submitted to the US Navy Geothermal Program Office, Contract No. N68936-02-R-0236.

An Update on Geothermal Energy Resource Investigations, Chocolate Mountains Aerial Gunnery Range, Imperial Valley, California

Steven BJORNSTAD[1], Steven ALM[1], Wei-Chuang HUANG[1], Andrew TIEDEMAN[1], Lindsey FRAZIER[1], Christopher PAGE[1], Andrew SABIN[1], Daniel VEAZEY[2]

[1]USN Geothermal Program Office, China Lake, CA,
[2]Epsilon System Solutions, Inc.

Keywords: geothermal, exploration, temperature gradient, self-potential, SP, Chocolate Mountains, US Navy

Abstract

The US Navy's Geothermal Program Office (GPO) conducted self-potential (SP) geophysical surveys in the Chocolate Mountains Aerial Gunnery Range (CMAGR) during November and December 2010 with assistance from Epsilon Systems Solutions, Inc. The focus of this work was the Camp Billy Machen training area extending northeast to a region east of the Hot Mineral Spa KGRA. The objective was to further define the controls on the 5.3 to 23.5 degrees F/100 feet temperature gradients identified through a temperature gradient hole drilling campaign in 2010.

Over 1,200 stations at 200 foot spacing were occupied in a ~20 mi^2 region in this western piedmont of the Chocolate Mountains. Two major anomalies were identified in the survey area. A negative 108-mV anomaly in the North (HMS-A) and a negative 96-mV anomaly in the South (HMS-B), both of which appear to be electro-kinetically produced anomalies. The anomalies are generally coincident with the higher shallow temperature gradients. The radial nature of the South anomaly suggests a flow of thermal fluids structurally controlled by faults analogous to regional patterns. Two target areas were identified and the drilling of two deeper test holes (programmed to 3,000 feet) is to be completed in mid-2011.

Introduction

The US Navy's Geothermal Program Office (GPO), has continued its geothermal exploration in the Chocolate Mountains Aerial Gunnery Range (CMAGR) with a focus on the Camp Billy Machen training area, extending generally northeast of Niland, California to east of the Hot Mineral Spa Known Geothermal Resources Area (HMSpa) (Figure 1). The CMAGR is a military air and ground training range situated along the eastern margin of the Salton Sea in southern California. The range is managed by the Marine Corps Air Station, Yuma, AZ. The US Navy Geothermal Program Office (GPO) has conducted exploration activities within CMAGR a various times beginning in 1976 (Alm et al, 2010). Current exploration program begin in 2008 following the issuance of a directive from the Commandant, United States Marine Corps, in support of the development of geothermal resources on Marine Corps installations.

The prospect area is located along the far eastern margin of the Salton Trough where a thick section of Quaternary alluvium slopes gently westward from the Chocolate Mountains. Away from the mountainside, the alluvium overlies Lake Cahuilla and associated late-Holocene/Pleistocene sediments (Figure 2). The mountains themselves are here composed primarily of Tertiary intrusive, hypabyssal rocks - multiple parallel dikes of porphyritic quartz latite composition injected in fine-grained porphyritic quartz monzonite of possibly pre-Tertiary age. The abundance and regularity of the dikes gives the appearance of well-layered rock. Isolated occurrences of Tertiary volcanics (rhyodacitic to rhyolitic plug domes, lava flows) are present as well. Underlying these Tertiary units is a Precambrian igneous and metamorphic rock complex (also mapped as the Chuckwalla Complex) of quartz diorite gneiss, foliated hybrid granitic rocks, and granophyres, largely acidic to intermediate range in composition. Except for reconnaissance geologic mapping and a LiDAR survey, all of the prospecting has been focused on the alluvial slope.

Beginning in the summer of 2008 gravity and magnetic data were acquired over the prospect. Apparent buried basement fault structures were mapped and interpreted through both density and magnetic contrasts (Figure 3). In the exposed bedrock, major structures trend northwest (N35W to N55W) in the Tertiary outcrop, generally parallel to the San Andreas fault zone. In the prospect area, this anticipated major NW structural trend appears disturbed (cross-cut) by numerous N, NE, and almost east-west structures. These apparent structural trends appear to be generally consistent with trends both to the northeast in the mountains, as well as, in the subsurface to the south within Ormat NV's Wister project (Skip Matlick, personal communication). These appear to represent to reflect the local

structural pattern associated with the San Andreas fault System. These include NW-trending structures generally parallel to the San Andreas, as well as NNE and NE orientations which may be directly related to tensional and reidel structures extending outward along the northeastern edge of this fault system.

High resolution LiDAR (light detection and ranging) data were also acquired in 2008 over the CMAGR exploration areas to produce artificially illuminated hillshades and slope intensity maps used to identify subtle linear features, i.e. faults scarps, faceted hillsides, vegetation lineaments, and low relief slope inflections. Active or young structures within this western piedmont of the Chocolate Mountains are likely conduits for potential hydrothermal fluids near the surface. Several sets of geomorphic lineaments were identified based on alignments of slope breaks, drainage deflections, drainage confluences, and gravel bar terminations, however all were determined to be of a non-tectonic nature except one. This is a northwest striking, southwest dipping, 40 centimeter high structure that has 0.5 kilometer of well-defined surface expression and was roughly traced out in both directions for a total of ~6.5 kilometers – providing another potential geothermal target.

Shallow TGH Drilling Results

As previously reported (Alm et al, 2010), results of the above investigations were integrated and several target sites were defined for shallow temperature gradient drilling. This effort, consisting of a total of 13, 500-foot deep, test holes was completed in 2010, with temperature gradients ranging from 5.3 to 23.5 degrees F/100 feet (Figure 3). Test hole construction consisted two stages: 1) drilling a nominal 12-inch hole, setting and cementing in eight-inch diameter, 50-foot steel surface conductor; and 2) drilling a six-inch open-hole to 500 feet and completing with sealed 3-inch internal diameter coupled PVC pipe, bentonite and gravel-packed. The PVC is filled with fresh water and a locking cap installed on the surface conductor pipe. Chip samples were taken at 10-foot intervals and logged. Equilibrated temperature logs were run between 60 and 90 days following completion of each test hole.

A distinct areal distribution of shallow temperature gradient can be seen, with all test hole gradients above 8.8 degrees F/100 feet occurring in the northwest part of the prospect implying a significantly higher potential for the occurrence of a geothermal resource in the northwest. However, a part of the probable explanation for this can be seen in Figure 4, a generalized NW-SE cross-section through the prospect. All of the test holes with gradients less than 8.8 intersected mostly or entirely Pleistocene Lake Cahuilla and associated sediments – dominantly impermeable clays and muds, while the other holes intersected thick sections of highly permeable alluvial slope wash – sands, gravels and cobbles. In the southeastern area, even if open basement fractures are present and are conductive to deeper hot fluids, their thermal signature may be masked by the thick section of shallow clays.

Figure 5 shows the temperature profiles for all of the test holes. Most of the lower gradient profiles are clearly conductive. Projecting these conductive gradients to depth, temperatures in the range of 150° to 160°F would not be seen above about 1500 to 2000 feet and the area would not appear prospective. This is a good example of why temperature gradient drilling must be viewed in context with other geological and geophysical data.

Self Potential Surveys

Self-potential (SP) methods measure naturally occurring electrical potential in the earth. One source of these naturally occurring self-potentials is the "streaming potential" or electrokinetic potential which arises from the flow of fluid, such as groundwater, through a porous medium. For this reason, S-P can be applied to groundwater investigations and the identification of the shallow upwelling and/or outflow of geothermal fluids. The self-potential method has been identified as an effective low-cost geothermal exploration method for identifying electrical resistivity anomalies generated from electrokinetic and thermoelectric phenomena. These phenomena, when related to geothermal fluids, are a theorized (Corwin and Hoover, 1979) result of ion rich fluid transportation and electrical voltages produced from temperature differences. This method has been described as very successful in identifying shallow zones of upwelling geothermal fluids at a number of known geothermal resource areas such as; LongValley, California (Anderson and Johnson, 1976), Cerro Prieto, Mexico (Goldstein et al., 1989), East Mesa (Goldstein et al., 1989), Beowawe (Demoully and Corwin, 1980), and Newcastle (Ross et al., 1990).

Therefore, the SP method was chosen as a least cost way to potentially differentiate outflow from HMSpa versus fault-controlled upwelling beneath the TGH's. Elevated Temperatures in TGH-7, 9, 12, and ALT-3 along with known production of geothermal fluids for direct use at several nearby resorts and aquaculture developments inspired the initial survey location and design over this portion of the prospect area. Two detailed SP surveys were conducted in the

Camp Billy Machen/Hot Mineral Spa region of the CMAGR in November and December 2010 (Surveys 1 and 2). The first was designed to gather detail SP resistivity data in the region of those temperature gradient test holes with the highest gradients. The second survey was designed to augment and confirms the results of the first (Figure 6).

SP Method

All data were collected by two four-person survey crews. Each three or four-person crew consisted of one or two people laying out the survey lines and two people collecting the self-potential (SP) data. The November survey design was based on the "radial spoke" technique, which typically consists of lines being laid out in a radial pattern originating from a central stationary electrode or "base station." A similar method was applied to the second survey, however the layout of the lines was done in a more grid (90°) pattern. Stationary electrode type surveys with a single roving electrode, compared to leap-frog type surveys where there is no stationary electrodes, minimize cumulative errors that can result from intersecting profiles. In an effort to greatly reduce the potential for compound polarization and drift error, all new base stations were referenced back to the original or primary base station, plus the natural voltage between pots was monitored in an electrolyte bath before and after each survey leg. The temperature of the porous pots was regulated to the extent possible by keeping them shaded because temperature differences between pots can cause a significant amount of drift as well.

Line stations were marked at a 200-foot spacing using a Trimble Juneau SB handheld that operates at ~3-meter accuracy. Lines were designed in the field using the ESRI Arcpad program installed on the Trimble unit and spacing was determined using a 200-foot length of wire. The team operating the GPS unit would clear a small 4-6" wide depression of debris, add about a cup of water, take a GPS measurement, name the site, and then flag for ease of location by the SP team. Allowing one group to work ahead gave the water in the electrode holes time to allow the infiltration potential to completely decay and still provide enhanced electrical contact with the soil. It was observed by Ross (2009) that in a similar arid environment initial infiltration potentials after watering produced +30mV and then decreased to 0-5mV after a period of 10-30 minutes. Our survey was designed to allow for a period of 1-3 hours before an electrode measurement was ever taken. The voltage reading was often retested to verify that the reading was not still being affected by the infiltration potentials.

The survey lines were almost exclusively "cross-country" type traverses since our survey procedure equated to little more than hiking with geophysical equipment across the ranges. Survey lines were laid out by GIS technicians from ESS and a reasonable amount of flagging was used to mark the shortest path along the line as needed. In several instances large drainages were crossed and older alluvial terraces, incised as much as 15 feet, had to be ascended and descended with regularity. This rapid, local change in elevation is considered to be a potential source of error in the data since uneven topography may affect surface potential fields by distorting current flow patterns (Corwin, 1979).

Select data was processed in the field by doing a simplified base correction or tie-in calculation to allow for diligent survey expansion design on the fly. Every evening all data was processed in an Excel spreadsheet so that long integer calculations, which help reduce compound errors, could be swiftly completed with ease and the next day's survey could be designed to effectively map and define anomalies. Upon completion of the survey all data was reviewed for accuracy before being contoured in ArcMap 3D Analyst (Figure 6). Contouring was examined in detail to further delineate potential issues or concentrations of noisy/ inaccurate/misplaced data. From this visual inspection several corrections were made, several areas with increased noise were left to source speculation, and one survey line was omitted entirely.

SP Survey Interpretation

Four features in the Camp Billy Machen/Hot Mineral Spa SP survey area have compelling amplitude, extent, and orientation to be considered anomalies worthy of further testing. These are discussed below.

HMS-A. This anomaly occurs in the far NW portion of the survey, SW of the Salt Creek Wash. HMS-A trends NNW ~6000 feet along its long axis and ranges from -54 to -100mV with the heart of the anomaly approximately 2000 feet NW of TGH-12 (Figure 6). This dipolar self-potential anomaly has a 140mV peak to trough amplitude and 3000 feet peak to trough length. This high amplitude portion of the anomaly is about 1700 feet across on the short axis and has a similar range of -55 to -100 mV. The anomaly, as defined by Survey 1, had the potential to be a continuation of negative values cumulated in the reference base correction and was therefore heavily targeted for follow-up work in Survey 2. In Survey 2 five survey lines were run perpendicular to the long axis trend of the anomaly from new base stations. Three survey lines filled areas with little data and two

survey lines were laid very close to existing lines to test the repeatability of the data. The results were very encouraging. The fill-in lines did little to alter the contouring of the general shape of the defined anomaly and the parallel lines reproduced the data mostly within 1-10mV with a maximum difference of 20mV.

Potential survey noise can be generated from several sources and could have caused some of the minor issues in accurately reproducing the data. These include:

a. infiltration potentials that did not fully decay before readings were taken;

b. minor amount of rain occurred during the night before the first day of Survey 2. The rain could have concentrated groundwater flow across certain areas and created electrokinetic voltage, potentially altering the field; and

c. the variability in the short distance between the two lines could be valid, giving strength to the argument that when testing data reproducibility one should reoccupy the actual stations in order to create an accurate comparison.

Anomaly HMS-A appears to have a high potential for being real. The combined data strongly suggests that it probably arises from a natural source, potentially a upwelling of geothermal fluids. We have closure on all sides and were able to reproduce the data with a good deal of confidence, suggesting that this anomaly is distinct from the HMSpa…and that our field methods were thorough and well executed by all team members.

HMS-B. This broad anomaly occurs in the SE portion of the survey area with lows in the range of -40 to -87 mV along a 7500 feet NNW trending profile. HMS-B is well-defined with over 20 survey lines from 5 different base stations recorded over both phases of the survey (Figure 9). There is also an antithetic spur that trends off the southern section of the profile to the NE with negative values of -53 and -68. Although the anomaly has a well defined general trend the overall data has a noisy character to it. This causes some irregularity in the contouring that is difficult to account for.

Potential noise issues could be very similar to the ones mentioned in regards to HMS-A or the effects of uneven topography on electrical current flows patterns described by Corwin (1979). Figure 10 attempts to display relationships between uneven topography and data noise, showing survey profiles that represent the long axis of the anomaly in a side by side comparison with an elevation profile from our LiDAR dataset. The presence of a relationship between elevation irregularity and SP data noise is very difficult to discern at this scale since the resolution of the two data sets is very different. However it displays very well that the SP data in the NW is grouped much more tightly than that in SE. This seems to generally correlate with a much smoother elevation profile in the NW and a much more uneven profile to SE, again where we generally start to see an increase in the variability of the SP data or what could be interpreted as noise.

Similar to HMS-A, HMS-B should be considered to have a high potential for being associated with a natural SP source such as upwelling geothermal fluids. Even though there appears to be some significant noise associated with the data and the contouring is slightly irregular the dominant trend of the anomaly appears to align with the trend of HMS-A and regional structural patterns. Matched with encouraging thermal anomalies from nearby temperature gradient holes and similar patterning found in the magnetics and gravity interpretations make this anomaly a high priority for future exploration.

HMS-C. This is a very small smoothly contoured anomaly located 1000 feet from the southern tip of HMS-A. It has a circular contour pattern about 500 feet across with minimum values of -48, -76, and -88 mV (Figure 6). Several lines from various base stations in both phases of the survey were measured across this anomaly to fully delineate a potential source.

SP values rapidly increase in every direction as you move away from this minor anomaly. This is likely a continuation of HMS-A. A steep, well incised drainage in the range front may potentially be funneling ground water across and masking what would otherwise be a larger more continuous HMS-A. This would be a good target for further testing with lower cost surveys before attempting a deep borehole in the HMS-A/C area. 2-meter temperature probes could be an excellent way to see if there are elevated temperatures near the surface and how they compare with readings over nearby SP and thermal anomalies.

HMS-D. This anomaly appears to be a northwestward continuation of HMS-B and is separated by a broad zone of moderately low values in the range of -10 to -40 mV (Figure 6). The values across HMS-D range from -20 to -60 mV over 8500 feet. One of the major issues with this minor anomaly is the survey coverage. We acquired only a small amount of data perpendicular to what appears to be the general trend of the anomaly. This was a section of the survey area where there was little room between the range front and the Coachella Canal. The canal is another possible noise source for the

entire dataset since one of the primary applications of SP surveying is the identification of subsurface leaks in the dams and canal liners. The base stations were therefore kept at least 500 feet from the canal whenever possible and it was observed that data became more positive as survey lines approached the canal. It was for that reason data acquisition in this area was kept to minimum. However, looking back, a few short lines perpendicular to the regional trend would have been very useful to better define the extent and character of the anomaly.

The extent and potential source of this anomaly is very uncertain. Acquisition of additional SP data points along short lines perpendicular to the primary line may help define the true shape of the anomaly. Drilling a grid of 2-meter temperature probes across the anomaly may also be useful in defining the relationship between the SP anomaly, the high temperature gradient test hole, TGH-ALT3, and the nearby thermal features of the HMSpa KGRA.

Discussion and Conclusions

Integration and interpretation of several geological and geophysical data sets resulted in the targeting of 13, 500-foot deep temperature gradient test holes, drilled in a general southeast to northwest pattern through the Camp Billy Machen/Hot Mineral Spa prospect area. Chip samples revealed dominantly Pleistocene Lake Cahuilla sediments in the southern section and Quaternary alluvial slope wash sediments in the northern section. Equilibrated temperature logs were run between 60 and 90 days following completion of each test hole with resulting temperature gradients ranging from 5.3 to 23.5 degrees F/100 feet.

Self-potential surveys were designed to further investigate the northern portion of the prospect area. These identified several broad, high-amplitude SP anomalies coincident with the 500-foot thermal anomalies. These appear to be worthy of further exploration. These SP anomalies share several general characteristics. Their amplitudes generally range from -40 to -100mV and this range is well beyond that which could be associated with potential noise sources combined with the local background potentials. They are well defined on all sides with the exception of HMS-D, which is recognized to require further work to verify. Anomalies HMS-A and –B, especially, were both extensively verified with cross-cutting lines in Survey 2 in order to verify the reproducibility of the data from Survey 1.

Most importantly, the anomalies tend to share an elongated 2-dimensional shape which appear to reflect the local structural pattern associated with the San Andreas fault System. These include NW-trending structures generally parallel to the San Andreas, as well as orientations which may be directly related to tensional and reidel structures extending outward along the northeastern edge of this fault system. Whether this pattern actually reflects deep-seated permeable faults providing conduits for upwelling geothermal fluids directly beneath these SP anomalies or whether they simply provide relatively shallow conduits for the lateral distribution of geothermal fluids feeding the HMSpa area remains to be determined. This step is now being taken.

Based on the assemblage and interpretation of these results along with those of our earlier work, two potential deep target areas were identified, HMS-A and HMS-B. Of these, HMS-B has been selected for the drilling of two deeper test holes (programmed to 3,000 feet) (Figure 11). It is anticipated that these holes will be completed by the third quarter, 2011. Key elements to this work will be the acquisition of geophysical logs over the entire length of the drill holes, including acoustic and/or resistivity imaging logs. These should allow for three-dimensional mapping of fractures and faults, as well as the calculation of the active tectonic stress regime at this prospect

Acknowledgements

We appreciate the continued support for this exploration effort on the part of both the United States Marine Corps at Marine Corps Air Station, Yuma, AZ and the United States Naval Special Forces at Camp Billy Machen, Niland, CA. We also appreciate the committed assistance of Epsilon Systems Solutions as they have provided highly professional field and GIS support to this project.

References

Alm, Steve, Bjornstad, S., Lazaro, M., Sabin, A., Meade, D., Shoffner, J., Huang, W.C., Unruh, J., Strane, M., Ross, H., 2010, Geothermal Energy Resource Investigations, Chocolate Mountains Aerial Gunnery Range, Imperial Valley, California, Geothermal Resources Council Transactions, v. 34, p. 509-514.

Anderson, L. A., and Johnson, G. R., 1976, Application of the self-potential method to geothermal exploration in Long Valley, California: J. Geophys. Re$., v. 81. no. 8. p. 1527- 1532

Corwin, R. F., and Hoover, D. B., 1979, The self-potential method in geothermal exploration: Geophysics, v.44, pp.226-245

Corwin, R. F., DeMoully, G. T., Harding Jr., R. S., and Morrison, H. F. (1981), Interpretation of Self-Potential Survey Results from the East Mesa Geothermal Field, California, *J. Geophys. Res.*, 86(B3), pgs 1841–1848

Goldstein, N. E., Halfman. S. Corwin, R. F. and Alvarez, J.R., 1989. Self-potential anomaly changes at the East Mesa and Cerro Prieto geothermal fields. Proceedings of the 14th workshop on geothermal reservoir engineering, Stanford University, p. 145-153.

Hunter, C.C., 1998, An investigation of the Hot Mineral Spa geothermal resource area, Riverside and Imperial Counties, California, in Lindsay L., and Hample, W.G., eds., Geology and Geothermal Resources of the Imperial and Mexicali Valleys: San Diego Association of Geologists, Annual Field Trip Guidebook, p. 93-108.

Matlick, Skip, 2011, personal communication, Ormat NV LLC

Ross, H. P., Blackett, R. E., Shubat, M.A., and Mackelprang, C. E., 1990, Delineation of fluid upflow and outflow plume with electrical resistivity and self-potential data, Newcastle geothermal area, Utah: Geothermal Resources Council Transactions, v. 14, pp.1531-1536.

Ross, Howard, 2009, Self-Potential Surveys at MCAGCC Marine Base, Twentynine Palms, CA, Twentynine Palms MCAGCC, CA

Figures

Figure 1. Chocolate Mountains Aerial Gunnery Range, California (MCAS Yuma).

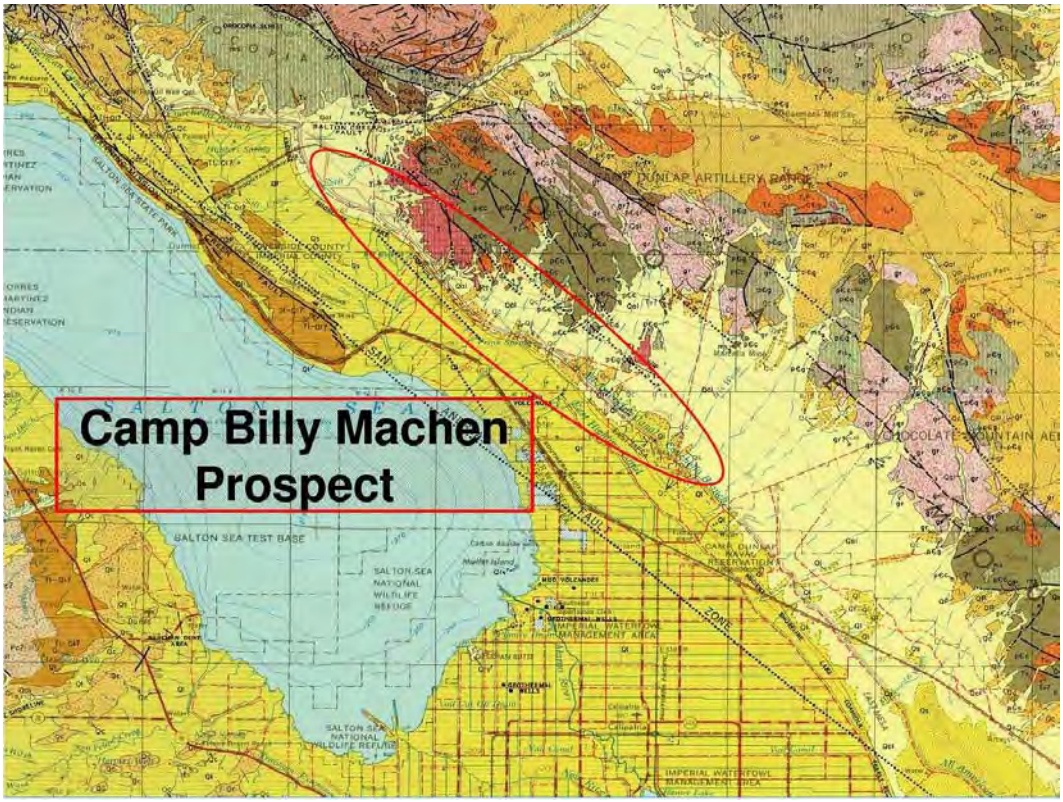

Figure 2. Camp Billy Machen prospect area superimposed on the CDMG Salton Sea 1° x 2° geologic map.

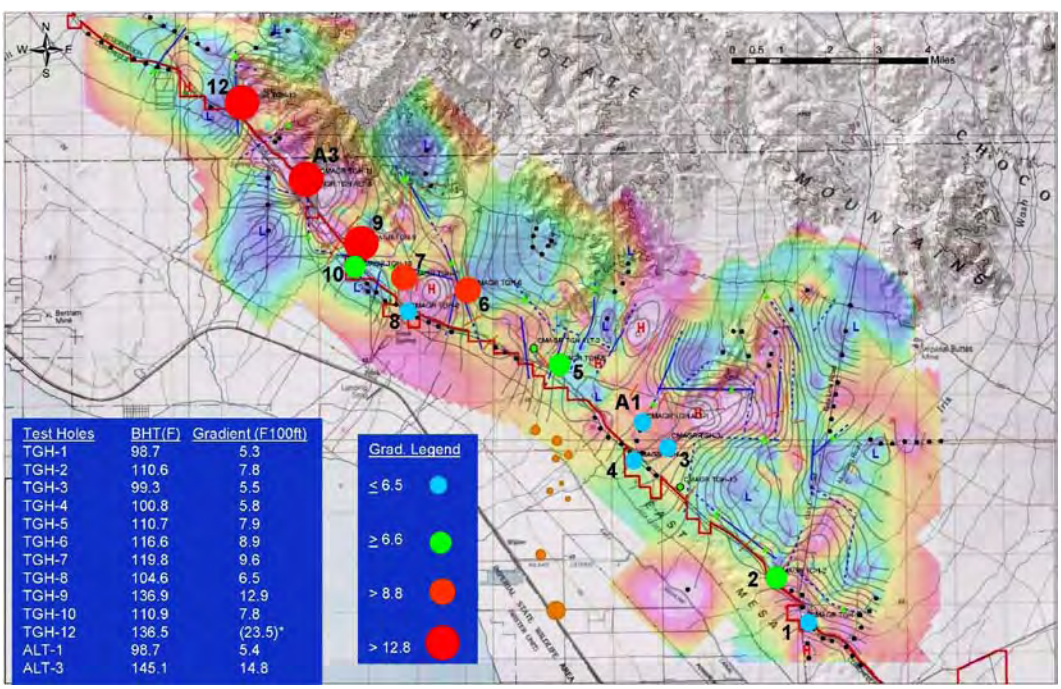

Figure 3. Temperature gradient drilling results over detailed prospect gravity map.

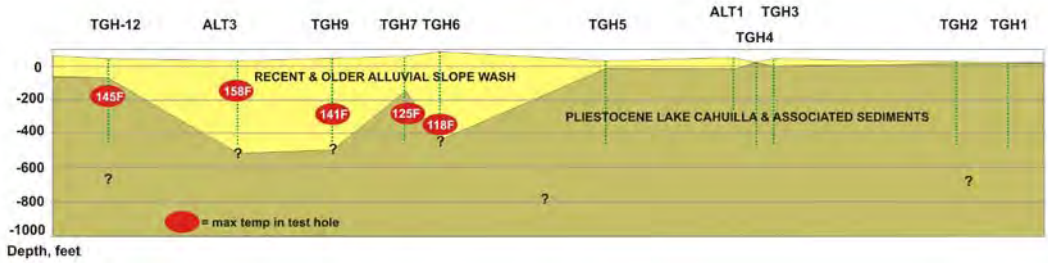

Figure 4. Shallow cross-sectional fence diagram, NW-SE, of the TGH test holes showing general lithology and location of highest temperature in the five hot holes.

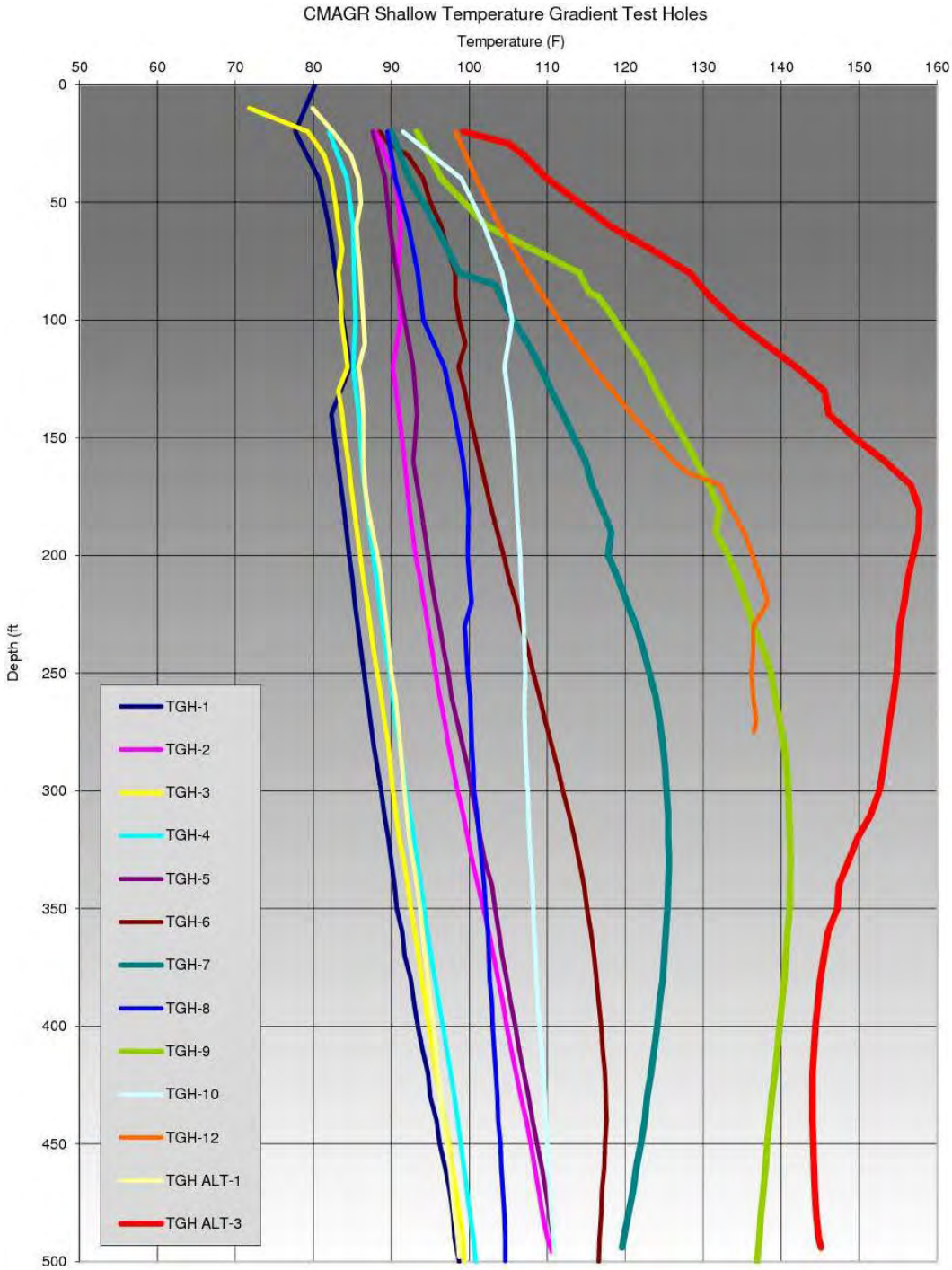

Figure 5. Equilibrated temperature profiles, 500-foot TGH test holes

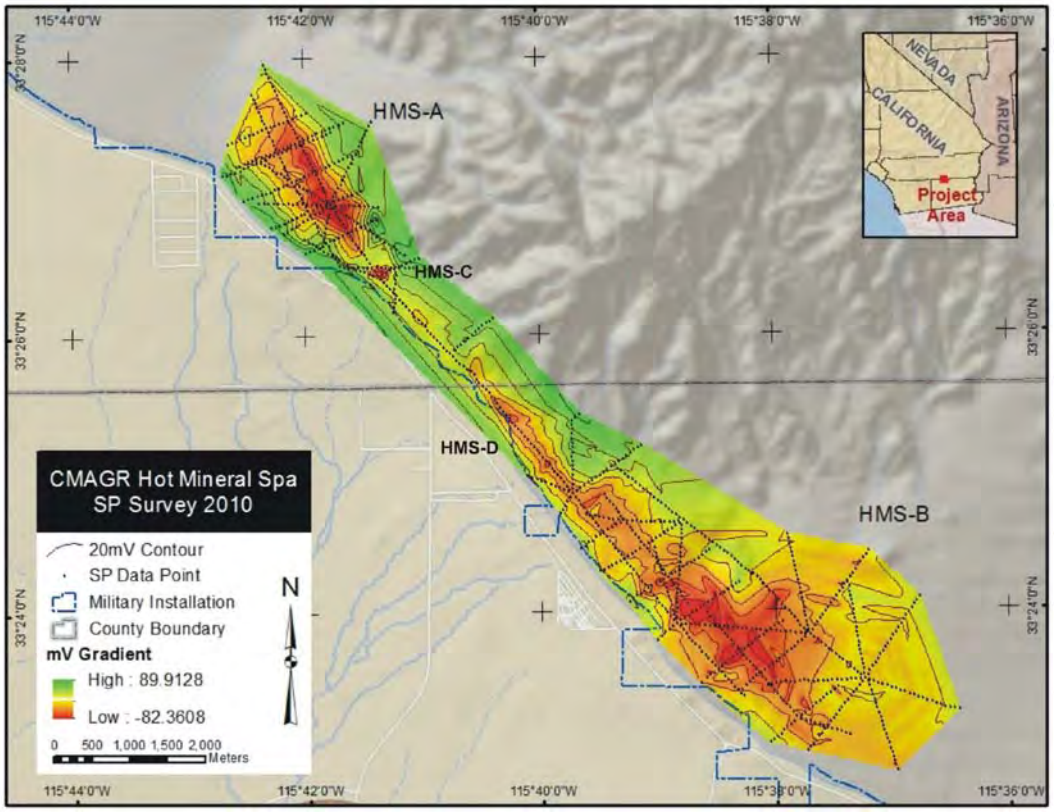

Figure 6. SP surveys – layout and processed data contour map.

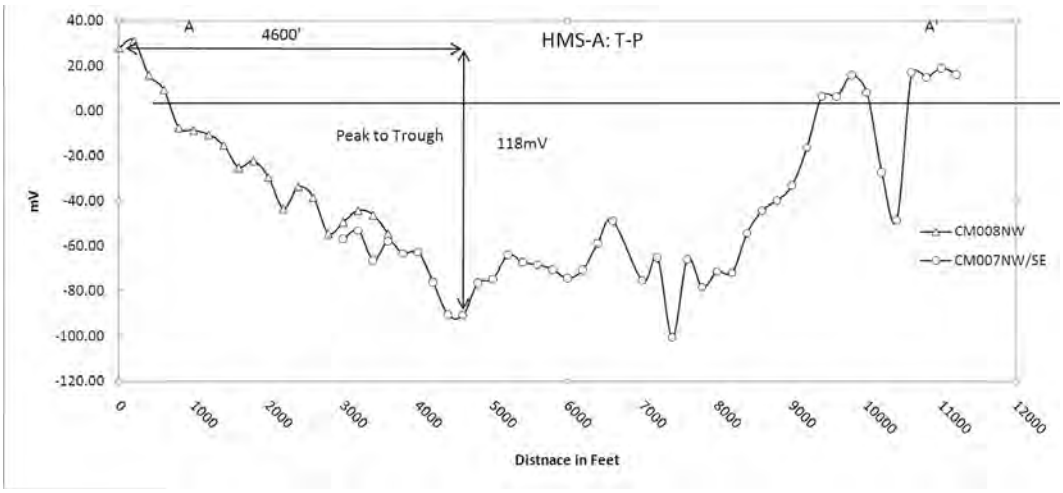

Figure 7. Section A-A' across anomalies HMS-A and HMS-C.

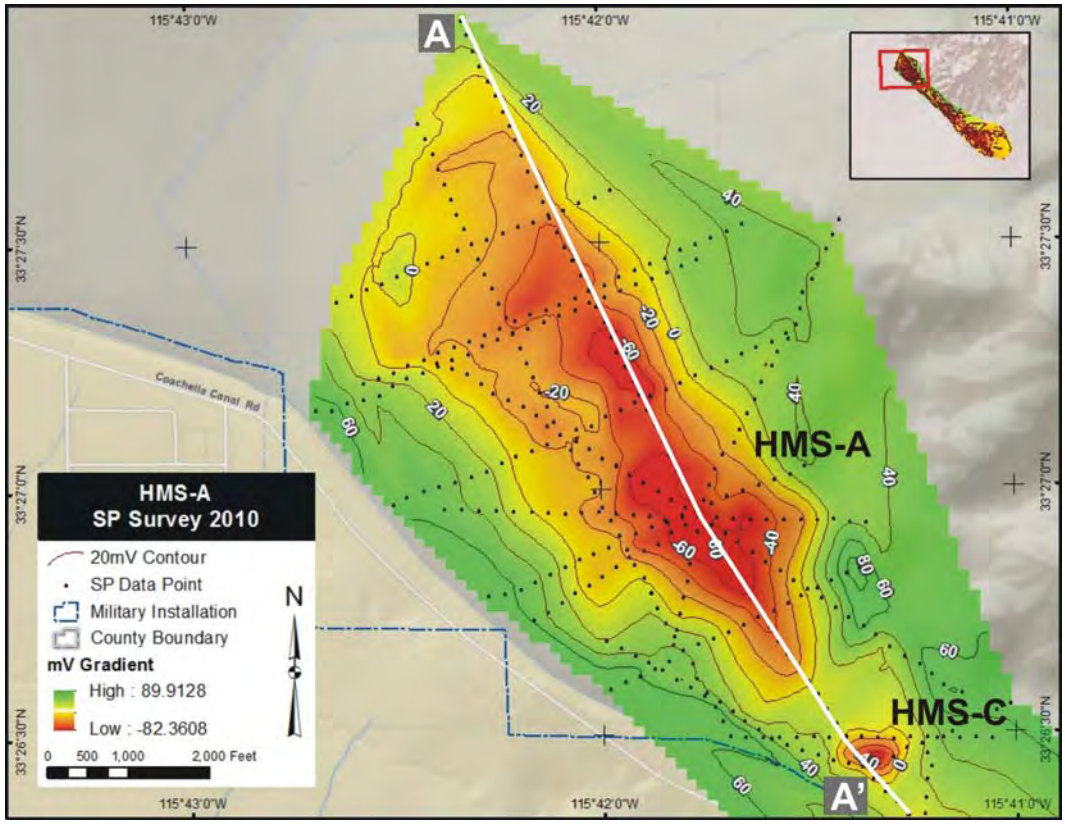

Figure 8. SP anomalies HMS-A and HMS-C.

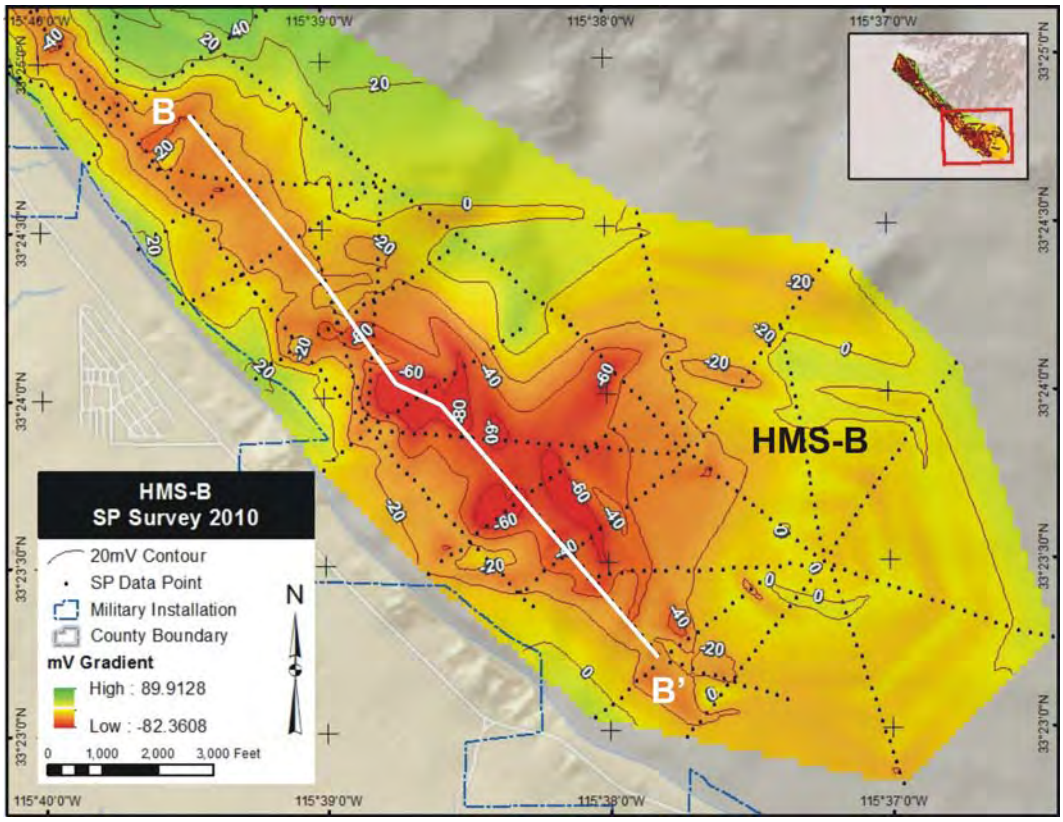

Figure 9. SP anomaly HMS-B.

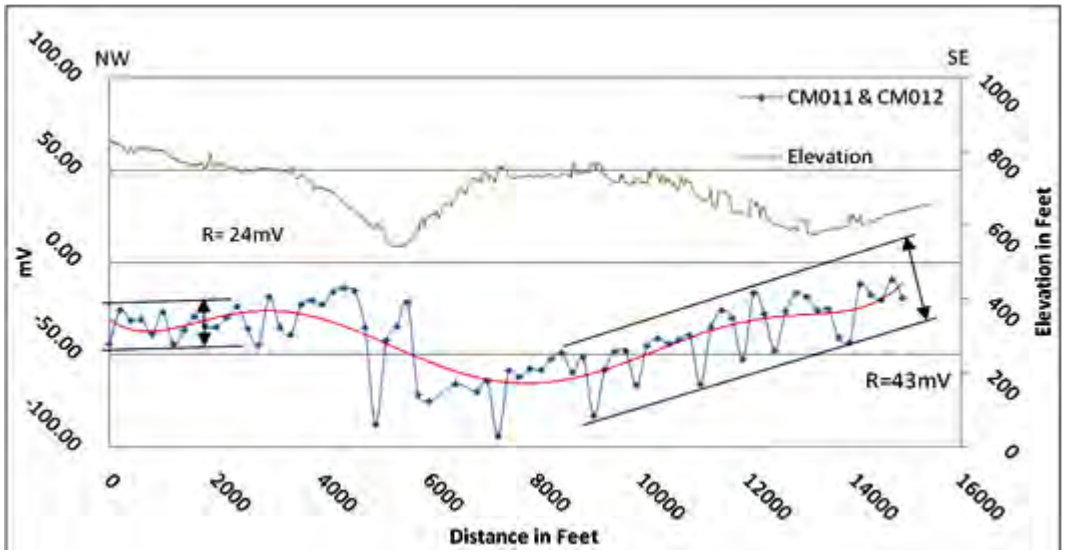

Figure 10. A comparison of SP profile B-B' across anomaly HMS-B' against the detailed elevation profile (from LiDAR data). An increase in SP data noise appears to coincide with an increase in topographic irregularity.

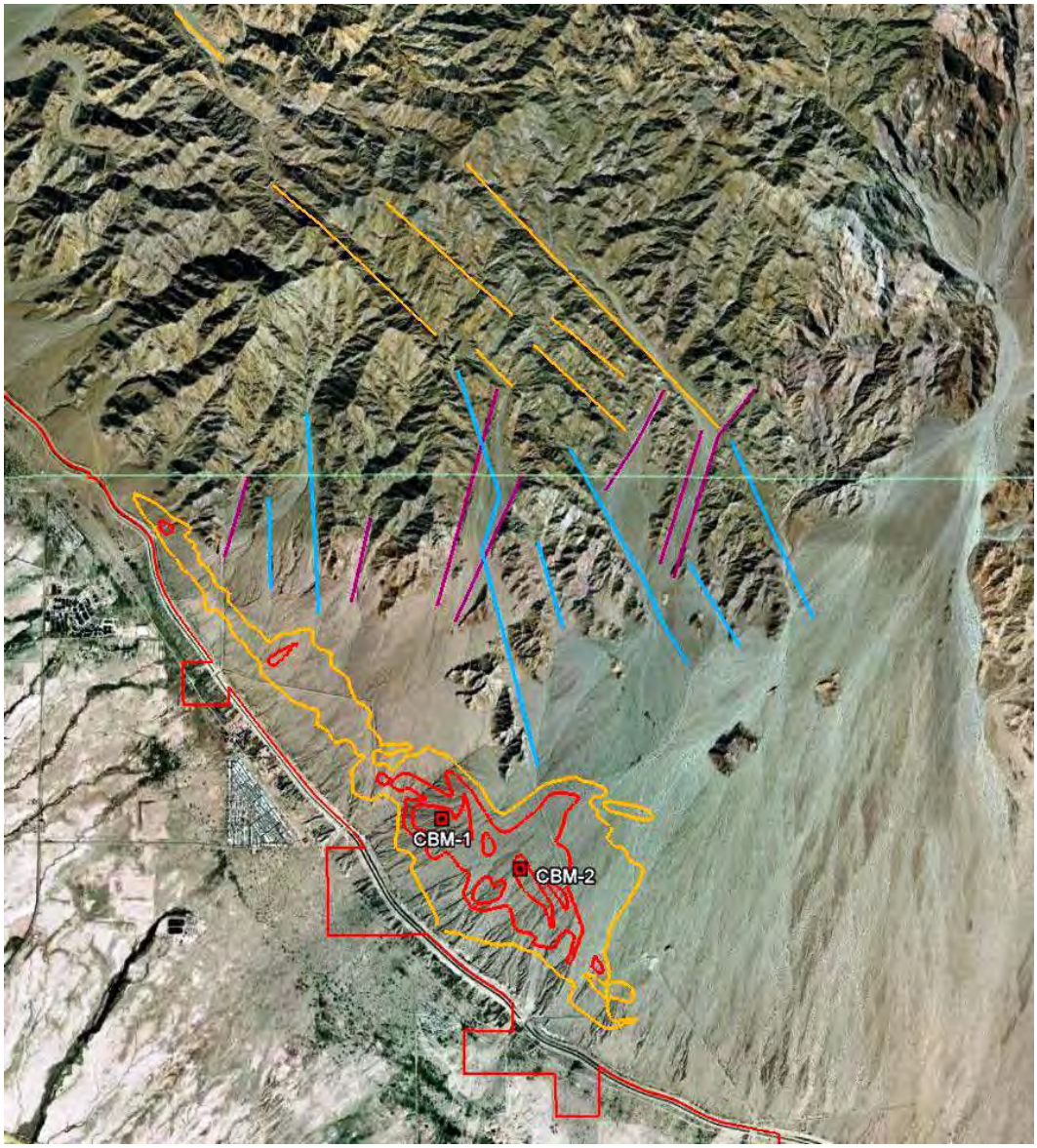

Figure 11. 2011 Intermediate-depth drilling targets, with SP anomalies and potential local structural framework.

NAVAL AIR FACILITY EL CENTRO,

IMPERIAL VALLEY,

CALIFORNIA

GEOTHERMAL RESOURCE EXPLORATION, NAF EL CENTRO – SUPERSTITION MOUNTAIN AREA, IMPERIAL VALLEY, CALIFORNIA

Steven C. Bjornstad[1], Bethiah Hall[1], Jeff Unruh[2], Keith Richards-Dinger[3]

[1]USN Geothermal Program Office, China Lake, CA
[2]William Lettis & Associates, Walnut Grove, CA
[3]Dept. of Earth Sciences, University of California, Riverside, CA 92507
e-mail: steven.bjornstad@navy.mil

Keywords
Superstition Mountain, Imperial Valley, West Mesa, geothermal, neotectonic, seismogenic, kinematic

Abstract

The geothermal potential of West Mesa has historically been assumed to be small because it is thought to be dominated by a left-stepping transpressional regime that is generally tight and not conducive to open fluid pathways. This may not be the complete picture, however. The 85 MWe Heber geothermal project appears to be located in a right stepover from the northwest trending seismogenic extension of the Cerro Prieto fault, placing it outside the Imperial-San Andreas fault system and on a separate, sub-parallel, extensional trend to the west. A similar right stepover appears to be present at Superstition Mountain where shallow drilling in the 1980's found temperature gradients exceeding 300ºC/km (17.5ºF/100 ft.). Through the use of detailed surface mapping, electrical and potential fields geophysical methods and analysis of a relocated earthquake catalog for the region, the Navy Geothermal Program Office is beginning to define the hydrothermal history and the structural and tectonic framework of this thermal anomaly and to delineate active transtensional areas and critically stressed fractures which may serve as conduits for upwelling geothermal fluids.

Introduction and Geological Background

The Superstition Mountain geothermal prospect is located in the West Mesa area of northwestern Imperial Valley, California (Figure 1) and occurs within the Shade Tree bombing and parachute range of the Naval Air Facility, El Centro. The geothermal potential of West Mesa has historically been assumed to be small because, while the central Salton Sea trough is dominated by the Imperial fault-San Andreas fault trend, a right-stepping transtensional regime that allows for the upward circulation of heat and geothermal fluids, West Mesa has been thought to be dominated by a left-stepping transpressional regime (San Jacinto, Laguna Salida and Elsinore fault zones) that is generally tight and not conducive to open fluid pathways. Recent seismotectonic studies indicate this may not be the complete picture.

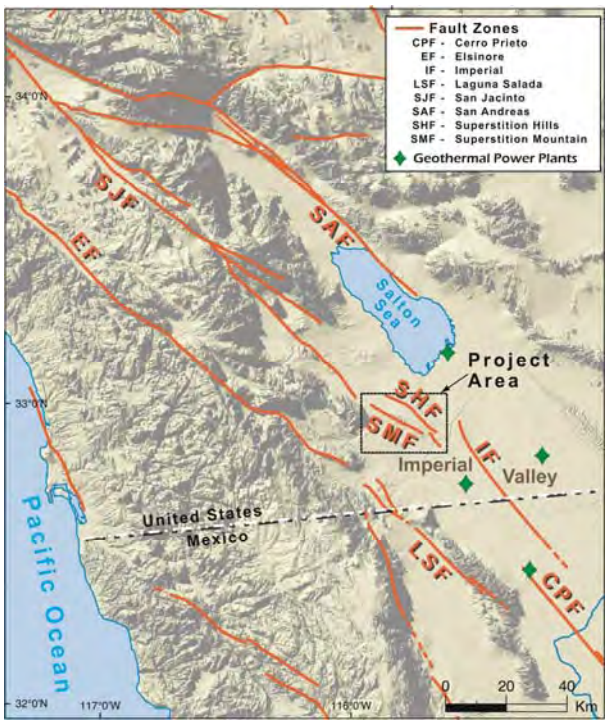

Figure 1. NAS El Centro project location and the regional structural framework.

Edmunds (1977) noted the hypothesis that current tectonic activity on the west side of Imperial Valley may be opening new heat sources there. The 85 MWe Heber geothermal project successfully operates using fluids fed from intersecting northwest trending right lateral strikeslip and northeasterly-trending normal faults (James, et al, 1987) and appears to be located in a right stepover from the northwest trending seismogenic extension of the Cerro Prieto fault (Magistrale, 2002) (Figure 2).

This evidence appears to place Heber on a structural trend outside the Imperial-San Andreas fault system and on a separate, sub-parallel, extensional trend to the west. Such a right step would be releasing, creating the critically stressed fractures found at Heber which are

optimally oriented to be open pathways for upwelling geothermal fluids.

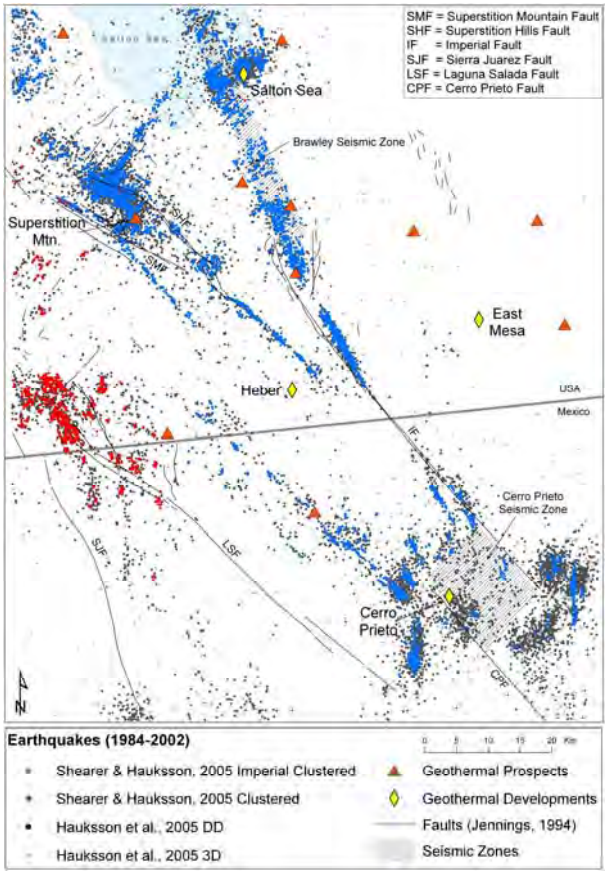

Figure 2. Plot of relocated regional earthquake catalogs relative to mapped fault zones and geothermal developments and prospects.

Further up the valley a similar, but currently more active, right step appears to be present at Superstition Mountain – one that cuts across the mapped Superstition Mountain Fault (SMF) and connects with the Superstition Hills Fault (SHF) and associated northeast trending Elmore Ranch fault. As at Heber, such a right step would allow for critically stressed fractures and upwelling of geothermal fluids. Within the Superstition Mountain prospect area shallow drilling in the 1980's indicated temperature gradients exceeding 300ºC/km (17.5ºF/100 ft.). There are no deep thermal or fluid data available for this site, so understanding the basement structure, the current state and orientation of local tectonic stresses and how these operate together to create pathways for ascending geothermal fluids are critical keys to defining the geothermal potential - and potential drilling targets - in this area.

To test this hypothesis and identify potential targets the Navy Geothermal Program Office is conducting a multi-faceted investigation consisting of: 1) analysis of local gravity survey data; 2) surface mapping of hydrothermal alteration and active (neotectonic) late Quaternary faults; 3) kinematic analysis of the seismic events catalogs to create visualizations of the seismogenic faults, the local stress field and the potentially critically stressed faults; and 4) analysis of magnetotelluric data to further characterize the seismogenic faults. Through this work we anticipate being able to connect the shallow thermal and electrical anomalies to deeper geothermal resource targets.

The geology of the project area is dominated by a granitic knob (Superstition Mountain), a Pliocene to Recent marine/lacustrine system around the mountain, and the western Imperial Valley tectonics, specifically the Superstition Mountain and Superstition Hills faults. Superstition Mountain is a northwest-southeast trending elongate feature rising abruptly above the Imperial Valley floor to a height of 231 m (759 ft) asl. It is composed primarily of pre-Tertiary (probably Mesozoic) intrusive rocks – granite, granodiorite, quartz monzonite – and is probably closely related to the Fish Creek Mountains eight kilometers (five miles) to the west. The shallow sedimentary cover consists primarily of Pliocene to Pleistocene sediments and there appears to be no evidence for an older meta-sedimentary sequence here as is present in the central region of the valley. A small section of Tertiary rocks occur on the northeast section of the mountain including a thin section of Miocene volcanics. These flows and pyroclasitics do not play a role in the geothermal potential of the prospect, however. The depth to crystalline basement in the Superstition/West Mesa area is substantially less than the central part of the valley with the boundary between the two being very sharp. Fuis, et al (1982) estimate as little as 2.1 km to basement near the south end Superstition Hills dropping quickly to 5-6 km to the southeast.

Superstition Mountain and Hills are dominated by two sub-parallel northwest-trending dextral strike-slip faults (SMF and SHF) which are part of the San Jacinto fault system to the north and connect to the Imperial Valley and/or Cerro Prieto faults to the south. It is assumed that additional northwest-trending structures are present beneath the sedimentary cover between the two. These buried structures are indicated by the subtle northwesterly patterning of topographic contours and imply a single 3 to 5 mile wide fault zone. There is also strong evidence (both in aerial orthophotos and outcrops) for northeast-trending faults striking through the mountain in several places, creating conjugate pairing with the northwesterly faults. This orientation of dominant northwesterly dextral and subordinate northeasterly sinistral faults is well defined in the Superstition Hills. On Superstition Mountain the subordinate northeasterly structures appear to be sinistral as well.

Superstition Mountain is located in a region of significant seismicity. In 1987 a magnitude 6.2 earthquake occurred on the (previously unmapped) northeast-trending sinistral strike-slip Elmore Ranch fault, followed less than 12 hours later by a magnitude 6.6 event on the SHF resulting in significant surface rupture in the Hills, but little apparent movement on the adjacent SMF (Faneros, 2005). Shearer, et al (2005) and Hauksson and Shearer (2005) obtained precise relative locations for over 340,000 southern California earthquakes between 1984 and 2002, many of them in the Superstition area (Figure 2). Results of a kinematic analysis of these data are described below.

The presence of a thermal anomaly at Superstition Mountain has been known for many years. The USGS heat flow database lists a well (SUPR) which is located near the southeast end of Superstition Mountain and has a thermal gradient of 64°C/km, while one zone along the northeast flank of Superstition Mountain has a calculated thermal gradient exceeding 300ºC/km (17.5ºF/100 ft.) based on shallow temperature gradient drilling done by Chevron in the 1980's. California Department of Oil and Gas drilling records and information provided to the Navy by Layman Energy Associates corroborate the existence of this second anomaly (Figure 3), which is generally elongate northwesterly on the northeastern flank of the mountain and the broad valley that separates it from the Superstition Hills to the north. These areas are part of the Shade Tree bombing range, and are under Navy jurisdiction.

Geothermal Investigations

A 2003 electrical survey conducted by Innovative Technical Solutions, Inc for the Navy resulted in the identification of an 120 mV SP anomaly (ITSI, 2003) over Quaternary to Recent sediments about 450 m (1500 ft) north of granite outcrops of Superstition Mountain (Figure 3). The anomaly is elongate sub-parallel to the range front, with a half-amplitude length of about 1800 m (5900 ft) and a half-amplitude width of about 500 m (1600 ft). The considerable elongation of the anomaly suggests a SP source associated with covered faults and fractures. The data suggest a fairly shallow (~150 m (500 ft) deep) SP source area. The source of the SP anomaly may not be a geothermal system or upflow zone, however, this interpretation is very permissive given the dimensions and shape of the anomaly, the location near other geothermal systems, and spatial association with the Chevron thermal anomaly.

Through reconnaissance mapping, we have also documented the presence of a previously unmapped northwest-striking, northeast-dipping range-front fault (SMFF) along the northeastern flank of Superstition Mountain that marks the contact between the bedrock and the Quaternary to Recent sediments. This fault is associated with a moderately well-expressed northeast-facing bedrock escarpment that can be traced for about 1.25 km (0.8 mi) southeast along the mountain front. It is coincident with the thermal and SP anomalies and appears to be the extension of a previously mapped short splay from the main trace of the Superstition Mountain fault. The range-front fault shows clear evidence of hydrothermal alteration and mineralization and, as described below, also shows clear evidence of neotectonic activity.

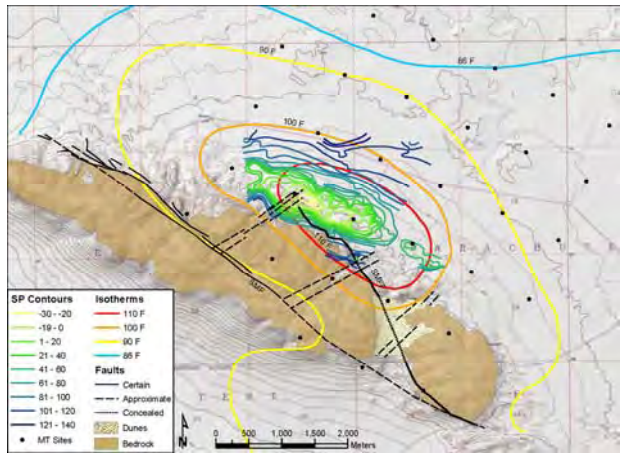

Figure 3. Superstition Mountain thermal and self-potential electrical anomalies, magnetotelluric survey stations, and the generalized geology and structure of the mountain, including the northwest-trending active range-front fault.

A gravity and magnetics survey consisting of 112 km (70 mi) of transects was conducted in December 2004. (Due to a magnetometer malfunction, the magnetic data were subsequently excluded from this analysis). The gravity survey data were processed and various corrections applied to obtain the simple Bouguer, complete Bouguer, and isostatic residual grids. The resulting gravity maps show a small, but prominent, gravity high associated with Superstition Mountain. The bulk of this high is shifted, in a parallel fashion, approximately 1100 m (3600 ft) to the northwest (Figure 4) and may be interpreted as shallow basement dipping gently away from the northeast side of the mountain contrasted by a sharp break and a significant down-dropping of the basement on the southwest side of the mountain. Additional detail on the gravity high appears to be related to prominent faults – both mapped and inferred - reflecting the broken, blocky nature of this small granitic knoll and it may, in part, be a product of localized cementing of sediments by mineralizing fluid at depth.

Three cross-sections were modeled using the gravity data and based initially on the Dibblee (1984) geologic cross-section, the refraction seismic analysis of Fuis and

Kohler (1984), including their velocity model used in the Superstition area, plus published fault maps and recent fault mapping described in this paper. The cross-sections all have a reasonable fit (~0.5 mgal error) when the sedimentary beds extend no deeper than about 3 km (10,000 ft). Section A-A' (Figure 5) is representative of the three sections and was oriented in a northeast-southwest direction in order to perpendicularly cut the apparent dominant northwest-trending fabric of the Superstition Mountain/Superstition Hills area, as well as, the previously mapped temperature and SP anomalies.

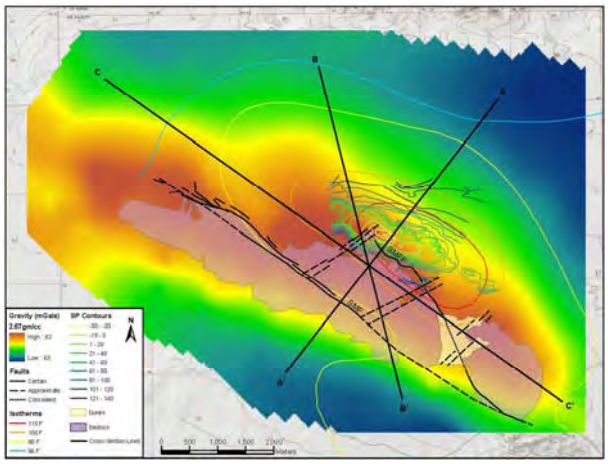

Figure 4. Superstition Mountain isostatic residual gravity map showing cross-section locations.

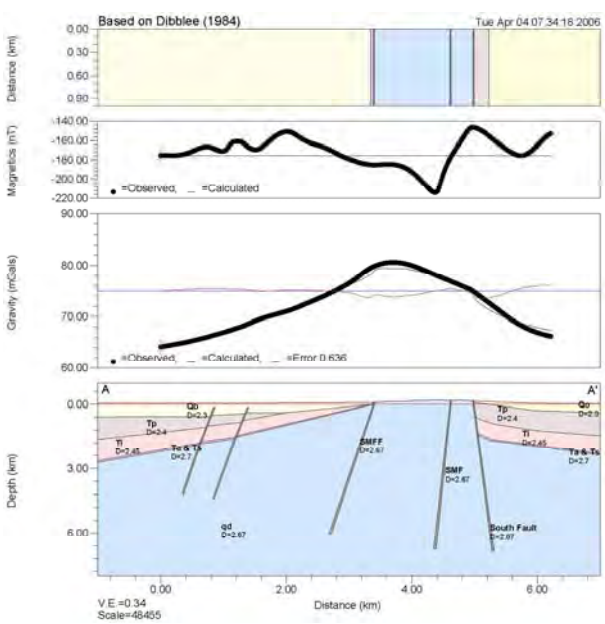

Figure 5. Gravity cross-section A-A'

At the northeastern extent of the gravity survey area, the beds in the model are extended down to about 3 km, whereas in Dibblee's model they extend no deeper than about 1.3 km. However, a large fit error (>1.50 mgals) occurred when the basement was placed above 1.3 km. A much smaller fit error (0.636 mgals) remained after increasing the thicknesses of the sedimentary units to more closely match the sedimentary section of an oil and gas drill hole (~8750 ft deep) located about four miles to the east-northeast of the project area (Loeltz, et al, 1975). Plus, the overall fit of the model is best when the sedimentary column is thickened rather than made denser.

This best-fit model is relatively simple, but it is consistent with the available geologic data. None of the subsurface geologic/geophysical data for the project area are tightly constrained, however the model is consistent with the mapped faulting, as well as, the extent of surface exposure and the generally expected regional distribution and range of thicknesses of the Tertiary to Recent sediments and the density contrast between these and the bedrock. The model is also generally consistent with the refraction seismic interpretation of Fuis and indicates that granitic basement is shallow in the area of the thermal and electrical anomalies and that both conjugate and additional *en-echelon* structures are permissive between the major northwest-trending Superstition structures.

A 3-D analysis of the relocated earthquake catalog identified several distinct seismogenic faults in the Superstition area. Planar alignments of the relocated seismicity define a number of faults in the study area, some of which clearly correspond to previously mapped faults on the surface and others which do not. For our current purposes, the most interesting are: 1) the lineament (L1 of Magistrale, 2002) SW of the mapped surface trace of the SE end of the SMF; 2) an ENE trend of seismicity crossing beneath the southeastern end of Superstition Mountain towards the broad valley NE of the mountain; and 3) a broad, NW trending cluster of seismicity underlying this valley between Superstition Mountain and the Superstition Hills. The seismicity in the lineament L1 defines a steeply dipping (80 deg to the SW) plane which strikes approximately 25 degrees more northerly than the main mapped surface trace of the SMF. The seismicity in this lineament shallows abruptly at its NW end to merge with the seismicity in the ENE trend. Its geometry in map view somewhat suggests a releasing step transferring some of the slip from the southern SMF to the Superstition Hills Fault (SHF). The seismicity underlying the valley between Superstition Mountain and the Superstition Hills seems to form a zone of subparallel, NW striking, subvertical dextral faults and on NE-striking sinistral faults. The low hills in the center of the valley may be neotectonic landforms associated with the seismogenic faults at depth.

The planar alignment clusters were combined with other, spatially distinct, clusters of earthquakes. The focal

mechanisms of these events were inverted for stress and strain with the results shown in Figure 6 as the vertical stress ratio. The results show that the Imperial Valley-San Andreas trend is predominantly strike-slip faulting with the maximum compressive stress subhorizontal and striking N20E. In general, the stress and strain states in the western side of the Imperial Valley (including our study area) are similar but rotated approximately 35 degrees counter-clockwise so that the maximum compressive stress strikes N15W. However in the Superstition Mountain area itself (and to a lesser extent the area between Superstition Mountain and the Superstition Hills) there are signs of significant heterogeneity in the stress and strain states, both between small groupings of seismic events and within individual groups. Small areas of apparent crustal thickening are adjacent to areas of apparent crustal thinning implying a dynamic state of strain and a mixed transtensional and transpressional tectonic environment.

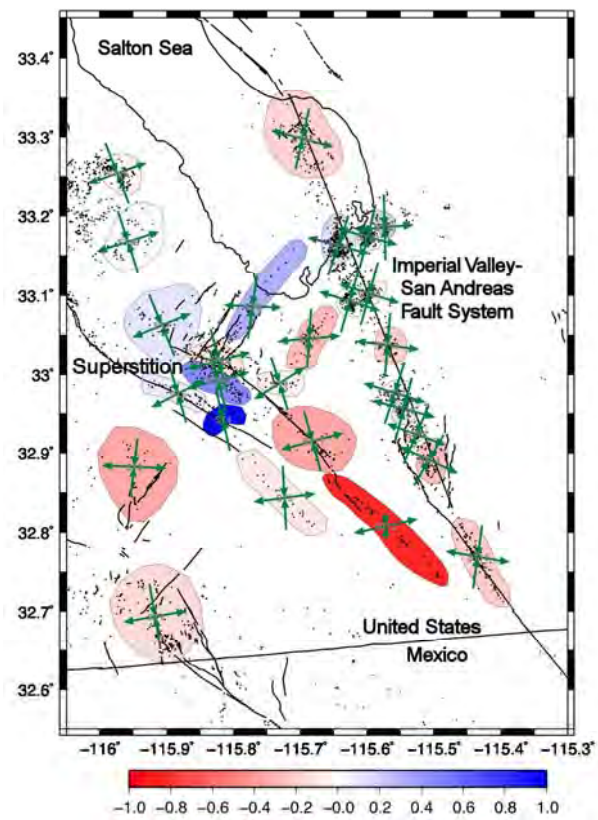

Figure 6. Earthquake clusters and vertical stress ratios. This is the ratio of the vertical stress to the maximum extensional stress. Negative (red) values indicate crustal thinning and positive (blue) values crustal thickening.

Reconnaissance neotectonic mapping along the southern portion and northeast side of Superstition Mountain and the broad valley to the north confirmed the active nature of the range-front fault (SMFF) through a series of Quaternary to Recent up-lift/erosion cycles. The rate of normal separation on this fault appears to be at least 1-2 mm/yr (Unruh, J.R., 2006).

Based on the map-scale pattern of surface faulting, the SMF through the mountain is comprised of at three geometric segments that exhibit a left-stepping *en echelon* pattern. The southern segment of the fault splays or steps north-northwest, projecting NNW and emerging along the northeastern flank of Superstition Mountain as the range-front fault (SMFF). Displacement appears to die out to the northwest and is likely transferred in a left en echelon step to the main trace of the SMF. The SMFF strikes more toward the north than the main fault, suggesting that it is kinematically distinct. Kinematic analysis of earthquake focal mechanisms from the Superstition Mountain area indicates that the style of deformation is dominantly strike slip, and that the direction of regional right-lateral shear strain is oriented approximately N60°W. The central segment of the Superstition Mountain fault strikes about N55°W, and thus is optimally oriented to accommodate strike-slip faulting, not transpression as is commonly assumed in the literature. The SMFF strikes about N26°W, nearly normal to the direction of the maximum extensional principal strain obtained from the focal mechanism inversion (i.e., N76°E), and thus is optimally oriented to accommodate extension and normal faulting in the modern seismotectonic setting. As stated above, the temperature and SP anomalies are associated with this fault.

It is not clear if transfer of slip is occurring from the SMFF to the seismogenic faults, or if the seismicity is more directly associated with the Superstition Hills fault. Any transfer of slip from the SMFF to the seismogenic faults in the valley would be right step, and thus potentially a releasing geometry relative to the direction of regional NW right-lateral shear. The SMFF has a releasing geometry relative to regional dextral shear, and thus is locally "transtensional" in the vicinity of the SP and temperature anomalies. Also, it is possible that some slip is transferred from the southern segment of the Superstition Mountain fault to the system of seismogenic faults in the valley to the east, which would be a right, releasing transfer in the regional NW dextral tectonic regime. The SMFF dips toward the temperature and SP anomalies. If the average dip of the SMFF at depth is comparable to the dip observed at the surface (about 55-60°), then the intersection of the fault and the source of the anomalies is at a depth of less than 1000 m.

Conclusions and Further Work

Through a combination of mapping, electrical and potential fields methods, and seismicity and kinematic analysis, we have begun to define the hydrothermal history and the structural and tectonic framework of the thermal anomaly at Superstition Mountain. A significant

SP anomaly has been defined within the heart of the thermal anomaly and there is clear evidence for an active range-front fault adjacent to it on the northeast side of the mountain. We interpret that the range-front fault is a segment of the Superstition Mountain fault, and that it has a more northerly strike than the main sections of the fault. While this geometry is not a true releasing stepover, the more northerly strike is a releasing geometry relative to the direction of regional NW dextral shear in the southwestern Imperial Valley. The rate of normal separation on the southern segment is at least 1-2 mm/yr, and the fault dips northeast toward the temperature and SP anomalies. Based on the observed dip of the fault at the surface, it predictably would intersect the source of the anomalies in the upper 1 km (3300 ft) of the crust.

Future work will include determining focal mechanisms for additional events in the project area in order to better characterize the stress/strain heterogeneity recognized here. A reduction of the heterogeneity will allow for a more detailed characterization the dynamics of this translational tectonic environment and a differentiation of the critically stressed faults within it. In addition, in early 2006, MT data were acquired at 31 stations on an ~1000 meter grid (Figure 3) in order to image the resistivity structure of the study areas using one-dimensional (1D) and two-dimensional (2D) inversions techniques, and to represent this structure using grids of 2D depth models. A contract is in place for the data analysis and modeling, with the work to be completed by December, 2006. It is anticipated that the MT analysis will provide sufficient detail to the resistivity structure to link surface and near-surface anomalies and the deep seismogenic structure.

References

Dibblee, T.W. Jr., 1984, Stratigraphy and Tectonics of the San Felipe Hills, Borrego Badlands, Superstition Hills and Vicinity (mapped 1954), *in* The Imperial Basin Tectonics, Sedimentation and Thermal Aspects, Rigsby, C.A., ed., Society Economic Paleontologists & Minerologists Pacific Section, Los Angeles, CA, p. 31-44.

Edmunds, S.W., 1977, Geothermal Development in Imperial County, Geothermal Resources Council Transactions, v. 1, p. 81-83.

Faneros, G., 2005, Structure and Neotectonics of the Superstition Mountain Fault, Imperial County, California, Masters Thesis, San Diego State University.

Fuis, G.S., W.D. Mooney, J.H. Healey, G.A. McMecham and W.J. Lutter, 1982, Crustal Structure of the Imperial Valley Region, *in* The Imperial Valley, California, Earthquake of October 15, 1979, United States Geological Survey Professional Paper 1254, p. 25-50.

Hauksson, E., and P. Shearer, 2005, Southern California Hypocenter Relocation with Waveform Cross-correlation, Part 1, Results using the Double-Difference Method, Bulletin of the Seismological Society of America, v. 95, n. 3, p. 896-903.

Innovative Technical Solutions, Inc., 2003, Geothermal Energy Resource Assessment on Military Lands, final technical report submitted to the US Navy Geothermal Program Office, Contract No. N68936-02-R-0236.

James, E.D., V.T. Hoang and I.J. Epperson, 1987, Structure, Permeability and Production Characteristics of the Heber, California Geothermal Field, PROCEEDINGS, 12th Workshop Geothermal Reservoir Engineering, Stanford University, SGP-TR-109, p. 267-271.

Loeltz, O.J., B. Irelan, J.H. Robinson and F.H. Olmsted, 1975, Geohydrologic Reconnaissance of the Imperial Valley, California, United States Geological Survey Professional Paper 486-K, 52p.

Magistrale, H., 2002, The Relations of the Southern San Jacinto Fault Zone to the Imperial and Cerro Prieto Faults, *in* Barth, A., ed., Contributions to Crustal Evolution of the Southwestern United States: Geological Society of America Special Paper 365, p. 271-278.

Shearer, P., Hauksson, E., and Lin, G., 2005, Southern California Hypocenter Relocation with Waveform Cross-Correlation, Part 2: Results using Source-Specific Station Terms and Cluster Analysis, Bulletin of the Seismological Society of America, v. 95, n. 3, p. 904-915.

Treiman, J.A., 1989, Superstition Hills, Superstition Mountain, and related faults: California Division of Mines and Geology Fault Evaluation Report FER-207, 21 p.

Unruh, J.R., 2006, Results of Neotectonic Reconnaissance, Superstition Mountain, NAFEC, William Lettis & Associates, Inc. letter report to US Navy Geothermal Program Office under contract N68936-04-C-0072.

Geothermal Exploration Activities, Including Intermediate Depth Temperature Gradient Drilling, at the Naval Air Facility, El Centro, California

Andy Tiedeman, Steven Bjornstad, David Meade, Michael Lazaro, Andrew Sabin, Steve Alm

U.S.N. Geothermal Program Office, China Lake, CA 93555

Keywords
Superstition Mountain, Imperial Valley, Geothermal, U.S. Navy, Exploration

Abstract

The US Navy Geothermal Program Office (GPO) is conducting geothermal energy exploration adjacent to Superstition Mountain in western Imperial Valley, California, within the Target 101 bombing range of the Naval Air Facility, EI Centro. Shallow temperature gradient drilling (~600 feet (~183m)) completed by Chevron in the early '80's indicated higher than background temperature gradients along the northeast side of Superstition Mountain. Exploration activities conducted by the Navy over the past few years indicates that this thermal anomaly appears to coincide with an active transtensional right stepover occurring between the parallel northwest trending Superstition Mountain fault and the Superstition Hills fault to the north. Critically stressed fractures appear to serve as conduits for upwelling geothermal fluids.

Based on the earlier shallow drilling, detailed geologic mapping, seismogenic fault mapping and stress analysis, and a variety of geophysical surveys, including gravity and magnetic, self-potential electrical and magneto-telluric, the Navy sited two moderate depth test holes on this target. These were completed in December 2008 confirming the existence of a moderate temperature anomaly with temperatures reaching approximately 186°F (85.6°C) at less than 2300 feet. This thermal anomaly coincides with hydrothermal alteration in both Pliocene sediments and Miocene volcanics intersected by the test holes.

A third slim test hole is planned for 2010 and is designed to explore the heart of the thermal and SP anomalies, as well as the down-dip extension of the northwest-trending range-front fault and a conjugate structure extending northeastward from Superstition Mountain.

Introduction and Geological Background

The Superstition Mountain geothermal prospect is located in the West Mesa area of northwestern Imperial Valley, California *(Figure 1)* and occurs within the Shade Tree bombing and parachute range of the Naval Air Facility, El Centro (NAFEC). The range is mostly flatland immediately north-northeast of Superstition Mountain but overlaps onto the mountain. It is a primary inert bombing practice range for Navy and Marine Corp aviators, and is also the winter training range for the Navy's Blue Angels aerial exhibition team.

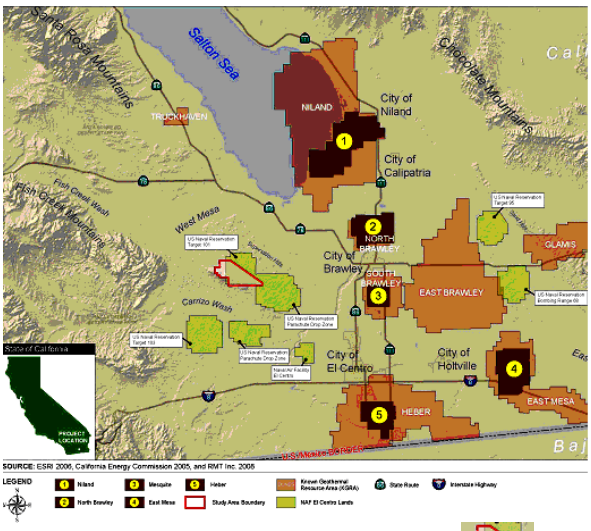

Figure 1: NAS El Centro project location:

The dominant physiographic feature within the project area is Superstition Mountain which trends northwest-southeast and rises to a height of 759 ft (231m) asl above the Imperial Valley floor and composed mostly of pre-Tertiary intrusives of granite, granodiorite, and quartz monzonite. Occurring in the northeast section of the mountain is a small section of Tertiary rocks including some Miocene volcanics. In the area surrounding the mountain and lower lying playa is primarily a Pliocene to recent marine/lucustrine system consisting of Pliocene to Pleistocene sediments (Bjornstad et al, GRC 2006).

There has been a history of significant seismic activity in the region where Superstition Mountain is located. Between the period of 1984 to 2002, Shearer, et al (2005) and Hauksson and Shearer (2005) collectively acquired precise relative locations in excess of 340,000 southern California earthquakes, many occurring near the Superstition area (*Figure 2*). Within the Superstition project area are two significant sub-parallel northwest-trending dextral strike-slip faults, the Superstition Mountain fault and the Superstition Hills fault. The faults are part of the San Jacinto fault system to the north and connect to the Imperial Valley and/or Cerro Prieto faults to the south (Bjornstad et al, GRC 2006).

The depth to crystalline basement within the Superstition/West Mesa area is thought to be much less than the rest of the valley, estimated by Fuis, et al (1982) to be approximately 2.1 km (1.3 miles) near the south end of Superstition Mountain. Drilling records from the California Department of Oil and Gas and information provided to the Navy by Layman Energy Associates, indicate the presence of a thermal anomaly located near the northeast flank of Superstition Mountain. This is indicated from shallow temperature gradient holes drilled by Chevron in the 1980's with a calculated temperature high of 300°C/km (17.5°F/100 ft) (Bjornstad et al, GRC 2006).

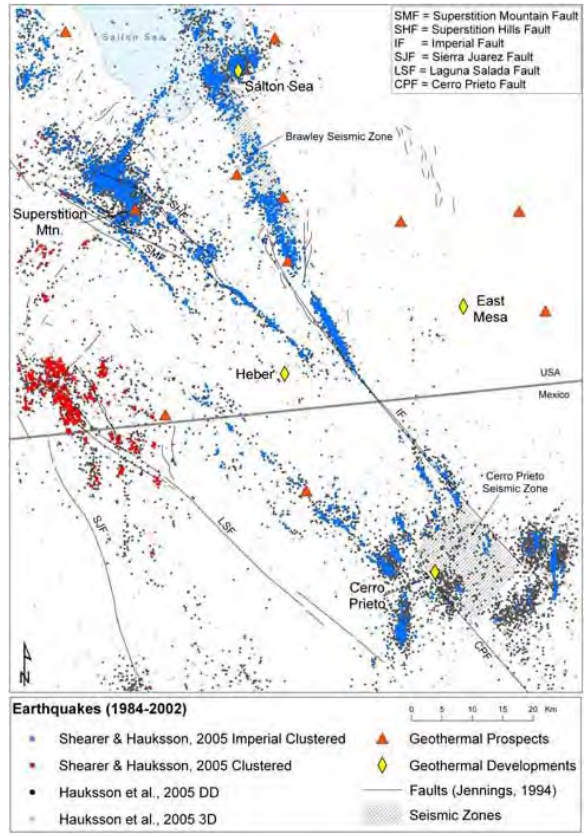

Figure 2. Plot of relocated regional earthquake catalogs relative to mapped fault zones and geothermal developments and prospects.

Previous Ivestigations:

The GPO started exploration work at NAFEC after initial information was provided by Layman Energy Associates in late 2001. Geothermal data has since then, been accumulated by various organizations contracted by the Navy as well as the GPO. Beginning with an electrical survey that Innovative Technical Solutions, Inc conducted resulting in the identification of an 120 mV SP anomaly (ITSI, 2003) within the project area.. Reconnaissance mapping was performed and a previously unmapped northwest-striking, northeast-dipping range-front fault (SMFF) was discovered, marking the contact point between the bedrock, Quaternary to recent sediments as well as

hydrothermal alteration and mineralization being observed (Bjornstad et al, GRC 2006).

With the use of a geologic cross section based initially from Dibblee (1984), published fault maps and recent fault mapping, refraction seismic analysis of Fuis and Kohler (1984), which included their velocity model used in the Superstition area, and gravity/magnetics data gathered, a cumulative of three cross-sections were modeled. Using these cross-sections, a best fit model was put together (Loeltz, et al, 1975). The model produced was consistent with mapped faulting, the extent of surface exposure, generally expected regional distribution as well as being generally consistent with the refraction seismic interpretation of Fuis. (Bjornstad et al, GRC 2006).

A 3-D analysis of the relocated earthquake catalog identified several distinct seismogenic faults in the Superstition area. Planar alignments of the relocated seismicity defined a number of faults and some of the more intriguing were the lineament (L1 of Magistrale, 2002) southwest of the mapped surface trace of the south-eastern end of the Superstition Mountain Fault and a northwest trending cluster of seismicity underlying this valley between Superstition Mountain and the Superstition Hills. The planar alignment clusters were combined with other spatially distinct, clusters of earthquakes. The mechanisms of these events were inverted for stress and strain (*Figure 3*) (Bjornstad et al, GRC 2006).

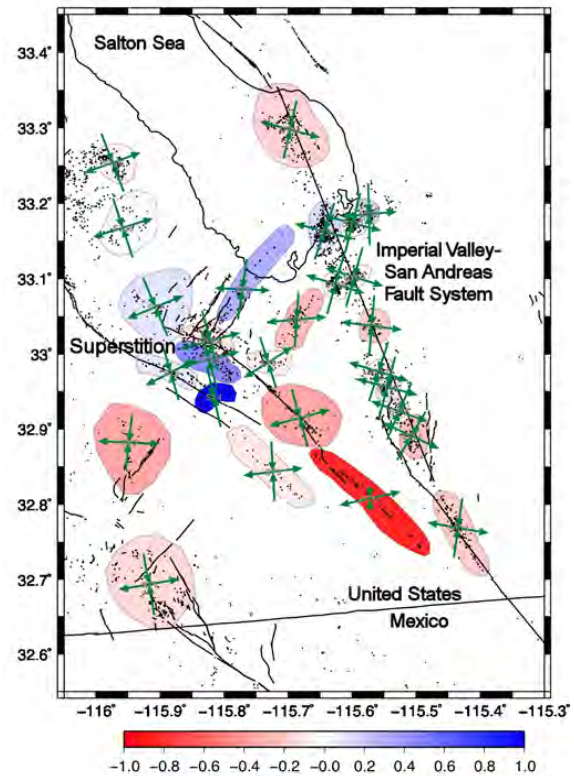

Figure 3: Earthquake clusters and vertical stress ratios. This is the ratio of the vertical stress to the maximum extensional stress Negative (red) values indicate crustal thinning and positive (blue) values crustal thickening.

Geothermal Investigations

Magnetotelluric

A magnetotelluric (MT) survey at the NAFEC geothermal prospect was contracted out to Cumming and Mackie through Solicitation Number N68936-06-T-0115 in early 2006 by the

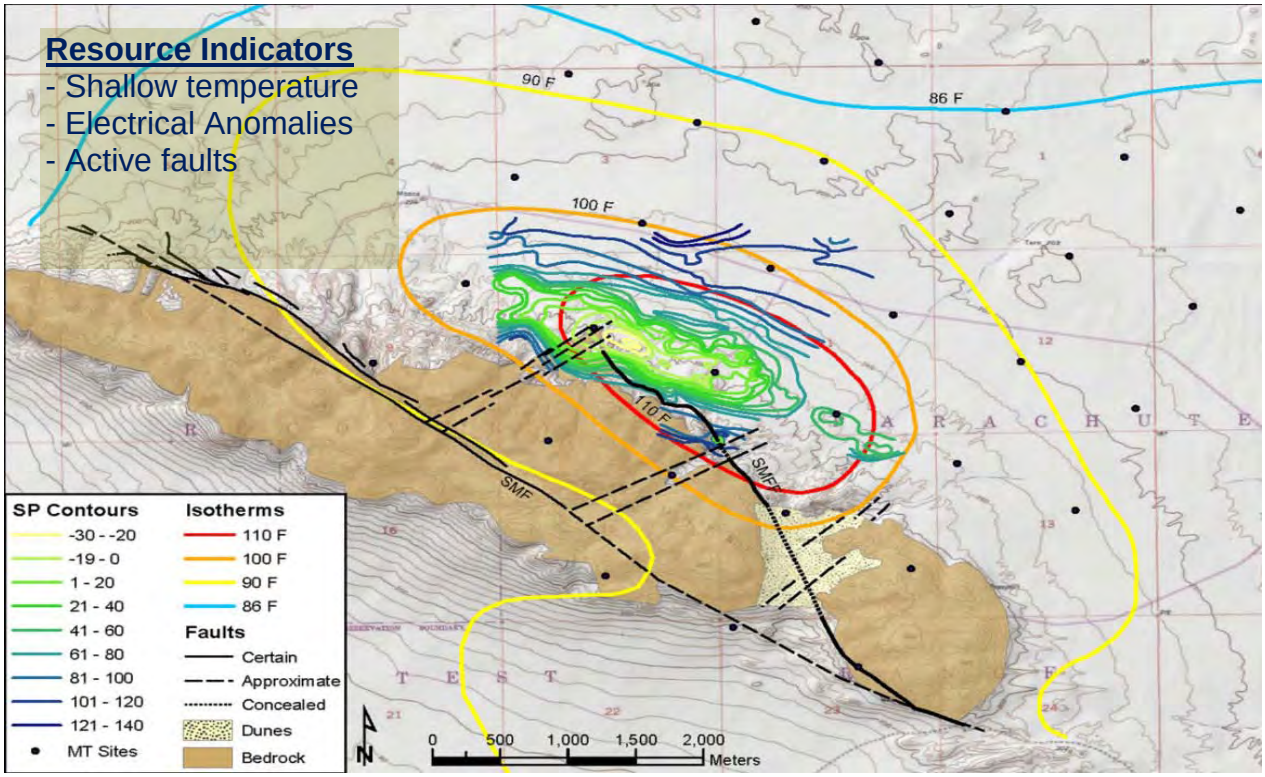

Figure 4
Superstition Mountain thermal and self-potential electrical anomalies, magnetotelluric survey station, and the generalized geology and structure of the mountain, including the northwest-trending active range fault (Bjornstad et al, GRC 2006).

GPO and completed and reported on in April 2007. A survey of a total 31 MT stations were analyzed and imaged in 1D and 2D as specified by the GPO. The data collected was to image major structural features at depth where geothermal fluids could possibly be present or where signs of geothermal alteration are apparent. The MT results were also integrated with gravity and other related geoscience data including temperature gradient information from holes drilled by Chevron into a coherent model to effectively target 4000' temperature gradient holes to assist in the exploration of a developable geothermal resource (*Figure 4*).

Through an interpretation of the integrated MT data as well as the other geoscience data of gravity, heat flow, geology, structure, SP and alteration information, a number of conclusions as to the possibilities of a geothermal resource at NAFEC are supported. From these conclusions, the most likely source for a developable resource may be the sediments. The MT data also detected two low resistivity features that could possibly be associated with sedimentary clays altered by hydrothermal fluid in sub-surface aquifers. During the study and from the information gathered it was decided to illustrate a resource conceptual model using isotherm patterns rather than of specific temperatures (Cumming and Mackie, 2006). However, it is also noted in the final report that, "the deep circulation along faults in relatively hot granite may be the ultimate source of the heat of a NAFEC geothermal resource,…" (Cumming and Mackie, 2006). By integrating the MT results with gravity and other related geosciences data reported in Bjornstad et al. (2006) and Hall and Bjornstad (2005), as well as the conceptual model that is illustrated (*Figure 5*), the GPO was able to effectively target two moderate depth exploratory geothermal test wells to explore for a developable geothermal reservoir at NAVFEC.

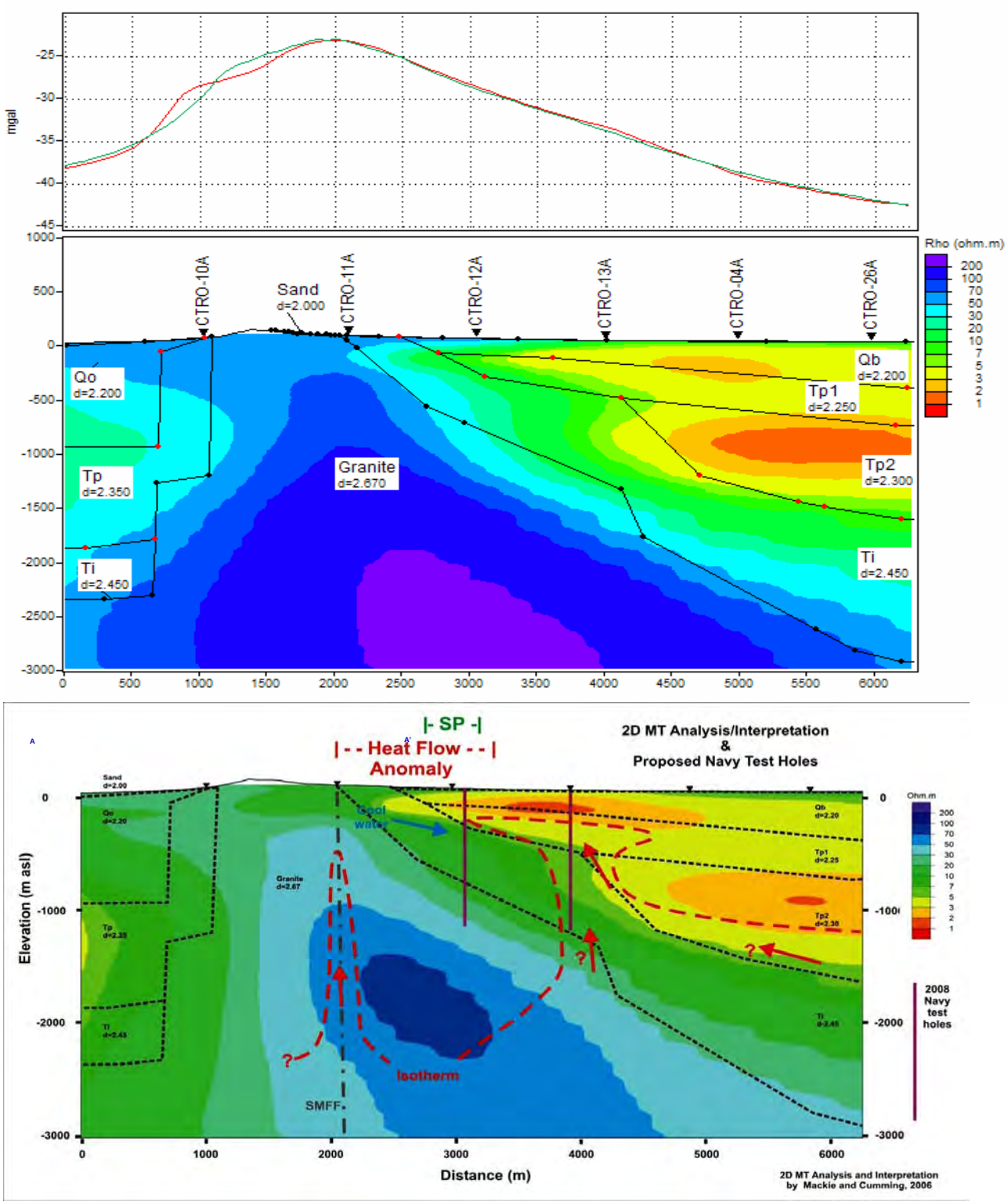

Figure 5:
NAVFEC profile: MT resistivity cross-section with gravity model. The upper 2D MT inversion image is derived from static stripped data; the lower one from 2D static corrections of MT at 115° azimuth. Due to the differing approaches to correcting static and dimensional distortion, the average resistivity of the images differs. However, the pattern is similar. Several geothermal resource conceptual elements are shown in the lower image (Cumming and Mackie,2006). The figure also shows Navy test hole locations.

Deep Drilling:

With the analysis of geophysical data gathered during 2006 and earlier, the Navy GPO revealed a possible resource at the Superstition Mountain area. Two moderate to deep wells were determined to be the next logical decision in going forward. In 2007, the GPO proposed to drill two moderate depth exploratory geothermal core test wells at NAF El Centro within the Shade Tree bombing and parachute range. These test wells were to be drilled to 3,000 feet with an option to go to 4,000 feet. Thermasource was then contracted by the GPO in mid 2008 to drill two moderate to deep wells in order to determine if a viable resource was present.

With the information that has been gathered through various geophysical studies as well as utilizing the shallow temperature gradient holes that were drilled by Chevron in the late 1970's and early 1980's which indicated higher than normal temperature gradients in the area, Navy GPO holes NAFEC 1 and NAFEC 2 were strategically located and drilled (*Figure 6*). The test holes were sited on the north-eastern side of Superstition Mountain and within the profile data gathered through MT, gravity, and SP as well as the isotherm profile which had been obtained from Layman Energy Associates through the temperature gradient holes drilled by Chevron.

The drilling of NAFEC 1 commenced on August 2nd, 2008 and was completed to a depth of 2,321 feet on November 5th, 2008. Bottom hole temperatures of a maximum 170.7° F. were measured by the GPO in April of 2009. NAFEC 2 began drilling of the test hole on November 8th, 2008 and was drilled to a total depth of 2682 feet, but was only able to be fully completed with temperature gradient tubing to a total depth of 2,168 feet in late December 2008. Bottom hole temperatures of this hole reached 186.6° F at 2168'.

Once drilling was completed and allowed to equilibrate, the Geothermal Program Office returned to NAFEC 1 and 2 in April of 2009 to measure and gather the temperature gradient information within the test holes. Temperature gradient profiles were then compiled and

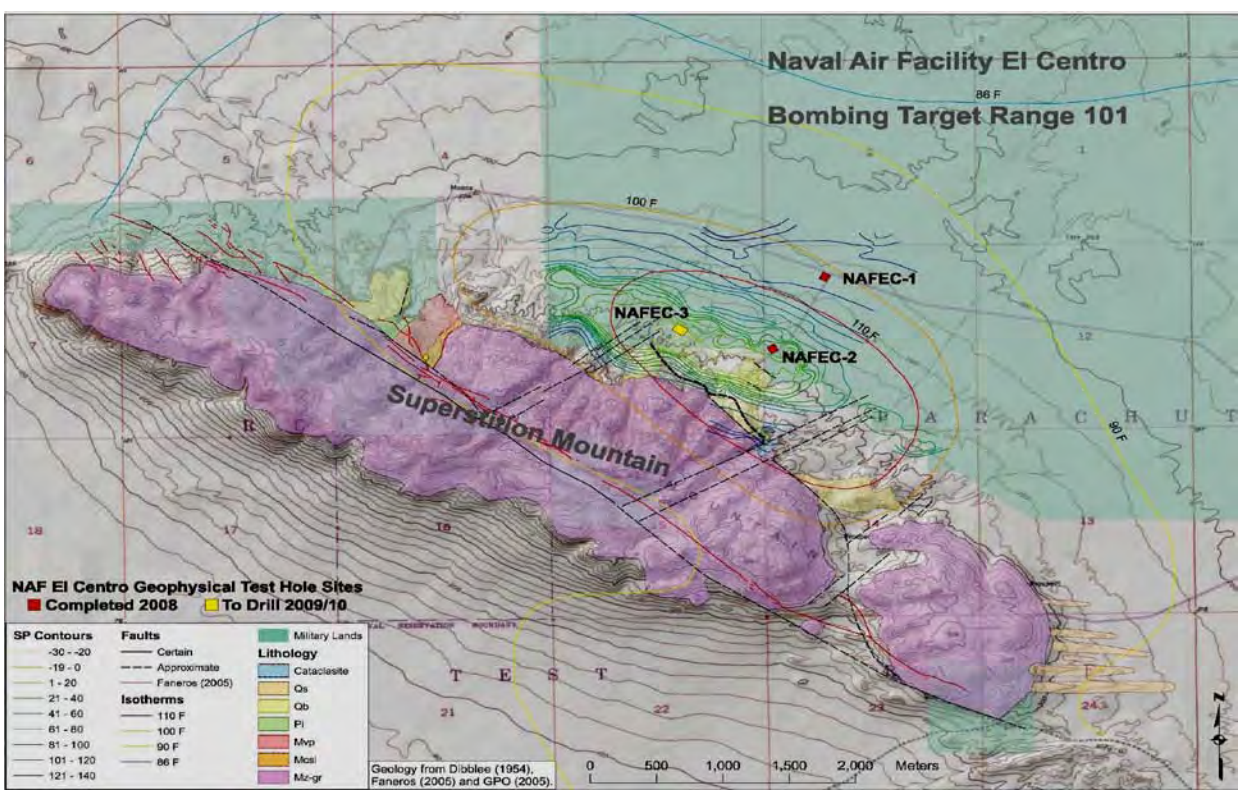

Figure 6

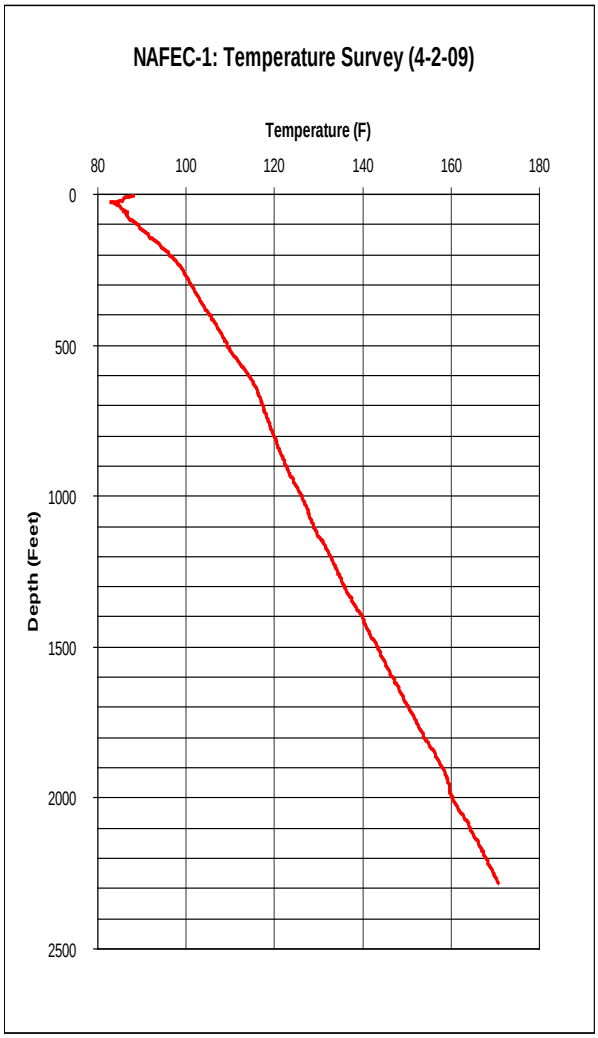

Figure 7: NAFEC 1 Temperature Survey

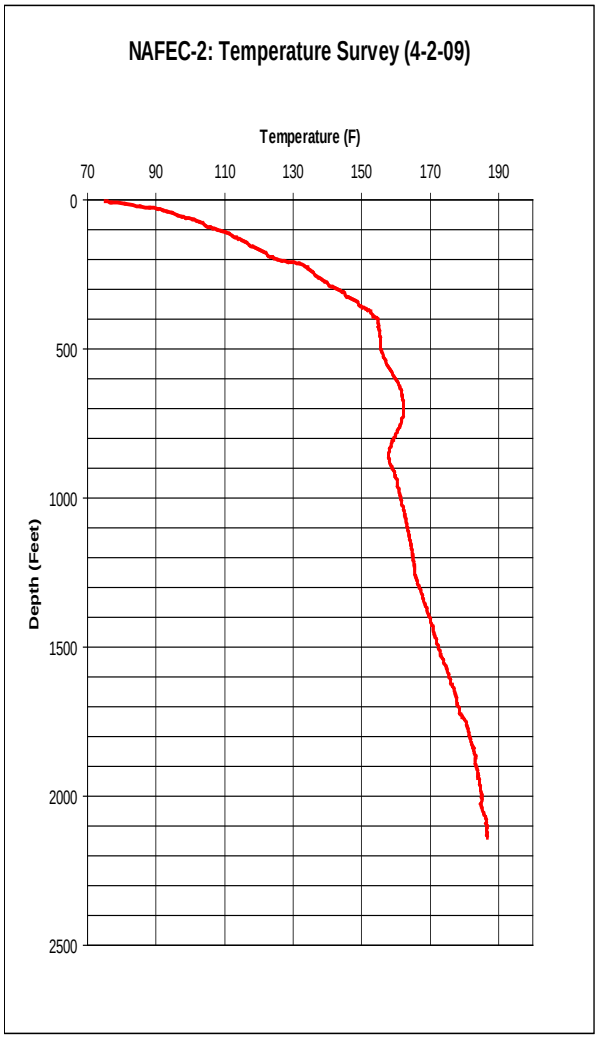

Figure 8: NAFEC 2 Temperature Survey

graphed (*Figure 7 & 8*). NAFEC 1 which was drilled further from Superstition Mountain than NAFEC 2, has a fairly linear profile. NAFEC 2 on the other hand, is warmer as well as being located within closer proximity to Superstition Mountain and shows a more non-linear profile. As these two test holes show promising results, the GPO will be drilling a third moderate depth test hole NAFEC 3 during 2010 to early 2011. See figure 6 for location of future test hole.

Conclusions and Further Work

The potential discovery of a geothermal resource at NAF El Centro is becoming more defined through our previous works as well as our recent moderate or deep exploration geothermal core test that were completed late 2008. The hydrothermal history, the structural and tectonic framework of the thermal anomaly at Superstition Mountain continues to become more apparent. The reported analysis of an MT survey that was combined with other geosciences such as gravity and SP, provided a resource conceptual model that best concluded that a developable resource may be within the sediments. The MT data also detected two low resistivity features that could possibly be associated with sedimentary clays altered by hydrothermal fluid in sub-surface aquifers. However, the ultimate source of heat could be from deep circulation along faults in relatively

hot granite. The moderate depth drilling of NAFEC 1 and 2 provided promising temperatures and a view of hydrothermally altered rock from the core samples taken. This has now enabled us to better locate a future 4000 foot slim hole NAFEC 3 which will commence between mid 2010 to early 2011. The location of NAFEC 3 was chosen due to the proximity of faulting along the Superstition Mountain front as well as being within the SP and gravity contours associated with the thermal anomaly. It is anticipated that a successful outcome of drilling NAFEC 3, we help define a potential resource.

References

Bjornstad, S.C., Hall B., Unruh J., Richards-Dinger K., 2006, "Geothermal Resource Exploration, NAF El Centro – Superstition Mountain Area, Imperial Valley, California", GRC 2006.

Cumming, W. and Mackie, R. (2006) Final Report on Analysis and Modeling of Magnetotelluric Data From the Superstition Mountain (NAFEC) Prospect. Report dated 2007-04-30 for the US Navy Geothermal Program Office, Solicitation N68936-06-T-0115.

Dibblee, T.W. Jr., 1984, "Stratigraphy and Tectonics of the San Felipe Hills, Borrego Badlands, Superstition Hills and Vicinity (mapped 1954)", in The Imperial Basin Tectonics, Sedimentation and Thermal Aspects, Rigsby, C.A., ed., Society Economic Paleontologists & Minerologists Pacific Section, Los Angeles, CA, p. 31-44.

Edmunds, S.W., 1977, "Geothermal Development in Imperial County", Geothermal Resources Council Transactions, v. 1, p. 81-83.

Faneros, G., 2005, "Structure and Neotectonics of the Superstition Mountain Fault, Imperial County, California", Masters Thesis, San Diego State University.

Fuis, G.S., W.D. Mooney, J.H. Healey, G.A. McMecham and W.J. Lutter, 1982, "Crustal Structure of the Imperial Valley Region", in The Imperial Valley, California, Earthquake of October 15, 1979, United States Geological Survey Professional Paper 1254, p. 25-50.

Hauksson, E., and P. Shearer, 2005, "Southern California Hypocenter Relocation with Waveform Cross-correlation, Part 1, Results using the Double-Difference Method", Bulletin of the Seismological Society of America, v. 95, n. 3, p. 896-903.

Innovative Technical Solutions, Inc., 2003, "Geothermal Energy Resource Assessment on Military Lands", final technical report submitted to the US Navy Geothermal Program Office, Contract No. N68936-02-R-0236.

James, E.D., V.T. Hoang and I.J. Epperson, 1987, "Structure, Permeability and Production Characteristics of the Heber, California Geothermal Field", PROCEEDINGS, 12th Workshop Geothermal Reservoir Engineering, Stanford University, SGP-TR-109, p. 267-271.

Loeltz, O.J., B. Irelan, J.H. Robinson and F.H. Olmsted, 1975, "Geohydrologic Reconnaissance of the Imperial Valley, California", United States Geological Survey Professional Paper 486-K, 52p.

Magistrale, H., 2002, "The Relations of the Southern San Jacinto Fault Zone to the Imperial and Cerro Prieto Faults", in Barth, A., ed., Contributions to Crustal Evolution of the Southwestern United States: Geological Society of America Special Paper 365, p. 271-278.

Shearer, P., Hauksson, E., and Lin, G., 2005, "Southern California Hypocenter Relocation with Waveform Cross-Correlation, Part 2: Results using Source-Specific Station Terms and Cluster Analysis", Bulletin of the Seismological Society of America, v. 95, n. 3, p. 904-915.

Treiman, J.A., 1989, Superstition Hills, Superstition Mountain, and related faults: California Division of Mines and Geology Fault Evaluation Report FER-207, 21 p.

Unruh, J.R., 2006, "Results of Neotectonic Reconnaissance, Superstition Mountain, NAFEC", William Lettis & Associates, Inc. letter report to US Navy Geothermal Program Office under contract N68936-04-C-0072.

Intermediate Depth Drilling and Geophysical Logging Results at Superstition Mountain, Naval Air Facility El Centro, California

Andrew Tiedeman, Steve Bjornstad, Steve Alm, Lindsey Frazier, Dave Meade, Chris Page, Mike Lazaro, Jeff Woolford: Navy Geothermal Program Office, China Lake, CA
Bob Crowder; Crowder consulting, LLC, Holyoke, CO

U.S.N. Geothermal Program Office, China Lake, CA 93555

Keywords
Superstition Mountain, Imperial Valley, Geothermal, U.S. Navy, Exploration

Abstract

The US Navy Geothermal Program Office (GPO) is conducting geothermal energy exploration adjacent to Superstition Mountain in western Imperial Valley, at the Naval Air Facility, El Centro (NAFEC), CA. Exploration activities conducted by GPO over the past few years indicates that a thermal anomaly appears to coincide with an active transtensional right stepover occurring between the parallel northwest trending Superstition Mountain fault and the Superstition Hills fault to the north.

Based on the earlier shallow drilling, detailed geologic mapping, seismogenic fault mapping and stress analysis, and a variety of geophysical surveys, including gravity and magnetic, self-potential electrical and magneto-telluric, two moderate depth test holes completed in December 2008, and a third test hole, NAFEC-3, completed in November 2010, further confirmed the existence of a m oderate temperature anomaly with temperatures reaching 255°F (124°C) at less than 3500 feet (1067m). The thermal anomaly coincided with hydrothermal alteration within the granodiorites intersected by the test hole.

Fracture and stress field analysis has been conducted through the total length of the hole. Geophysical logs, including UBI, Sonic, Resistivity, Gamma Ray, Borehole Caliper, and Temperature, were acquired through the entire length of NAFEC-3 and have been used in conjunction with the drilling log. Additional geological studies are in process for NAFEC-3, in combination with two other nearby test holes, NAFEC-1 and NAFEC-2, including a Fluid Inclusion Stratigraphy (FIS) study and a petrographic and hydrothermal alteration study.

Introduction and Geological Background

The Superstition Mountain geothermal prospect is located in the West Mesa area of northwestern Imperial Valley, California *(Figure 1)* and occurs within the Shade Tree bombing and parachute range of the Naval Air Facility, El Centro (NAFEC). The range is mostly flatland immediately north-northeast of Superstition Mountain but overlaps onto the mountain. It is a primary inert bombing practice range for Navy and Marine Corp aviators, and is also the winter training range for the Navy's Blue Angels aerial exhibition team.

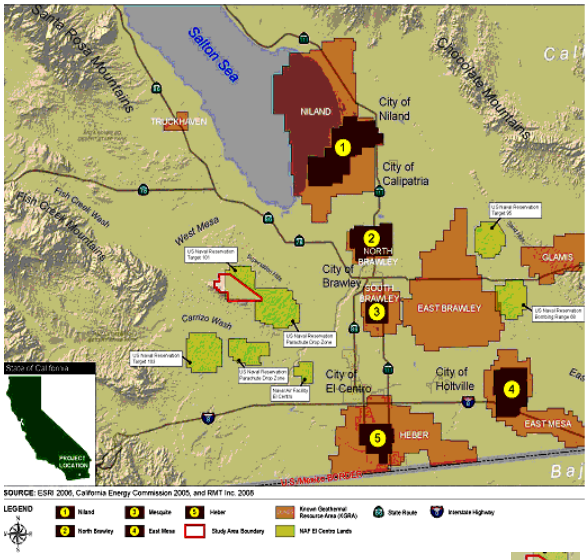

Figure 1: Location of NAFEC project location:

Superstition Mountain is the dominant physiographic feature within the project area that trends northwest-southeast and reaches heights of 759 ft (231m). Superstition Mountain is predominately comprised of pre-Tertiary intrusives of granite, granodiorite, and quartz monzonite. The surrounding areas range from Miocene volcanics and Pliocene to recent marine/lucustrine sediments. There has been a significant history of seismic activity which has been documented through collectively acquired precise relative locations in excess of 340,000 southern California earthquakes from a period of 1984 to 2002 (Shearer(2005) and Haukksson and Shearer (2005)) *(Figure 2)*. Two significant dextral strike slip faults that are sub-parallel and northwest-trending are located within the Superstition Mountain area (Bjornstad et al, GRC 2006). Depth to crystalline basement is thought to be approximately 2.1 km (1.3 miles) near the south end of Superstition Mountain. Drilling records from the California Department of Oil and Gas, and information provided by Layman Energy Associates, indicated the presence of a thermal anomaly with a calculated temperature high of 300°C/km (17.5°F/100 ft) located near the northeast flank of Superstition Mountain.

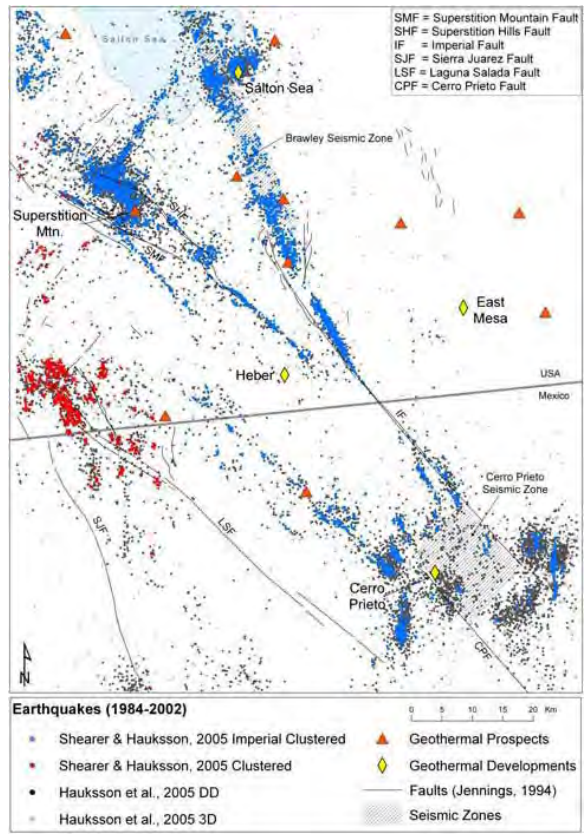

Figure 2: Plot of relocated regional earthquake catalogs relative to mapped fault zones and geothermal developments and prospects.

Previous Investigations:

The GPO since 2001 has accumulated significant geothermal data through various organizations contracted by the Navy as well as the GPO. Beginning with an electrical survey that Innovative Technical Solutions, Inc conducted in 2003, resulted in the identification of a 120 mV Self Potential anomaly (ITSI, 2003). The previously unmapped northwest-striking, northeast-dipping range-front fault (Superstition Mountain Fault) was discovered through reconnaissance mapping which marked the contact point between the bedrock, Quaternary to recent sediments as w ell as hydrothermal alteration and mineralization being observed (Bjornstad et al, GRC 2006).

A best fit model, that was consistent with mapped faulting, extent of surface exposure, and generally expected regional distribution, was put together with the use of a geologic cross section (Dibblee 1984), published fault mapping, refraction seismic analysis (Fuis and Kohler 1984), and gravity/magnetic data. Other data acquired consisted of a 3-D analysis of the relocated earthquake catalog, a magnetotelluric survey, thermochronology, and two intermediate depth slim test holes completed in late 2008 along with equilibrated temperature gradient data. Maximum temperatures ranged from ~187°F (86°C) at NAFEC-2 and ~171°F (77°C) at NAFEC-1 (*Figure 3) (Tiedeman et al, GRC 2010).* With these two test holes showing promising results, the decision was made by the GPO to drill a third moderate depth test hole, NAFEC 3, which was drilled late 2010 (*Figure 4*).

NAFEC-3

The GPO at China Lake, California contracted work to Barbour Well Inc., of Henderson, NV – to drill a slim temperature gradient test hole to a depth of 3500' (1067m) for further exploration

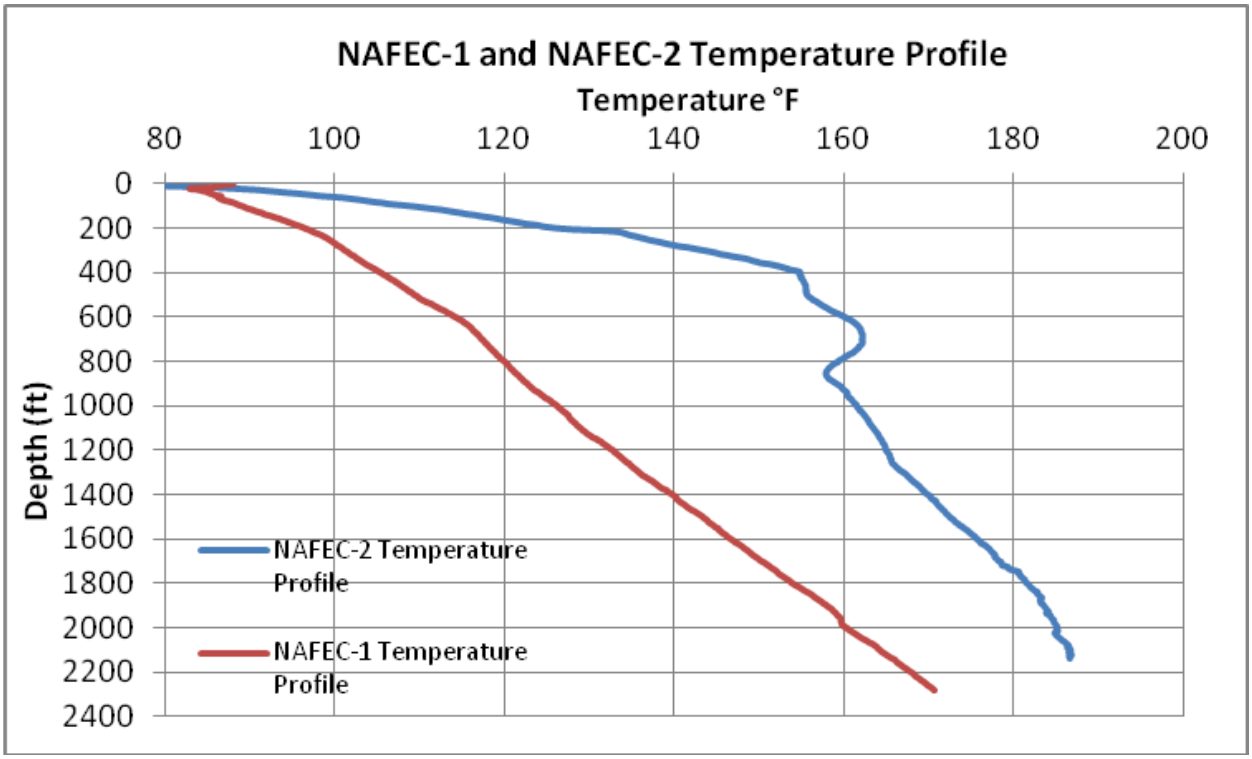

Figure 3: Temperature gradient profiles of NAFEC-1 (171°F) and NAFEC-2 (187°F).

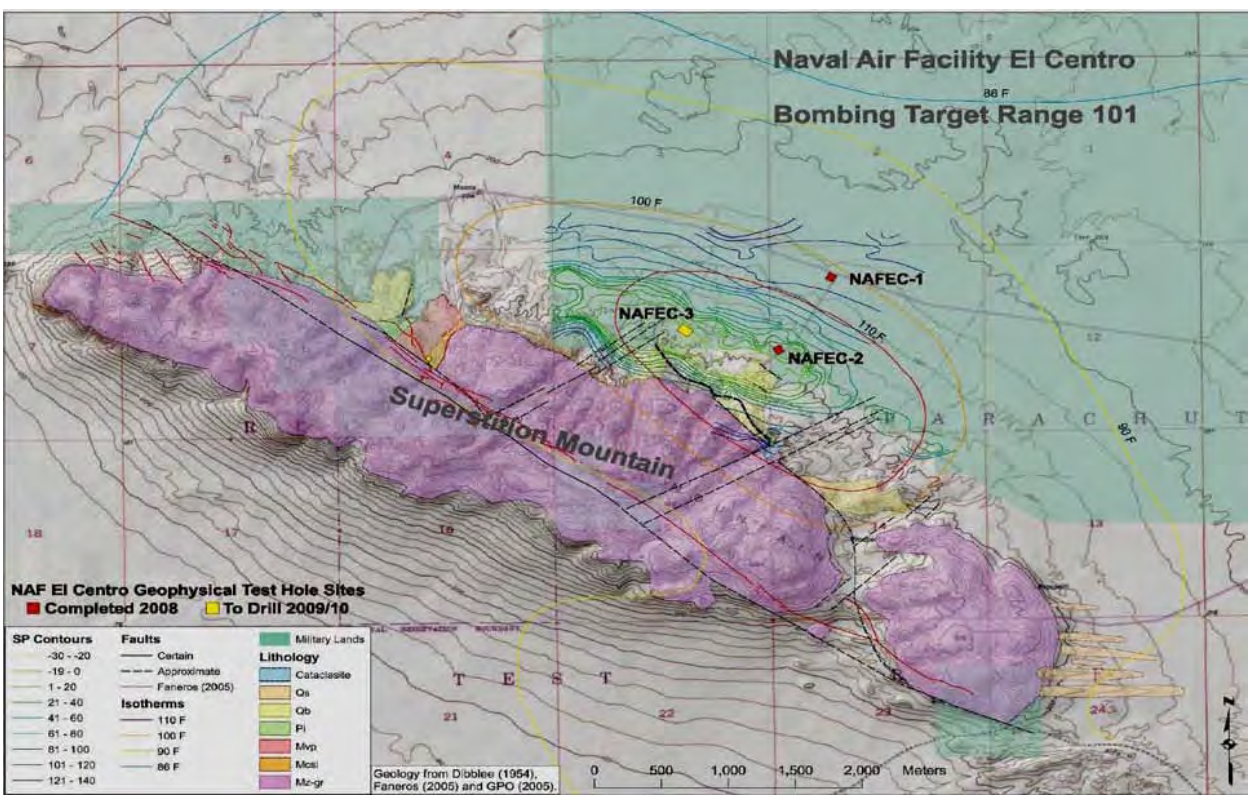

Figure 4: Locations of temperature gradient holes NAFEC-1, NAFEC-2, and NAFEC-3.

of the potential geothermal resource at Naval Air Facility El Centro (NAFEC), CA, through Contract N68936-10-D-0021, Task Order 0001.

The chip sample logging, complete lithology log, and daily drilling reports were provided by Prospect Geotech, Albuquerque, New Mexico. Geophysical hole logging was performed by Schlumberger Wellfield Services, Long Beach, California. The hole was logged with a UBI (Ultrasonic borehole imager), GR, SP, Caliper, Temperature, AIT (Array induction tool), and a BHC (Borehole Compensated Sonic tool). Temperature logging was performed by Southwest Exploration Services, Gilbert, Arizona. Maximum equilibrated temperatures reached a high of 255°F (124°C) between the depths of ~2800'-2900' (853-884m) within the Mesozoic basement.

Drilling Summary

Drilling commenced on October 21, 2010 with the construction of a 24" conductor hole to 106' (32m). The hole was then cased with steel casing and cemented to the surface. Barbour Rig #77 was then positioned over the borehole and continued drilling with mud rotary and the use of a 12 ¼" mill tooth bit to a TD of 1220' (372m). On 26 Oct. 2010 the top section of the hole was logged by Schlumberger and then cased with 33 joints of 9 5/8" steel casing to 1220' (372m) and cemented to the surface. From 28 Oct. to 03 Nov. 2010 the middle section of the test hole was drilled utilizing a 8 ½" mill tooth bit to a depth of 2520' (768m). The borehole was then logged by Schlumberger and then cased with 60 joints of 7" steel casing to 2520' (768m) and cemented to the surface. From 06 Nov. to 12 Nov. 2010 the bottom section of the test hole was drilled utilizing a 6 1/8" mill tooth bit to the total depth of 3520' (1073m). A final single-shot survey of the hole was then performed with a recording of 13.6° off vertical. The borehole was logged and then cased with 4 ½" capped temperature tubing/casing to 3506' (1069m) and filled to surface with water. Barbour Well then de-constructed the drilling equipment, restored area, and moved off-site. The test hole was then allowed to equilibrate for 90 days before Southwest Exploration arrived to acquire temperature gradient data on 15 Feb. 2011.

Lithology and Temperature Profile

A detailed mud/lithologic log was prepared by Prospect Geotech. From this a general formational log was prepared as follows.

0'-126' (0-38m) - No samples were collected within this interval (Drilling Conductor Casing)

126'-480' (38-146m) - *Brawley Formation* - The lithology consisted primarily of sand with some clay and silt, described as being multicolored, fine to coarse sand, rounded to sub rounded, bluish green claystone, with quartz, potassium feldspar, biotite, epidote(yellowish/green), and some green andesite fragments and granitic wash.

480'-580' (146-177m) - *Palm Springs Formation group - Arroyo Diablo Formation (potentially)* - Described as orange, fine-grained sandstone and siltstone, red-brown claystone (Cassiliano, M 2002). The lithology consisted of moderately dark red clay with inter-bedded sand and silt that is sub-angular to sub-rounded, ranging from silt to pebble size with abundant quartz, potassium feldspar, and biotite.

580'-990' (177-302m) - *Palm Springs Formation group- Canebrake Conglomerate (potentially)* - Described as b oulder conglomerate and arkose (Cassiliano, M 2002). The lithology is Granite Conglomerate and sand.

990'-2451' (302-747m) - *Split Mountain Formation* (upper and lower) – There appears to be possible inter-tonguing of the *Alverson Andesite Formation*. The lithology is a mix of sand, conglomerate, and sandy conglomerate with the presence of ash tuff periodically.

2451'-3520' (747-1073m) - Mesozoic basement - alternating between Granodiorite and Quartz Monzonite. The lithology is described as Granodiorite: clear, light grey, black, white, tr orange, translucent, medium-coarse grain cuttings, dominated fine groundmass @ 2820'. Continuous biotite with/and slightly weathered appearance, tr-com black amphibole, white plagioclase, very rare amber spheen crystals, and slight to moderately calcareous.

The equilibrated temperature profile (*Figure 5*) indicates that subsurface temperatures climb quickly to 215°F (101°C) at a depth of 407 feet (124m). From that point downward to about 2,800 feet (853m) the temperature climbs slowly but steadily to a maximum of 255°F (124°C). The granodiorites within the depths of roughly 2600'-2850' (792-869m) host the zone of maximum temperature.

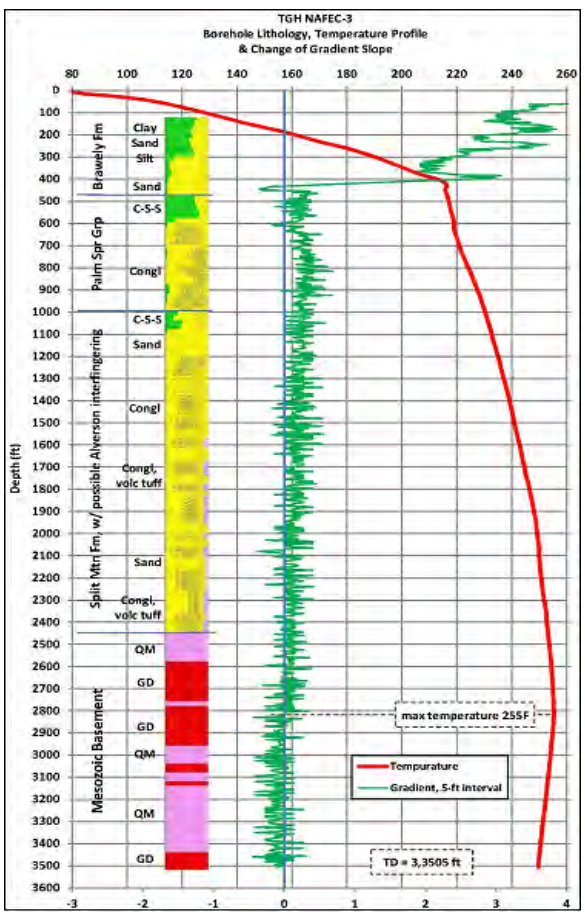

Figure 5: Temperature gradient profile compiled and graphed in combination with 5 foot interval change in gradient slope and lithology log NAFEC-3

Fracture Analysis

In early 2011 the GPO contracted with Robert Crowder to conduct a detailed fracture stress field analysis of NAFEC-3. Schlumberger and Southwest Exploration logged NAFEC-3 in three intervals, 114'-1214' (35-370m) (top section), 1215'-2515' (370-767m) (middle section), and 2450'-3506' (747-1069m) (bottom section). The logging method used for each tool is as follows. The UBI tool uses selectable heads that have a low frequency of 250 k Hz with vertical resolution of about 0.4" and a high frequency of 500 kHz with a vertical resolution of about 0.2" vertical resolution. The top and middle sections used an 8.7" and 6.7" diameter probes with low frequency, respectably, and a 4.3" diameter probe with high frequency on the bottom section. All the gamma resistivity, sonic porosity, caliper, temperature, and array induction tools collected data with 2' vertical resolution at 10", 20", 30", 60" and 90" in all sections of the test hole. The BHC tool included P and S-wave transit time, sonic porosity hole imagery, and PR where both P and S-waves were evaluated. The tools were combined and logged from bottom to top. All the data was depth correlated and had corrected azimuth with a declination of 11.93 degrees to true North. The log data was provided in LAS and DLIS format as well as hard copy plots in pdf and pds forms. The log data was processed and produced NAFEC-3 UBI Summary for top, middle, and bottom sections, NAFEC-3 Feature Summary, NAFEC-3 Breakout Summary, NAFEC-3 Geophysical Summary, and NAFEC-3 Feature Picks.

Feature Picks

UBI image features were picked and classified and presented graphically as sinsusoids, tadpoles and various lithologic symbols and output into an Excel spreadsheet (*Figure 6*). These features are listed by depth, dip direction and degree, aperture, classification, continuity, condition, form, and remark for open versus closed fracturing.

Lower Section -- ~2450' to 3506': nominal 6 1/8" hole w/ 9.8 lb/gal mud. UBI sampled 2 deg horizontally and 0.017' (vertical res of 0.042 due to 500kHz head, ~ 4.3" dia.)								
Image quality generally much higher than above due to high frequecy, smaller beam width and sample interval, though there were numerous zones where the probe jumped: probably due to deviation of drill hole.								
Portions of the drill hole are extremely oval shaped; possiblity due to borehole breakouts.								
Depth*	Dip Dir	Tilt	Aperture	Classification	Continuity	Condition	Form	Remark
ft	Deg	Deg	inch/10					
2658.99	186.6	84.38	0.00	109 - Partially Open Joint/Fracture	C3 Moderately continuous 75-100%	0 - Smooth	1 - Planar	Partially Open
2660.24	43.8	44.14	14.39	305 - Major Joint/Fracture	C5 Very continuous - wide	3 - Brec / Crushed	1 - Planar	Open
2662.68	47.2	49.69	56.10	305 - Major Joint/Fracture	C5 Very continuous - wide	3 - Brec / Crushed	1 - Planar	Open
2664.92	116.1	51.99	0.00	109 - Partially Open Joint/Fracture	C4 High continuous - thin	0 - Smooth	1 - Planar	Partially Open
2665.90	156.9	50.89	32.36	305 - Major Joint/Fracture	C5 Very continuous - wide	0 - Smooth	1 - Planar	Open
2669.14	137.2	75.97	9.83	305 - Major Joint/Fracture	C5 Very continuous - wide	3 - Brec / Crushed	1 - Planar	Open
2671.30	163.0	78.51	0.00	109 - Partially Open Joint/Fracture	C3 Moderately continuous 75-100%	0 - Smooth	1 - Planar	Partially Open
2674.28	4.8	27.15	209.16	305 - Major Joint/Fracture	C5 Very continuous - wide	3 - Brec / Crushed	1 - Planar	Open
2676.11	359.8	49.95	0.00	109 - Partially Open Joint/Fracture	C4 High continuous - thin	0 - Smooth	1 - Planar	Partially Open
2677.28	350.8	10.83	0.00	109 - Partially Open Joint/Fracture	C3 Moderately continuous 75-100%	0 - Smooth	1 - Planar	Partially Open
2677.64	53.3	53.77	0.00	109 - Partially Open Joint/Fracture	C3 Moderately continuous 75-100%	0 - Smooth	1 - Planar	Partially Open
2678.14	33.7	50.88	0.00	109 - Partially Open Joint/Fracture	C3 Moderately continuous 75-100%	0 - Smooth	1 - Planar	Partially Open
2678.84	337.7	60.95	0.00	109 - Partially Open Joint/Fracture	C3 Moderately continuous 75-100%	0 - Smooth	1 - Planar	Partially Open
2680.54	4.8	52.39	0.00	109 - Partially Open Joint/Fracture	C3 Moderately continuous 75-100%	0 - Smooth	1 - Planar	Partially Open
2681.03	14.7	37.54	0.00	109 - Partially Open Joint/Fracture	C3 Moderately continuous 75-100%	0 - Smooth	1 - Planar	Partially Open
2681.51	30.9	38.74	0.00	109 - Partially Open Joint/Fracture	C3 Moderately continuous 75-100%	0 - Smooth	1 - Planar	Partially Open
2682.02	74.7	31.11	0.00	110 - Minor Joint/Fracture	C4 High continuous - thin	0 - Smooth	1 - Planar	Tight
2683.33	176.0	18.58	0.00	110 - Minor Joint/Fracture	C3 Moderately continuous 75-100%	0 - Smooth	1 - Planar	Tight

Figure 6: Example of Excel spreadsheet showing features and classification.

There were multiple fractures identified from the logs, but only the more significant were chosen for further analysis. The overall total of identified features from the UBI was 1578 and of these were 30 major features with measureable aperture, 484 partially open features, 724 minor features, 141 near vertical features, 48 breccia/conglomerate/vugs zones, and 89 breakout features. The more significant fractures were identified in separate categories as Near Vertical Joints/Fractures, Breccia/Conglomerate/- Vugs/Vesicles, and Breakouts/Tensile Fractures (*Figures 7-9*). The analysis shows that the majority of open/partially open fractures and major fractures are located within the Mesozoic Basement Granodiorites.

UBI Summary

From the analysis of the UBI summaries for the top, middle, and bottom sections, image quality improves at depth and as the formations become more competent.

Top section - Poor image quality in the top section could be from the large diameter of the borehole, heavy drill mud and softer formation. This is fairly apparent throughout until lower in the top section where the formation transitions from soft clays and sands to conglomerate formations and image quality is not as inhibited as much by factors noted above.

Middle section - Image quality improves a little more in the middle section where sands and conglomerates become more competent and transition into the Mesozoic basement formations (*Figure 10*).

Bottom section - The bottom section has the highest resolution due to the formation being in the much harder Mesozoic basement, higher vertical resolution and frequency (500 kHz head), smaller beam width and sample interval than above (see *Figures 11-14*).

Breakouts/Tensile Fractures 0 = Broken Zone Undifferentiated 1 = Major Breakout 2 = Minor Breakout 3 = Tensile Fracture					
Top Section -- ~114' to 1214'					
Depth	Azimuth	Tilt	Length	Opening	Ranking/Description
ft	Deg	Deg	m	Deg	
No apparent Breakout like features were picked in this interval					
Middle Section -- ~1215' to 2515'					
1809.66	125.19	0.14	5.34	25.38	0 = Broken Zone Undifferentiated
1813	207.69	-0.3	7.49	28.85	0 = Broken Zone Undifferentiated
1817.09	357.4	0.08	4.26	47.88	0 = Broken Zone Undifferentiated
Lower Section -- ~2450' to 3506'					
2800.2	193.85	-0.84	3.15	55.38	1 = Major Breakout
2805.96	191.54	0.39	5.16	34.62	2 = Minor Breakout
2806.67	7.21	0.41	2.95	54.81	2 = Minor Breakout
2809.68	349.9	-0.35	2.83	51.35	1 = Major Breakout
2809.72	180.87	0	1.56	52.5	1 = Major Breakout
2810.07	263.65	-0.19	2.1	27.69	0 = Broken Zone Undifferentiated
2811.94	183.17	-0.48	1.64	59.42	1 = Major Breakout
2813.49	339.52	-0.18	2.14	36.35	2 = Minor Breakout
2852.99	147.4	1.59	1.89	45.58	1 = Major Breakout
2853.24	20.48	0	1.19	36.35	1 = Major Breakout
2858.57	185.48	0.48	3.54	68.65	1 = Major Breakout

Figure 7: Example of Breakouts/ Tensile Fractures from Excel Feature Picks.

Near Vertical Joints/Fractures

VFx = 2 Near vertical Joints/Fractures
VFx-W = 2 Wide Near vertical Joints/fractures
33 = >2 near vertical Joint/fractures
IFx = Possible drilling induced near vertical tensile fractures
Vein = infilled near vertical joint/fracture

Depth	Btm Depth	Ranking/Description
ft	ft	
Top Section -- ~114' to 1214'		
681	684.62	VFx = 2 near vertical Fxs
827.26	830.22	VFx = 2 near vertical Fxs
833.12	837.26	VFx = 2 near vertical Fxs
866.56	871.66	VFx = 2 near vertical Fxs
Middle Section -- ~1215' to 2515'		
2361.21	2366.91	VFx = 2 near vertical Fxs
2369.43	2371.94	VFx-W = 2 Wide Near vertical Joints/fxs
2378.06	2381.73	VFx-W = 2 Wide Near vertical Joints/fxs
2458.26	2467.63	VFx-W = 2 Wide Near vertical Joints/fxs
2467.63	2485.06	VFx = 2 near vertical Fxs
2491.25	2508.19	VFx = 2 near vertical Fxs
Lower Section -- ~2450' to 3506'		
2684.84	2687.19	VFx-W = 2 Wide Near vertical Joints/fxs
2707.35	2711.02	VFx = 2 near vertical Fxs
2721.56	2726.59	>2 near vertical Joint/fractures
2727.87	2741.08	VFx = 2 near vertical Fxs
2746.64	2752.69	>2 near vertical Joint/fractures
2752.69	2757.53	VFx = 2 near vertical Fxs
2758.09	2769.09	VFx = 2 near vertical Fxs

Figure 8: Example of Near Vertical Joints/ Fractures from Excel Feature Picks.

Breccia/Conglomerate/Vugs/Vessicles

Bx = Breccia/Collapse Breccia
Lg V = Large Vug/ Vugs/ or Vesicles (> 6" diameter)
MV = Medium Vug/ Vugs/ or Vesicles (2-6" diameter)
CNG = Small Vug/ Vugs/ or Vesicles (< 2" diameter)

Depth	Btm Depth	Ranking/Description
ft	ft	
Top Section -- ~114' to 1214'		
630.4	677.82	Bx = Breccia/Conglomerate
692.78	844.02	Bx = Breccia/Conglomerate
849.17	884.14	Bx = Breccia/Conglomerate
Middle Section -- ~1215' to 2515'		
1363.01	1394.7	Bx = Breccia/Conglomerate
1459.52	1522.21	Bx = Breccia/Conglomerate
1522.21	1559.91	Bx = Breccia/Conglomerate
Lower Section -- ~2450' to 3506'		
2659.57	2666.34	Bx = Breccia/Conglomerate
2673.39	2675.39	Bx = Breccia/Conglomerate
2764.24	2769.09	Bx = Breccia/Conglomerate
2816.18	2819.29	Bx = Breccia/Conglomerate

Figure 9: Example of Breccia/Conglomerate/ Vugs/- Vesicles from Excel Feature Picks.

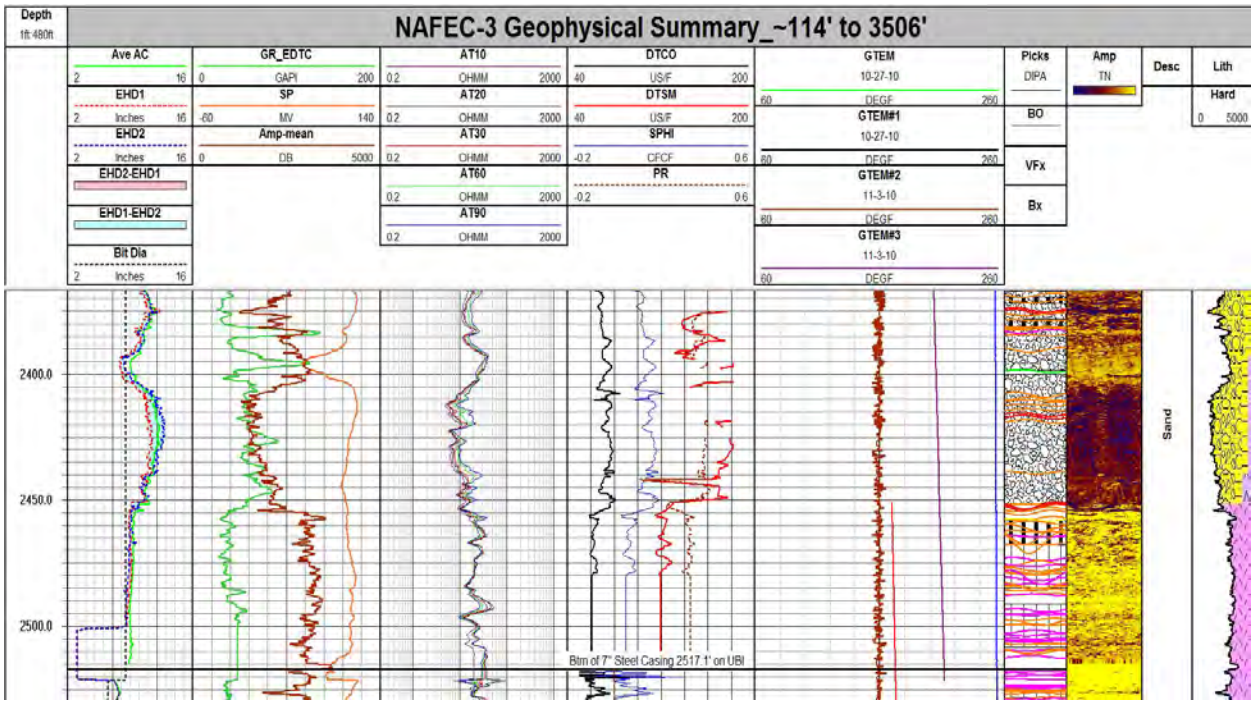

Figure 10: Geophysical Summary showing transition from Split Mountain Formation to Mesozoic Basement. Transition depth at approximately 2450'.

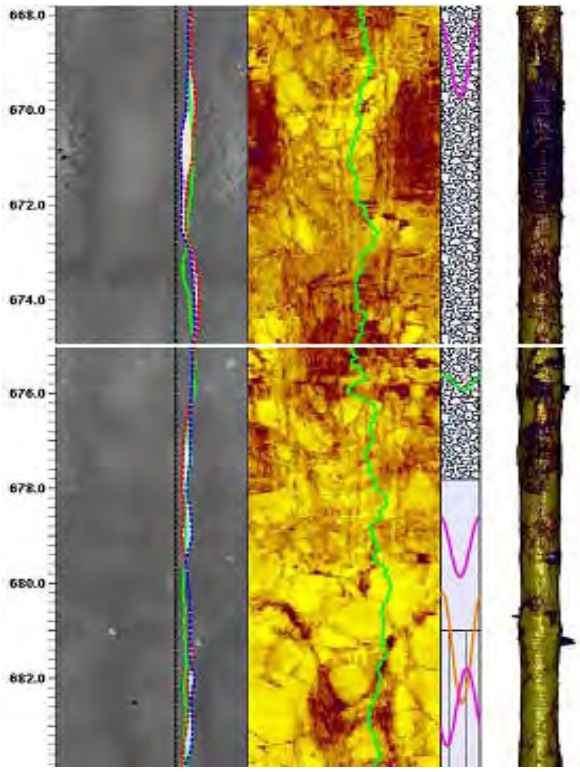

Figure 11: UBI Summary 662'-682'showing scalloped drill bit marks in softer formation transitioning to harder formation. Upper section.

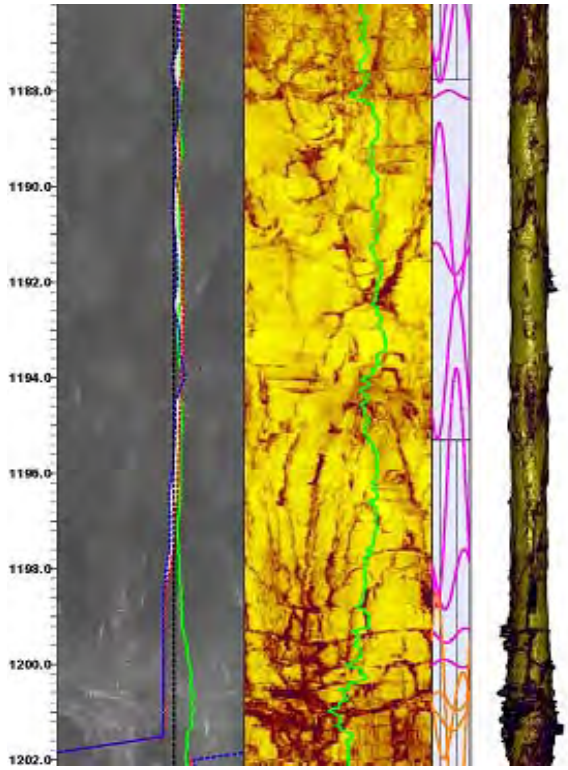

Figure 12: UBI Summary 1180'-1202' improved image quality in harder formation. Fractures visible in imagry.

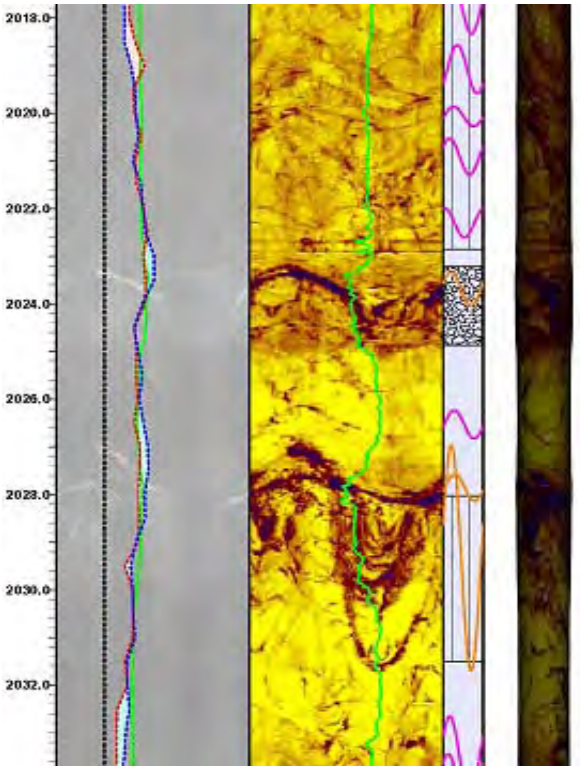

Figure 13: UBI Summary showing middle section imagry.

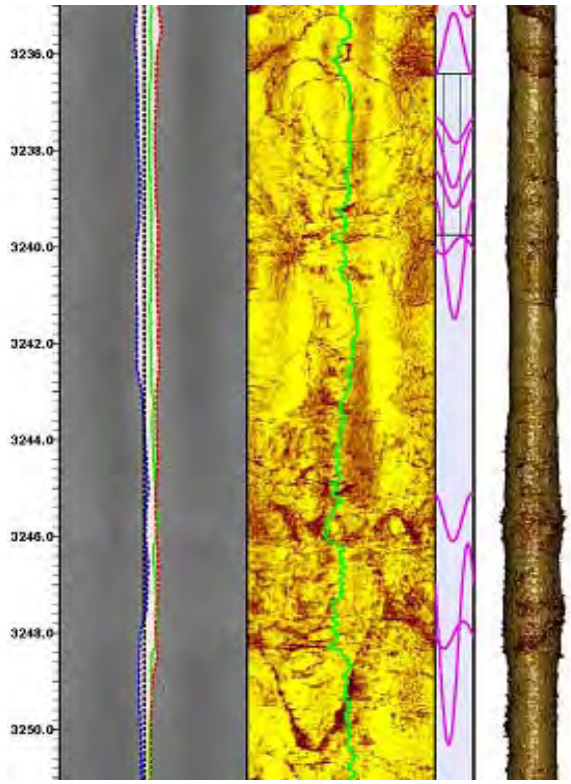

Figure 14: UBI Summary showing bottom section imagry.

The Mean Acoustic Amplitude may indicate relative rock hardness due to amplitude being higher in more competent less fractured formations and lower in less competent, fractured formations or a possible decrease in amplitude when detecting Argillic alteration. With that, the amplitude indicates that the granodiorite may be more altered than the quartz monzonite within the Mesozoic basement.

As noted above, the granodiorites within the depths of roughly 2600' to 2850 f eet (792-869m), host the zone of maximum recorded temperature, which coincides with a significant amount of major open fractures, breakouts, and brecciated zones, as well as having potential for fluid flow. However, cross flow within the well was not apparent during logging with Schlumberger's temperature tool. A fair amount of the major open fractures that occur in this zone appear to be constrained to brecciated zones within the granodiorites (*Figures 15 & 16*) These brecciated zones average nearly 5 inches wide and range up to 21 inches. Fracturing (not brecciated) with measureable apertures occurred from 1300 feet (396m) to TD, ranging from 0.5 to over 8 inches wide, dipping 15 to 72 degrees (average = 47°) in a wide range of directions from 25 to 313 degrees (average = 177° (S3E).

The temperature gradient slope (*Figure 5*) becomes negative at about 2810 feet (856m) and indicates the transition when temperatures begin to decrease. Below the transition, there are mostly minor to partially open fractures and no brecciated zones that have major open fractures for potential fluid flow as seen above.

UBI Feature Summary & Breakout Analysis

UBI imagery shows a v aried range of feature orientation over the entire hole, but has a few specific portions of the hole indicating common feature orientations. The general trend of the sediments tend to dip an average of 34° in the W-SW direction with a mean direction of about 220°-246°. There appears to be no dominant orientation trends within the Mesozoic basement directly below, but has a mean feature dip direction to the northwest within the first 550' (168m) of this bedrock (*Figures 17-18*).

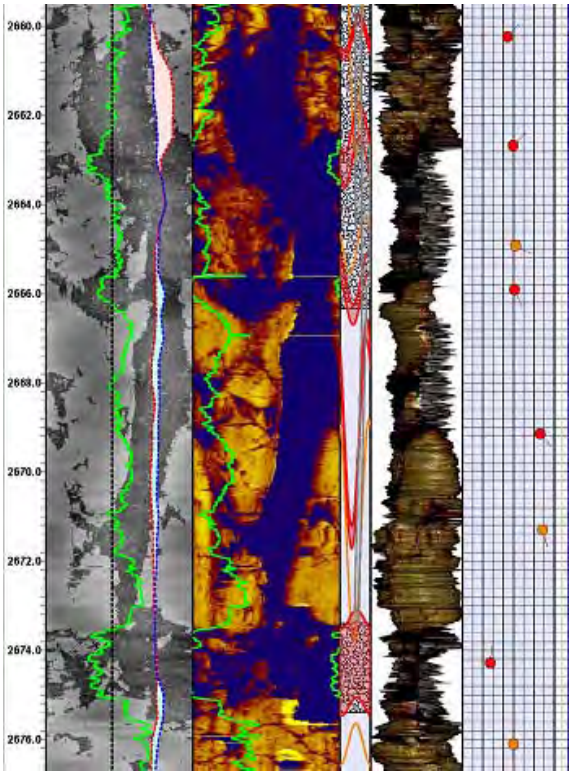

Figure 15: UBI Summary showing major open fractures in brecciated zones. Possible breakout features.

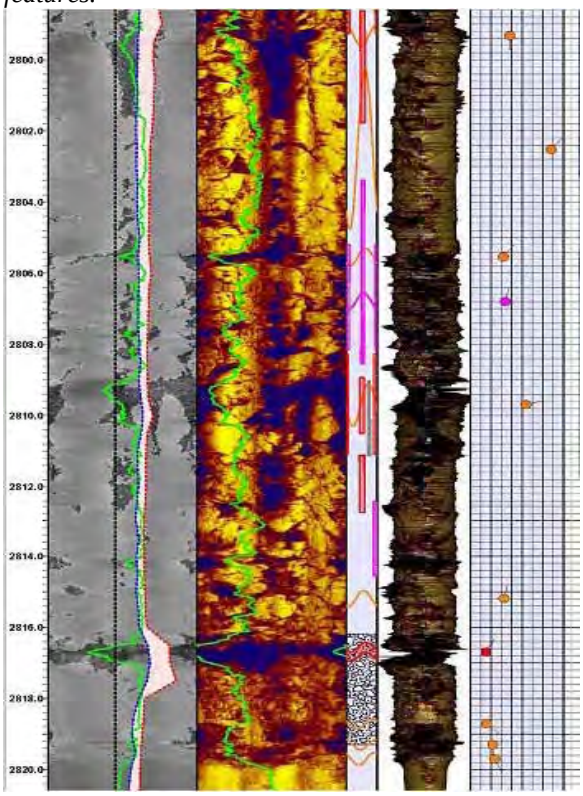

Figure 16: UBI Summary showing major open fracture and vertical joints/fractures.

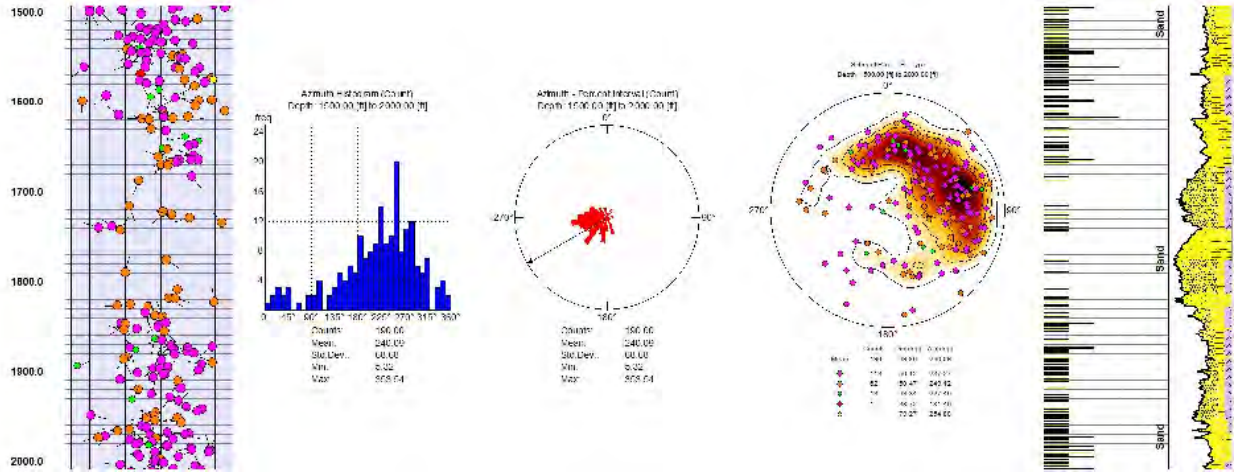

Figure 17: Showing feature orientations generally dipping to the W-SW within the sediments. Depths 1500'-2000'.

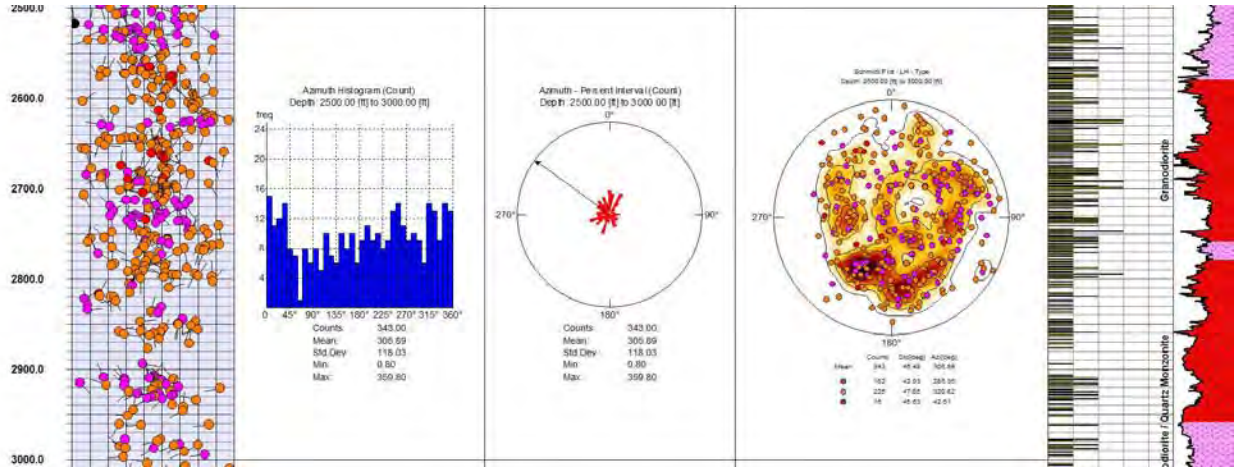

Figure 18: Showing feature orientations within the Mesozoic basement. Depths 2500'-3000'.

An earlier 3-D analysis of the regional relocated earthquake catalog defined a number of planar alignments of seismicity (apparent seismogenic faults) in the Superstition Mountain area (Bjornstad et al, 2006). These planar alignments were combined with other, spatially distinct clusters of earthquakes and their focal mechanisms inverted for stress and strain and displayed as t he vertical stress ratio. Based on seismicity data the Superstition Mountain area exhibits a maximum compressive stress sub-horizontal and striking N15W (345°) (*Figure 19*), however there is significant hetrogeneity in the magnitude of the stress between the small groupings of events, implying a dynamic state of strain in the area.

Based on a pparent borehole breakouts in NAFEC-3, the direction of maximum horizontal stress (Shmax) in the bedrock immediately adjacent to the borehole is ~N40W (320°), with a standard deviation in the data set of 78.9°. The breakout data set, at 66 samples, is relatively small. Coupled with the data's large standard deviation, it is difficult to extrapolate a strong Shmax direction for the prospect area. Instead, the heterogeneity defined by the seismic data, appears to be reflected in the borehole data.

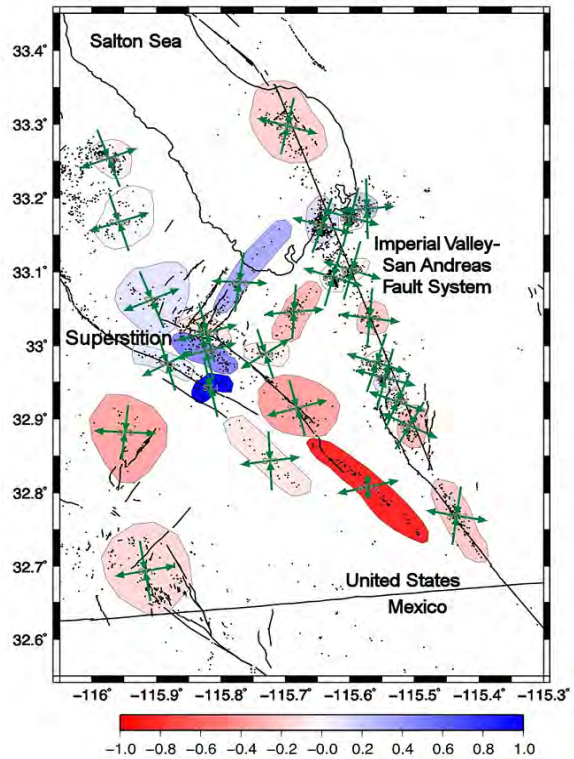

Figure 19: Earthquake clusters and vertical stress ratios. This is the ratio of the vertical stress to the maximum extensional stress. Negative (red) values indicate crustal thinning and positive (blue) values crustal thickening.

Summary and Conclusions

NAFEC-3 was successfully completed and analyzed through the combined efforts of the Navy Geothermal Program Office, Barbour Well Inc., Schlumberger Wellfield Services, Prospect Geotech, and Southwest Exploration. A variety of formations were encountered from the sands and clays of the Brawley Formation to Mesozoic basement granodiorite and quartz monzonite. After the completion of drilling a fracture and stress field analysis was performed in which approximately 1578 f eatures of fractures, brecciated zones, and breakouts were identified. Orientation trends within the sediments were generally found to dip in the W-SW direction while no dominant orientation trends were apparent within the Mesozoic basement. Also, horizontal stress directions were defined from breakout features.

The maximum equilibrated temperature that was recorded at ~255°F (124°C) plus a strong temperature profile through thick sections of porous conglomerates and sands have provided encouraging results and further defining the Superstition Mountain geothermal anomaly. The equilibrated temperature profile, along with the gradient profile, indicates a sh arp rise in temperatures to a depth of 407 feet (124m), after which the temperature climbs gradually to within the granodiorites which host the maximum temperatures recorded near 2800 feet (853m). Coinciding with maximum temperature, between the depths of roughly 2600' to 2850 feet (792-869m), a significant amount of major open fractures, breakouts, and brecciated zones occur as well. This could potentially indicate fluid heat flow, however, no c ross flow was apparent during drilling or logging nor were significant fluid flows or loses encountered while drilling the sedimentary section of the test hole.

Though it is difficult to define a strong maximum horizontal stress (Shmax) within the NAFEC prospect, it appears that heterogeneity defined by previous seismic data from the 3-D analysis of the regional earthquake catalog, may be reflected in the borehole data. Shmax within the bedrock is ~N40W (320°), with a standard deviation in the data set of 78.9°.

Completion of the geothermal test hole NAFEC-3 has provided a clearer picture and invaluable information about the potential geothermal resource at the Naval Air Facility in El Centro, CA within the Shade Tree Bombing Range. Significant temperatures are evident at relatively shallow depths. These temperatures occur both in the highly porous Tertiary sediments (up to 40% sonic porosity) and the fractured basement granodiorites with individual open fractures over 8 inches wide and porous breccia zones up to 21 inches wide. The potential for a producible geothermal resource here is significant.

References

Bjornstad, S.C., Hall B., Unruh J., Richards-Dinger K., 2006, "Geothermal Resource Exploration, NAF El Centro – Superstition Mountain Area, Imperial Valley, California", GRC 2006.

Cassiliano, M.L., 2002, "Revision of the Stratigraphic Nomenclature of the Plio-Pleistocene Palm Spring Group (New Rank), Anza-Borrego Desert, Southern California", Proceedings of the San Diego Society of Natural History, Number 38, 30 April 2002.

Crowder, R.E., 2011, "Borehole Geophysical Log Analysis and Discussion for Geothermal Test Well NAFEC-3, at NAF El Centro/Superstition Mountains for U.S.N. Geothermal Program Office", Crowder Consulting, LLC., for US Navy Geothermal Program Office under contract N68936-10-D-0021, contingency.

Dibblee, T.W. Jr., 1984, "Stratigraphy and Tectonics of the San Felipe Hills, Borrego Badlands, Superstition Hills and Vicinity (mapped 1954)", in The Imperial Basin Tectonics, Sedimentation and Thermal Aspects, Rigsby, C.A., ed., Society Economic Paleontologists & Minerologists Pacific Section, Los Angeles, CA, p. 31-44.

Fuis, G.S., W.D. Mooney, J.H. Healey, G.A. McMecham and W.J. Lutter, 1982, "Crustal Structure of the Imperial Valley Region", in The Imperial Valley, California, Earthquake of October 15, 1979, United States Geological Survey Professional Paper 1254, p. 25-50.

Hauksson, E., and P. Shearer, 2005, "Southern California Hypocenter Relocation with Waveform Cross-correlation, Part 1, R esults using the Double-Difference Method", Bulletin of the Seismological Society of America, v. 95, n. 3, p. 896-903.

Innovative Technical Solutions, Inc., 2003, "Geothermal Energy Resource Assessment on Military Lands", final technical report submitted to the US Navy Geothermal Program Office, Contract No. N68936-02-R-0236.

Shearer, P., Hauksson, E., and Lin, G., 2005, "Southern California Hypocenter Relocation with Waveform Cross-Correlation, Part 2: Results using Source-Specific Station Terms and Cluster Analysis", Bulletin of the Seismological Society of America, v. 95, n. 3, p. 904-915.

Tiedeman, A., Bjornstad, S.C., Meade, D., Lazaro, M., Sabin, A, Alm, S., 2010, "Geothermal Exploration Activities, Including Intermediate Depth Temperature Gradient Drilling, at the Naval Air Facility, El Centro, California", Geothermal Resources Council Transactions, Volume 34.

NAVAL AIR STATION FALLON,

DIXIE VALLEY,

NEVADA

Department of the Navy Geothermal Exploration on Naval Air Station Fallon (NASF) Managed Lands in Dixie Valley, Nevada

Michael Lazaro[1], Steve Alm[1], Andrew Tiedeman[1], Christopher Page[1], David Meade[1], Jeff Shoffner[1], Keith Bucher[2], University of Nevada Reno Great Basin Center for Geothermal Energy, Department of Geological Sciences and Engineering, University of Nevada, Reno, Nevada Bureau of Mines and Geology, University of Nevada, Reno

[1]Department of the Navy Geothermal Program Office, [2]SEI Group, Inc.,

Keywords: Geothermal, Dixie Valley, Exploration, Navy Geothermal Program Office, Temperature Gradient Drilling, Shallow Temperature Probe Surveys, LiDAR, Hyperspectral,

Abstract

The Department of the Navy Geothermal Program Office (DON GPO) is currently engaged in geothermal exploration on Naval Air Station Fallon (NASF) Training Ranges (Fallon, NV) with a focus on discovering a geothermal resource is Southern Dixie and Fairview Valley's. Results of the drilling of 20 (500-foot deep) temperature gradient holes, and 125 2-meter (2M) temperature probes have validated data from exploration activities in these valleys from the 1970's and 1980's, and have also identified previously unknown geothermal anomalies (Skord et. al, 2011).

2M temperature probes, LiDAR, and hyperspectral data were acquired and analyzed in partnership with SEI Group, Inc. and the University of Nevada-Reno Great Basin Center for Geothermal Energy (UNR-GBCGE). A primary goal of this work is to understand the nature of the left-stepping oblique to vertical slip transition zone between the Dixie Valley Structural Basin and the Fairview Valley Structural Basin. Previous geophysical studies in Dixie Valley (Mankhemthong 2008) suggest this transition zone to be the structural control of the geothermal anomalies at Eleven Mile Canyon and Pirouette Mountain. Additional geophysical surveys are currently being pursued to better define this apparent transition zone at depth. Those geophysical surveys include gravity, magnetic, and magneto-telluric (MT). The synthesis of these data will be used to generate several intermediate to deep slim-hole drilling targets to test our exploration model and further delineate potential geothermal resources at NASF.

Introduction

The Navy GPO is actively exploring for geothermal resources at a number of military bases throughout the world utilizing contractor support in conducting exploration /drilling to meet the renewable energy goals of the Department of Defense. The goal is to complete these exploration campaigns in a 2-year period, ultimately, trying to identify the presence of a geothermal resource that industry can develop and garner the DOD revenue and/or energy assurance.

Through American Reinvestment and Recovery Act (ARRA) funding, the Department of the Navy Geothermal Program has acquired LiDAR and Hyperspectral Imagery, acquired shallow probe temperature surveys, conducted fault mapping, and drilled twenty-four, five-hundred foot temperature gradient holes on NAS Fallon Managed lands; sixteen of those

temperature gradient holes were drilled in Fairview Valley, and Southern Dixie Valley. This paper will discuss the preliminary results from the surveys acquired, and the shallow temperature gradient drilling initiated in August 2010; it will also explain the exploration approach and methods the Navy GPO has engaged in and is currently pursuing at NAS Fallon through contractor support.

Study Areas

Naval Air Station (NAS) Fallon is located in the Lahontan Valley of west-central Nevada, approximately 70 miles east of Reno and six miles southeast of the city of Fallon. Geothermal exploration on NAS Fallon lands isn't a new concept; NAS Fallon main base, located approximately 10 miles southeast of Fallon, in the Carson Sink, has seen its share of geothermal exploration as in 2005 when a geothermal development contract with Ormat, Nevada Inc. was struck (Figure 1).

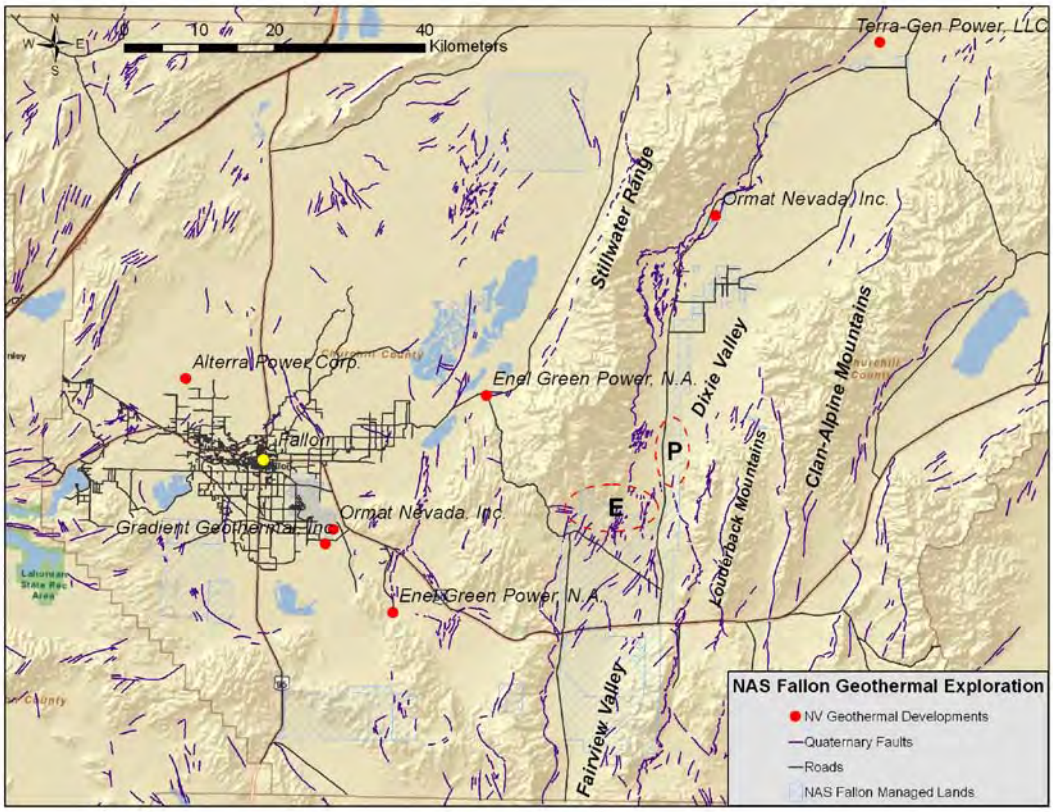

Figure 1. Map illustrating the location of NAS Fallon Managed lands (241,000 acres), in proximity to both current and pending geothermal developments. The (P) represents the Pirouette Mountain Geothermal Anomaly, while the (E) represents the location of the Eleven-Mile Canyon Geothermal Anomaly.

There are many support functions NAS Fallon provides to the Navy, however, NAS Fallon's primary mission is to support the Naval Strike and Air Warfare Center's (NSAWC) Navy Fighter Weapons School, Top Gun flight; The training ranges in Dixie and Fairview Valley's make for great flight simulation of forward deployed areas.

Naval Air Station Fallon Training Ranges cover an area of approximately 241,000 acres, and are in proximity to three current operating geothermal power plants (Figure 1), one being the hottest geothermal system in Nevada, Terra-Gen's Dixie Valley plant (Blackwell et. al., 2009). With two previously identified geothermal anomalies, Eleven-Mile Canyon, and Pirouette Mountain (Figure 1), and with a land position in proximity to known developments in Northern Dixie Valley (Terra-Gen), and pending developments in the central part of the valley at Dixie Meadows (Ormat Nevada Inc.) (Figure 1), the DON GPO suspects that NAS Fallon managed lands in Dixie Valley may yield a geothermal resource.

Geologic Setting

Southern Dixie Valley is bounded to the east by the NNE trending Stillwater Range and to the west by the north trending Louderback Mountains and the NNE trending Clan Alpine Range (Figure 1). The valley was formed as a result of late Miocene to Holocene E-W extension that exposed the Stillwater Caldera Complex and large sections of Pre-Cenozoic upper crustal material (John, 1993).

The navy property in Southern Dixie Valley is situated in the structural termination and transition of two major fault systems (Figure 1) associated with known geothermal occurrences. Our position at Eleven Mile Canyon and South to Hwy 50 (Figure 2) covers the southern termination of the Dixie Valley Fault, well known for the 1954 rupture and the highest temperature of produced geothermal fluid in the state of Nevada at the Terra-Gen facility ub Dixie Valley. This range bounding east dipping normal fault is the dominant structure controlling motion along the eastern front of the Stillwater Range.

The Pirouette Mountain (Figure 2) property is directly adjacent to the northern termination of the Gold King and Louderback Mountains faults. These are both west dipping normal faults that were recently active as part of the 1954 Fairview Peak rupture event that triggered the Dixie Valley Event. Analysis of static stress changes by Caskey and Wesnousky (1997) showed that the northward propagation of slip along four distinct faults in the Fairview Peak event, based on the stress changes modeled, were a driver in the Dixie Valley event. A 3.2 magnitude seismic event was recorded in this area as recently as April 22, 2011(NSL, 2011). This is one of the only parts of Dixie Valley with significant east-dipping neotectonic activity in the western part of the valley. The origin of geothermal fluids recognized in the Hunt Exploration data is thought to have a relationship with the confluence at depth of these east-dipping structures with the west dipping Dixie Valley Fault.

Geophysical Setting

Previous geophysical work has been limited in the southern Dixie Valley. Most recently, Mankhemthong (2008) performed a gravity study in Southern Dixie Valley and Northern Fairview Valley. This work directly overlay the Navy GPO project area at Pirouette Mountain and Eleven-Mile Canyon (Figure 1). The results show evidence to an inter-basin transition zone that has defined areas of compressional stresses and tensional stresses that correlate to shallow

temperature anomalies. North of the project area in the greater Dixie Valley, numerous geophysical surveys have proven to show insight to geology at depth. Numerous gravity surveys (Schaefer, 1983; Blackwell et al., 1999; Abbott and Louie 2001) have modeled faulting, basin depths, and geologic units, whereas aeromagnetic surveys have delineated previously unknown faulting (Grauch, 2002; Smith et al., 2002) and the locations of magnetic bedrock. These surveys have supplemented three seismic studies (Herring, 1967; Okaya and Thompson, 1985; Abbott and Louie, 2001). MT and other electrical methods have also been used for understanding the geothermal potential in Dixie Valley geothermal field with good success (i.e.: Wannamaker, 2005). While these surveys do not directly overlay our focus areas, they are very close in proximity and will be used to correlate with planned acquisition of geophysical data for this project.

Exploration Methods and Preliminary Results

Given the nature of pursuing geothermal exploration on military bases and training ranges, a number of factors come into play when considering exploration: prospect identification/potential, access to training ranges, and; mission compatibility. Also, prior to any exploration activities, the necessary environmental clearances must be obtained to ensure NEPA requirements, and tribal consultations are addressed. Like any good exploration strategy/plan, delays are expected and worked into the exploration timelines. Since the Navy GPO works at the pleasure of the commands we are servicing, planning the work around the training missions requires flexible contractor support and strong relationships with base personnel.

The Navy GPO scheduled a number of exploration endeavors (with contractor support from SEI Group, Inc.) in the summer of 2010; that work included: shallow temperature probe surveys, LiDAR and Hyper spectral acquisition/analysis, and temperature gradient drilling. The Navy GPO is also mining both existing geophysical and drilling data that was collected in Dixie Valley as part of previous research studies or exploration efforts. The following is a description of the ongoing exploration on NAS Fallon lands in Dixie Valley:

Temperature Gradient Drilling

The Navy GPO (with contract support from Dan's Water Well and Pump Service- Tracy, CA), drilled 24-500' Temperature Gradient Holes (TGH's) on NAS Fallon lands from August – November 2010 using ARRA funding. Twenty of those holes were drilled in Fairview and Southern Dixie Valley (Figure 2). Two of those twenty had temperatures > 50°C, with the hottest of those holes being TGH-77 (77.3^{o}C), followed by TGH-104 (51.1 ^{o}C) (Figure 3).

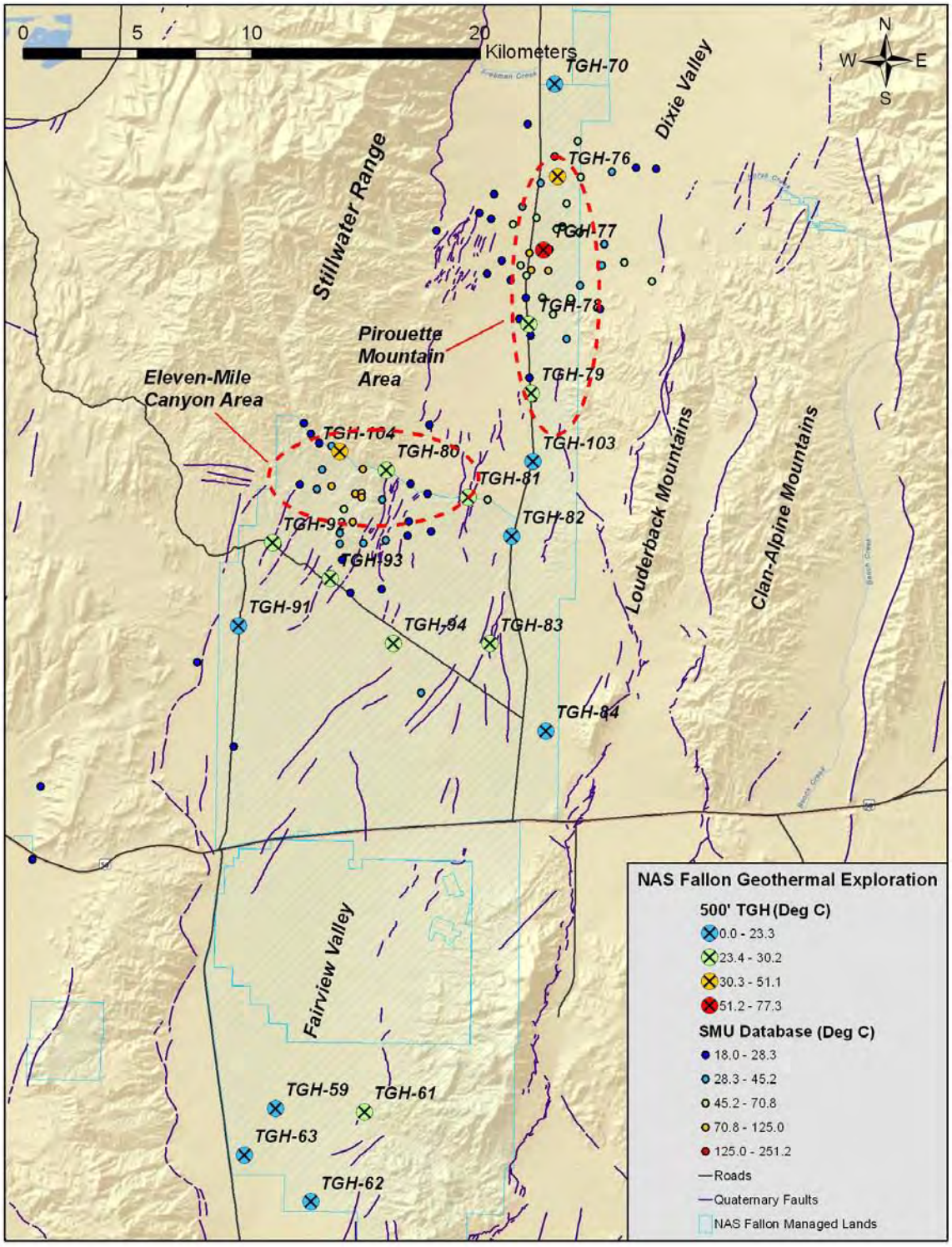

Figure 2. Location of twenty, shallow temperature gradient holes, drilled in Fairview and Southern Dixie Valley. The shallow gradients correlate with previous Hunt exploration drilling from the 1970's (courtesy of SMU database).

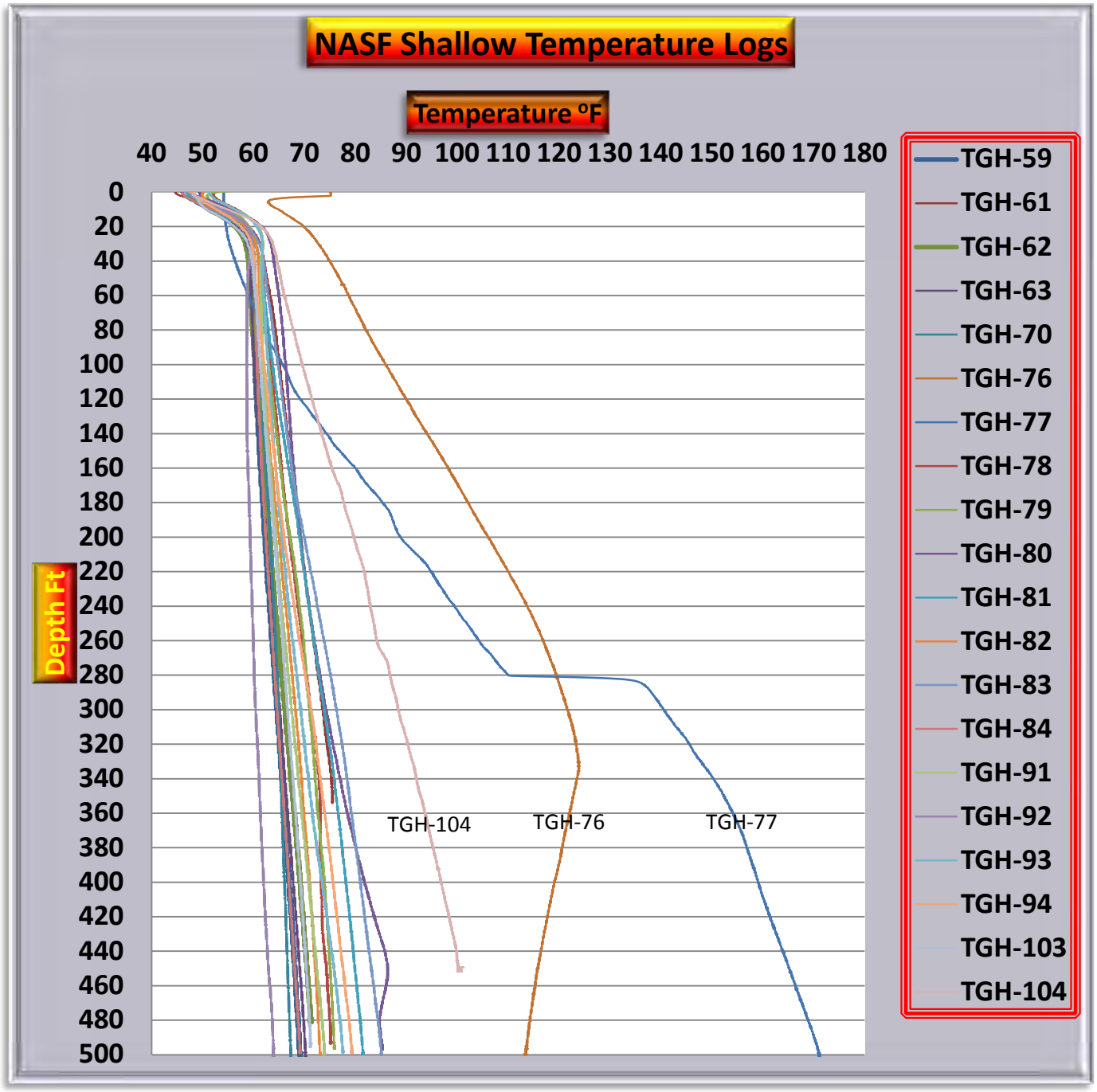

Figure 3. Graph of Temperature profiles for the 20-500' Temperature Gradient Holes drilled in Fairview Valley and Dixie Valley in the Fall of 2010. TGH-77 reached a maximum temperature of 171°F (77°C) at a depth of 500' (150m).

The temperatures encountered at the Pirouette Mountain and Eleven-Mile Canyon areas validate Hunt Exploration data the Navy GPO has been pursuing (Bowers, 2010-11). Hunt Energy

drilled multiple 500', 2000', and even a 7300' hole at the Pirouette Mt area (Figure 2); the Navy GPO is currently pursuing both geophysical and geological logs that may exist from Hunt Energy's files. This data is currently being stored at Southern Methodist University and the Navy GPO is currently working with SMU faculty and staff to acquire this data.

LiDAR Analysis

High resolution LiDAR was collected over NAS Fallon Managed lands with a vertical accuracy < 13 cm in the fall of 2010 (Figure 4). LiDAR permits the imaging of very small irregularities in the surface of the earth that generally go undetected by conventional field mapping. In particular, this technology can be extremely helpful in identifying fault scarps that are present in unconsolidated sediments that are indicative of Holocene tectonic activity (Monastero and Coolbaugh, 2007). Mapping young active faults that could be potential conduits for fluid flow is a common exploration approach for any geothermal exploration campaign; active faults are a common occurrence in geothermal systems (Sabin et. al, 2004, Bell and Ramelli, 2009). NAS Fallon lands cover more than 241,000 acres and by acquiring LiDAR data, the Dept. of the Navy and its sub-contractors are able to focus their efforts and field observations on areas where fault's are detected (Figure 4).

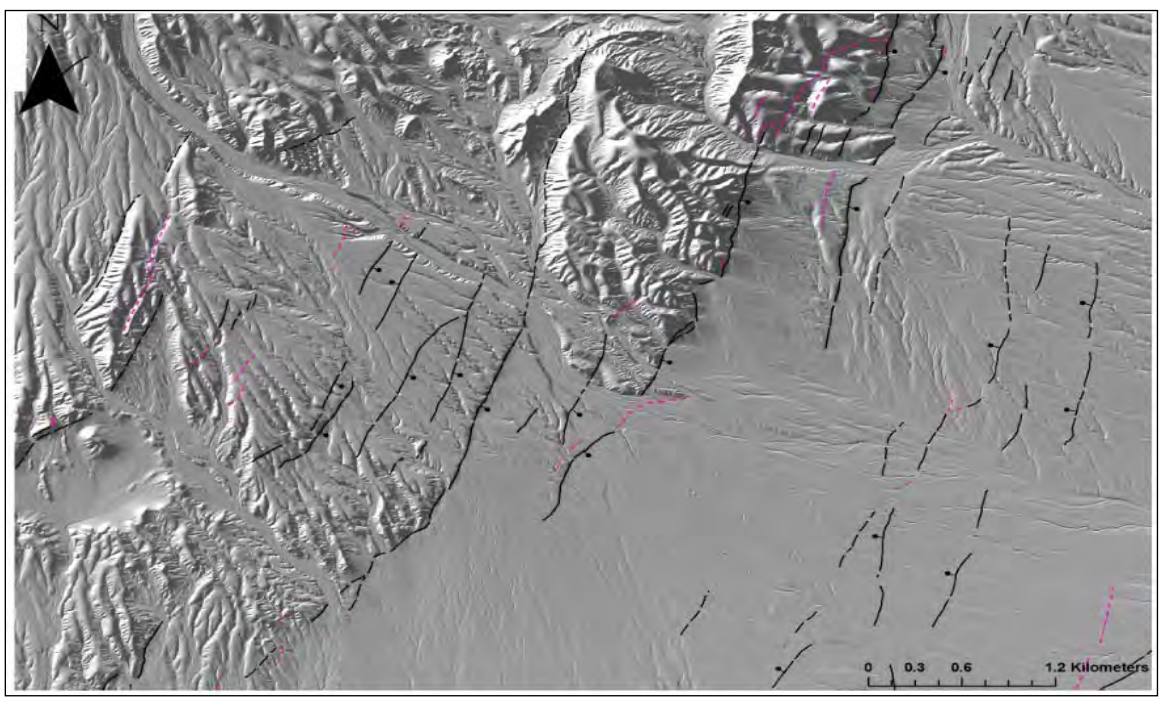

Figure 4. Map illustrating LiDAR imagery and NNE trending faults in LaPlata Canyon. Lines highlighted in red are faults that experienced 1954 rupture. (Figure courtesy of Helton et. al, 2011).

Shallow Temperature Probe Surveys

The most significant shallow temperature anomaly was found at the Pirouette Mountain area (Figure 5). This area was previously identified from drilling back in the late 1970's by Hunt Exploration. A more recent gradient hole (TGH-77), drilled by the Navy Geothermal Program, found a temperature of 171°F (77°C) at a depth of 500' (150m). No shallow temperature surveys have previously been conducted in the Pirouette Mountain area. The two-meter anomaly found here is characterized by temperatures 3-4 °C above background, and covers a north-south trending area 3-5km long (Skord et. al, 2011).

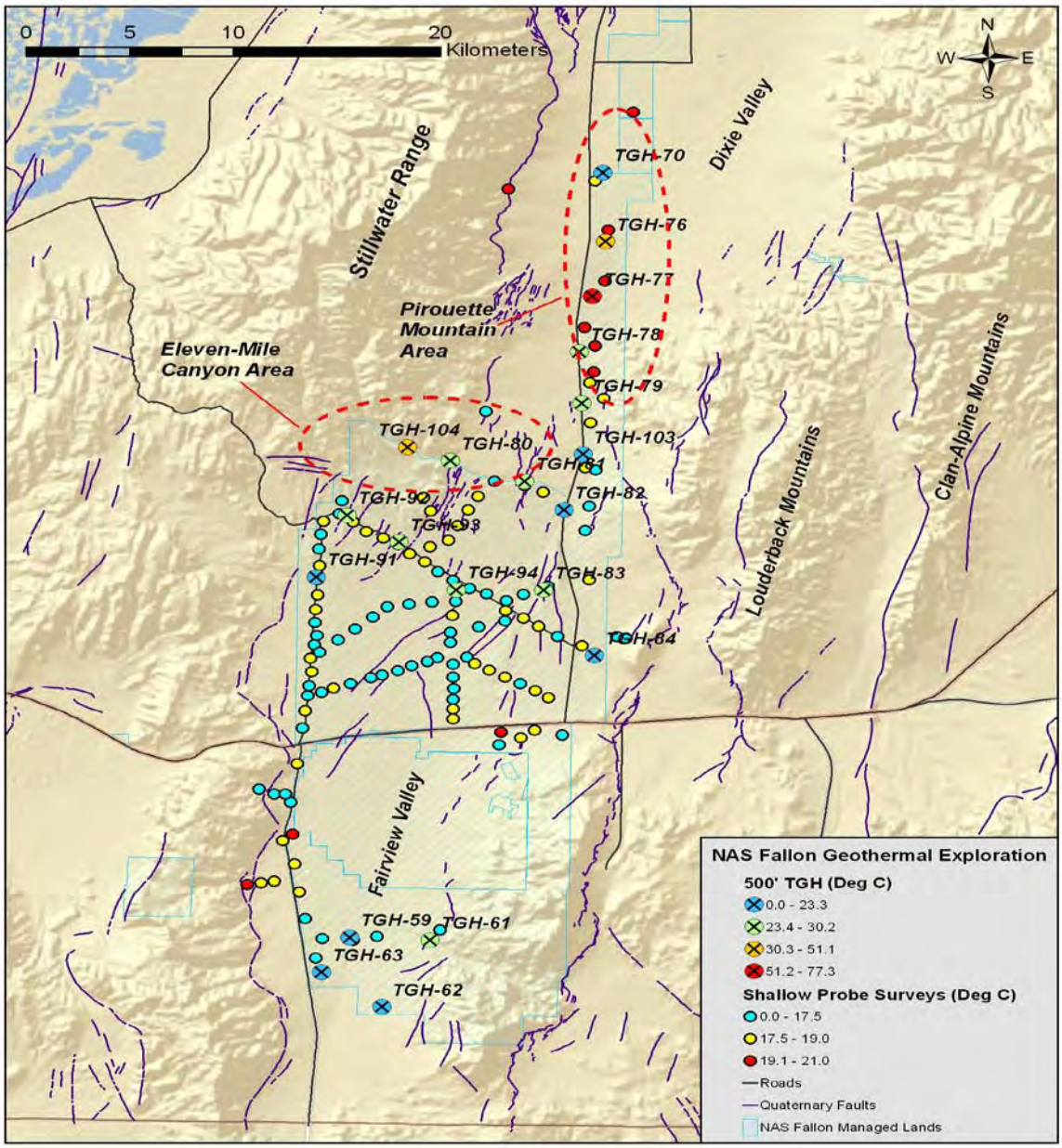

Figure 5. Map illustrating shallow probe survey results for Fairview Valley and Southern Dixie Valley.

Additional Geophysical Exploration

Based on the previous geophysical work in and around the project area, we have begun to implement an exploration strategy of collecting higher density gravity stations, an aeromagnetic survey, as well as ground MT work (Figures 6). The Navy is pursuing efforts to piggyback an existing Department of Energy funded EGS methodology project (DE-EE0002778). In 2010, the Department of Energy awarded a cost-share grant to AltaRock Energy, Inc.; AltaRock is conducting an Engineered Geothermal System (EGS) Exploration Methodology project in the northern portion of Dixie Valley approximately centered on the existing geothermal electrical production field (Figure 6).

A necessary consequence of this endeavor is also the definition of the geological exploration characteristics of the Dixie Valley hydrothermal system(s) (i.e., hot, high permeability, essentially fractured rocks, conducting fluid). As part of this proposal, various geophysics will be acquired such as MT, Gravity, and Aeromagnetics (Figure 6).

Existing gravity and magnetic data will be collated for Dixie Valley and joint magnetic/gravity inversion models will be created for these data, with a focus on improving site selection for hydrothermal geothermal resources.

In the efforts of progressing new technology to the geothermal industry, we are acquiring a small ZTEM spec survey through Geotech LTD. Geotech LTD. , coordinating flight acquisition through NAS Fallon Range Operations, is scheduled to acquire, process, and interpreting Z-TEM (Z-Axis Tipper Electromagnetic). The area of acquisition is the Eleven-Mile Canyon Area (Figure 6) This system is an innovative airborne EM system which uses the natural or passive fields of the Earth as the source of transmitted energy. GPO will use new inversion techniques and compare with MT results when acquired. With these datasets, as well as results from shallow drilling and previous geologic work, the Navy GPO will have a very good understanding of the density, susceptibility, and conductive properties of the subsurface in southern Dixie Valley.

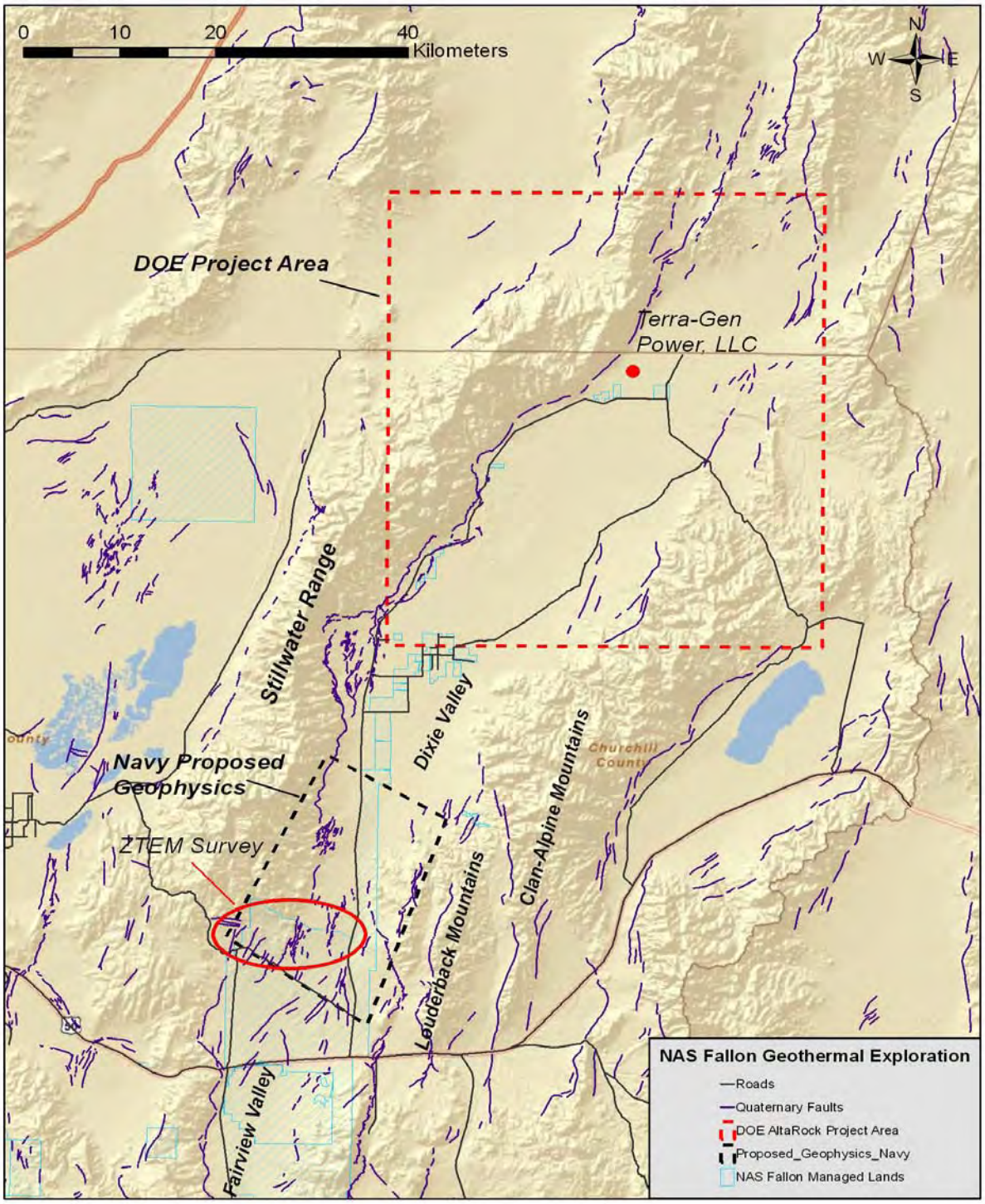

Figure 6. Map illustrating the location of geophysical surveys being pursued by the Navy GPO to further define the subsurface structure influencing shallow temperatures at the Eleven Mile Canyon and Pirouette Mountain Areas. The Navy GPO is pursuing detailed gravity, aeromagnetics, and MT surveys through DOE project (DE-EE-0002778).

Conclusions

Preliminary results indicate elevated shallow temperatures at depth in the Pirouette Mountain and Eleven Mile Canyon areas, verified by shallow probe surveys and shallow temperature gradient holes drilled. These elevated drilling temperatures validate previous drilling data that is currently being mined for geophysical and geologic data; also, to reduce redundant exploration and drilling efforts. As many as a dozen additional shallow temperature gradient holes will be drilled in Southern Dixie Valley to further determine the extent of the anomalies at Eleven-Mile Canyon and Pirouette Mountain as well as explore prospects from the ongoing data mining endeavor. LiDAR and Low-Sun Angle Photography have exposed previously unidentified faults in Dixie Valley and have validated the presence of fault terminations believed to be contributing to the Eleven-Mile Canyon and Pirouette Mountain geothermal anomalies (Mankemthong, 2008; Helton et. al, 2011). Additionally, the GPO is also pursuing several geophysical surveys that will yield detailed subsurface information, much needed to determine subsurface structures and conductivity of the Eleven-Mile Canyon and Pirouette Mountain areas. The synthesis of all these data will be tested with the drilling of two or three intermediate/deep slim holes, scheduled for calendar year, 2012.

Acknowledgements

The Department of the Navy Geothermal Program Office would like to recognize the NAS Fallon NSAWC Range Operations, NAS Fallon Range Scheduling, Public Works, and Environmental offices. These offices were responsible for coordinating access for drilling, assisting in the flight scheduling for acquiring LiDAR, Hyper spectral, LSA, and providing environmental oversight and guidance to ensure all NEPA requirements were met.

References

Abbott, R., E., and Louie, J., N., 2001. “Geophysical Confirmation of Low-Angle Normal Slip on the Historically Active Dixie Valley Fault, Nevada.” Journal of Geophysical Research, v. 106, p. 4169-4182.

Blackwell D, Wisian K, Benoit D, Gollan B., 1999, Structure of the Dixie Valley Geothermal System, a “Typical” Basin and Range Geothermal System, From Thermal and Gravity Data: Geothermal Resource Council Transactions. V. 23, p. 525-531.

Blackwell, D.D., Smith, R.P., Waibel, A., Richard, M.C., and Stepp, P., 2009, Why Basin and Range Systems are Hard to Find II: Structural Model of the Producing Geothermal System in Dixie Valley, NV: *Geothermal Resources Council Transactions*, v. 33, pp. 441-446.

Bowers, Roger. Multiple Telephone Interviews regarding Hunt Energy Exploration data (December 2010 - February 2011).

Caskey, S. J., and Wesnousky, S. G., 1997, Static Stress Changes and Earthquake Triggering during the 1954 Fairview Peak and Dixie Valley Earthquakes, Central Nevada, Bull. Of the Seis. Soc. Of America, Vol. 87, No. 3, pp. 521-527

Faulds, J.E., Coolbaugh, M.F., Vice, G.S., and Edwards, M.L., 2006, Characterizing Structural Controls of Geothermal Fields in the Northwestern Great Basin: A Progress Report: *Geothermal Resources Council Transactions*, v. 30, pp. 69-76.

Grauch, V. J. S., 2002. "High-Resolution Aeromagnetic Survey to Image Shallow Faults, Dixie Valley Geothermal Field, Nevada." United States Geological Survey Open File Report 02-384, 13pp.

Helton, E., Bell, J.W., Cashman, P.H., Lazaro, M., Alm, S. Structural Analysis of Southern Dixie Valley using LiDAR and low-sun-angle aerial photography, NAS Fallon Geothermal Exploration Project, Dixie Valley, Nevada, 2011 GRC Paper Submission.

Herring, A. T., 1967. "Seismic Refraction Study of a Fault Zone in Dixie Valley, Nevada, in Thompson, G. A., ed., Geophysical Study of Basin-Range Structure, Dixie Valley region, Nevada." Hanscom Bedford, Mass., Air Force Cambridge Research Laboratories, 274 pp.

John, D.A., Tilted middle Tertiary ash-flow calderas and sub adjacent granitic plutons, southern Stillwater Range, Nevada: Cross sections of an Oligocene igneous center, Geol. Soc. Am. Bull., 107, 180-200, 1995.

Kratt, C., Calvin, W., and Coolbaugh, M.F., 2006, Geothermal exploration with HyMap hyperspectral data at Brady-Desert Peak, Nevada; Remote Sensing Environment, v.104, p.313-325.

Mankhemthong, Niti. Structure of the inter-basin transition zone between Dixie Valley and Fairview Valley, Nevada, USA. MS theses. University of Nevada, Reno. 2008.

Monastero, F.C., Coolbaugh, M.F. 2007, Advances in Geothrmal Resource Exploration Circa 2007: Geothermal Resources Council Transactions, v.31, pp. 23-29.

Okaya, D. A., and G. A. Thompson, 1985. "Geometry of Cenozoic Extensional Faulting, Dixie Valley, Nevada." Tectonics, v. 4, p. 107-125.

Sabin, A.E., Walker, J.D., Unruh, J.R., and Monastero, F.C., 2004, Toward the development of occurrence models for geothermal resources in the western United States; Geothermal Resources Council Transactions, v. 28, p.41-46.

Schaefer, D. H., 1983. "Gravity Survey of Dixie Valley West-Central Nevada." U.S. Geological Survey Open-File Report, p. 82-111.

Skord, J., Sladek C., Coolbaugh M., Cashman P.H., Lazaro M., Kratt C. Two-Meter Temperature Surveys for Geothermal Exploration Project at NAS Fallon, 2011 GRC Paper Submission.

Smith, R. P., V. J. S. Grauch, and D. D. Blackwell, 2002. "Preliminary Results of a High- Resolution Aeromagnetic Survey to Identify Buried Faults at Dixie Valley, Nevada." Geothermal Resources Council Transactions, v. 26, p. 543-546.

Wannamaker, Philip E., William M. Doerner, and Derrick P. Hasterok. "Cryptic Faulting and Crustal Scale Fluid Interconnections in the Great Basin Extensional Province, Nevada and Utah; Implications from Deep MT Resistivity Surveying; Geological Society of America, 2005 Annual Meeting." Abstracts with Programs - Geological Society of America 37.7 (2005).

Structural analysis of southern Dixie Valley using LiDAR and low-sun-angle aerial photography, NAS Fallon Geothermal Exploration Project, Dixie Valley, Nevada

Erica L. Helton[1,2], John W. Bell[3], Patricia H. Cashman[1,2], Michael Lazaro[4], Steve Alm[4]

[1]Department of Geological Sciences and Engineering, University of Nevada, Reno, [2]Great Basin Center for Geothermal Energy, [3]Nevada Bureau of Mines and Geology, University of Nevada, Reno, [4]Department of the Navy Geothermal Program Office

Keywords: Dixie Valley, Nevada, geothermal, LiDAR, low-sun-angle aerial photography

Abstract

The goal of this study is to map and characterize Quaternary faults in southern Dixie Valley for the Department of the Navy Geothermal Program Office's NAS Fallon Geothermal Exploration Project. We will use this information to better characterize the regional structure and geothermal resource potential of the area, with a focus on determining the structural controls for two known geothermal anomalies. Previous structural investigations at other geothermal sites in Nevada have shown that Quaternary faults provide the best potential for geothermal fluid flow. Information on the structural characteristics, such as slip sense and relative age, will be synthesized into a structural kinematic model. The resulting structural kinematic model will help us identify the slip and dilation tendencies of the faults in southern Dixie Valley. This model will for allow a better understanding of what faults control these two geothermal anomalies and aid in exploration and selection of drilling targets.

In order to detect and characterize young faults, high resolution LiDAR and 1:12,000-scale low-sun-angle (LSA) aerial photography was acquired for the NAS Fallon study area. The LSA photos were flown during early morning, when the sun angle ranged between 10-25°. Slopeshades and hillshades using low sun angles (25-45°) were generated using LiDAR for fault detection. Elevation change and tonal lineaments were used to define possible faults in both the LiDAR and LSA photo data sets.

The LiDAR and LSA photo analysis has identified a large number of previously unmapped faults. Field investigations will determine slip sense and age of these newly mapped faults. Preliminary structural analysis using the newly mapped faults, in conjunction with shallow 2-meter temperature surveys, suggests that the two known geothermal temperature anomalies occur

in complex structural settings. A possible 3rd low temperature anomaly was also detected, but will require further investigation.

Introduction

The study area is located in southern Dixie Valley (Figure 1), which is 64 km south of the Dixie Valley geothermal power plant. The Dixie Valley geothermal power plant utilizes the hottest known geothermal system in Nevada (285°C at 3 km) (Blackwell et al., 2009). The Department of the Navy Geothermal Program Office's NAS Fallon Geothermal Project is evaluating geothermal resource potential in the southern part of the valley.

Although northern Dixie Valley has been termed a west-tilted half graben (Okaya and Thompson, 1985), the project area is bounded by active faults on both the east and west sides. Southern Dixie Valley (Figure 1) is bounded to the west by the northeast-trending, down-to-the-east Stillwater and Sand Springs range front faults. It is bounded to the east by the north-trending, down-to-the-west Louderback fault.

The project area experienced surface rupture during the December 16, 1954 Fairview Peak-Dixie Valley earthquakes (Figure 1; Caskey, 1996). The Fairview Peak (M_s 7.2) event was followed 4 minutes and 20 seconds later by the Dixie Valley (M_s 6.8) event. Caskey et al. (1996) described the surface rupture along the Louderback Mountains fault. Approximately 1-1.5 m of offset was recorded on the Louderback Mountains fault, and based on offset stream channels, the faulting was right-oblique. Kinematic models of the 1954 surface ruptures associate the rupture along the Louderback Mountains fault with the Fairview Peak event (Caskey et al., 1996).

Preliminary field reconnaissance and analysis of existing geologic mapping suggests that there is no surface expression related to recent geothermal activity in the study area, i.e. no hot springs, sinter or travertine deposits, or hydrothermal alteration (John, 1993; John and Silberling, 1994; John, 1995; John, 1997). Alteration related to Mesozoic plutonism and Tertiary volcanism is present throughout southern Dixie Valley, but plutonism and volcanism ceased by middle Miocene (John and Silberling, 1994).

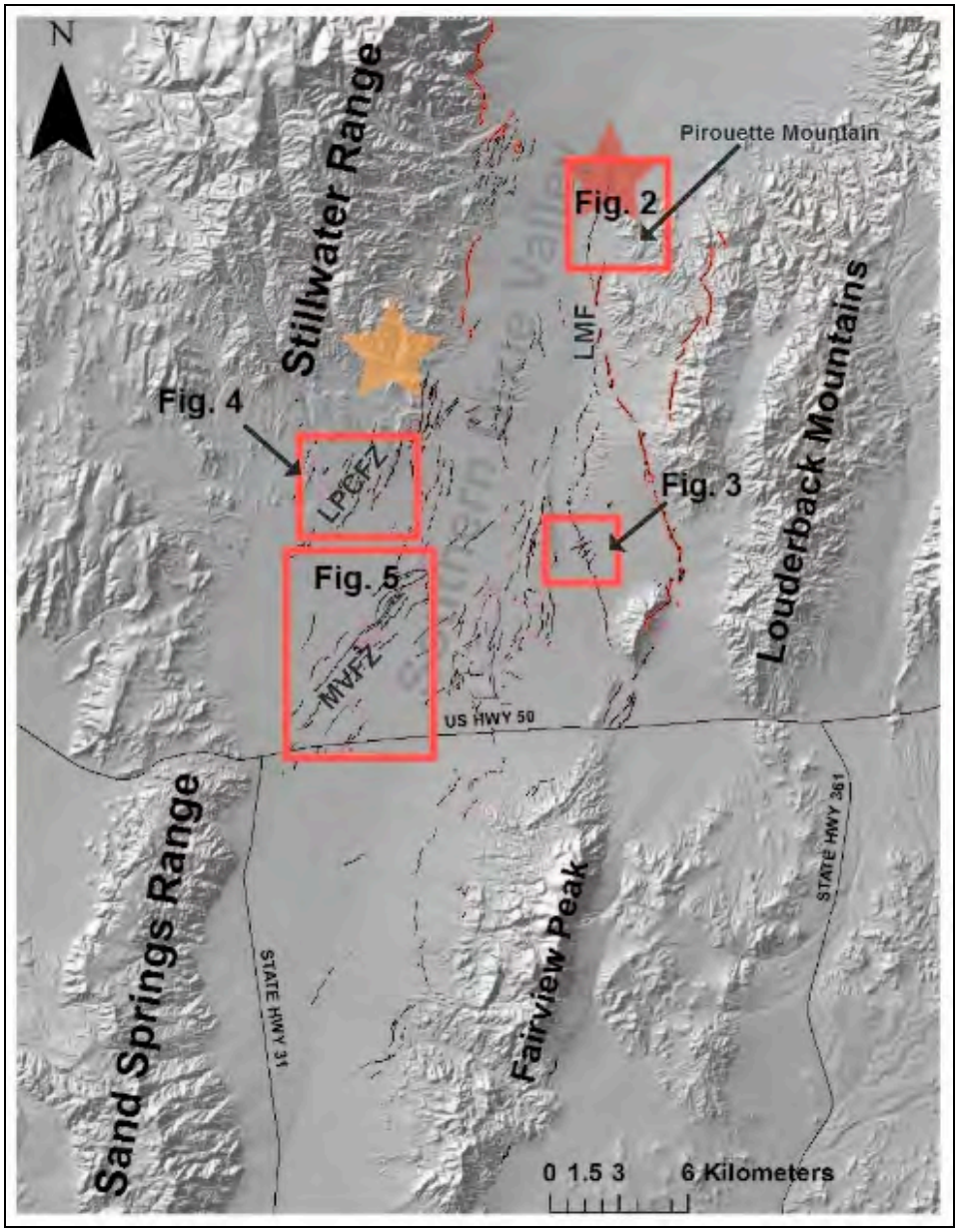

Figure 1. Location map of the general project area in southern Dixie Valley. Only Quaternary fault traces have been mapped. Solid black lines represent well located faults, dashed black lines represent approximately located faults, and dotted black lines represent faults that are inferred. Lines highlighted in red are faults that experienced 1954 rupture (Caskey et al., 1996). Pink dashed lines indicate lineaments seen in aerial photography and LiDAR. LMF: Louderback Mountains Fault. LPCFZ: La Plata Canyon Fault Zone. MVFZ: Mid-Valley Fault Zone. The red star represents the approximate location of the Pirouette Mountain geothermal anomaly. The orange star represents the approximate location of the Elevenmile Canyon geothermal anomaly. Red numbered rectangles indicate areas of subsequent figures.

Two potential geothermal resources in the project area have been identified based on existing temperature gradient well data: Elevenmile Canyon and Pirouette Mountain (Figure 1; Blackwell et al., 2009; Mankhemthong et al., 2008). Our goal is to characterize the age, slip-sense, and orientation of the structures within these two geothermal systems. These data will be used to create a conceptual structural-kinematic model of southern Dixie Valley

Methods

A spatial relationship between Quaternary faults and potential geothermal resources has been recognized in previous studies in Nevada (Bell and Ramelli, 2009). We have created a detailed preliminary Quaternary fault map of southern Dixie Valley to better understand the spatial relationship between Quaternary faulting and the geothermal anomalies in the project area (Figure 1). In addition to fault detection using the remote sensing techniques that are the focus of this paper, creation of the fault map also involved digitization of an historic fault rupture map (Caskey, 1996) using ArcGIS software. Information on the structural characteristics of the Quaternary faults, such as slip sense and relative age, will be synthesized into a conceptual structural-kinematic model of southern Dixie Valley. The resulting kinematic model will help us identify the slip and dilation tendencies of the faults in the study area, most importantly those within the two geothermal anomalies.

In order to detect and characterize Quaternary faults, high resolution LiDAR and large-scale low-sun-angle (LSA) aerial photography were acquired for the NAS Fallon study area. The LiDAR and LSA photo acquisitions were funded by the Department of the Navy Geothermal Program Office. LiDAR was acquired at a point resolution of 8.6 points/m^2, providing a vertical accuracy of 3.7 cm/m^2.

The LiDAR analysis involved processing various iterations of bare-earth slopeshades and hillshades of the area. We used elevation change and tonal variation to delineate potential fault scarps and other areas of interest to be investigated in the field. Preliminary hillshade analysis has shown that the best sun azimuths for fault detection are those that provide light oblique to the orientation of a fault. The best sun angles have been low, approximately 20-45°, mimicking either early morning or late afternoon sunlight.

Low-sun-angle aerial photography was flown at 1:12,000 scale under early morning sun conditions, with sun angles ranging between approximately 10-25°. The low-sun-angle methodology, like LiDAR, is useful for detecting small amounts of offset on young fault scarps and is considered a complementary tool. The newly acquired LSA aerial photos together with existing LSA photography were used to define tonal lineaments and vegetation that could not be detected as well in the LiDAR data set. Preliminary analysis of this data set has shown that LiDAR illuminates features that do not appear in the LSA aerial photos. Conversely, LSA aerial photos allow identification of cultural features that may appear to be faults on the LiDAR. Based on this information, the combination of these two techniques provide a more thorough structural investigation.

Results

Preliminary Quaternary fault mapping has shown that southern Dixie Valley is dominated by several structural zones: the Louderback Mountains fault (LMF), the La Plata Canyon fault zone (LPCFZ), and the Mid-Valley fault zone (MVFZ). Four areas illustrate the principal Quaternary faults detected in these structural zones using the LSA photos and LiDAR data set (Figure 1). These areas are likely the primary structural components for the kinematic fault model that may explain the occurrence of the geothermal anomalies.

Louderback Mountains Fault

The Louderback Mountains fault (LMF) bounds the western side of the Louderback Mountains and the eastern side of southern Dixie Valley. At the northern end of the LMF, near Pirouette Mountain, there is one main fault that has been identified (Figure 2). This fault trends approximately due north and is down-to-the-west. Preliminary LiDAR and LSA photo analysis have detected normal motion along this fault; however, the southern portion of the LMF ruptured in 1954, and right-oblique motion was recorded (Caskey et al., 1996). A trench study has been planned for the northern segment of the fault in Figure 2 for summer 2011 to better constrain the age and slip sense for the northern portion of the Louderback Mountains fault.

Shallow 2-meter temperature surveys were performed in this area during late summer and fall of 2010 (Skord et al., this volume). The highest shallow temperatures in the study area were recorded at the north end of the LMF, in the area of the Pirouette Mountain geothermal anomaly

(Figure 1; Figure 2). Previous authors have extended this anomaly farther to the north and west of the termination of the LMF (Blackwell et al., 2009; Mankhemthong et al., 2008), but these elevated temperatures at depth are also being reflected at shallow depth near and directly west of the LMF trace.

At the southern end of the LMF, we detected fault sets of two different orientations on the LiDAR: due north and NNE (Figure 3). Based on the crisp tone and sharpness of the lineaments in contrast with other faults and lineaments in the project area, we interpret the NE trending faults that cross-cut the N-S trending fault in Figure 3 to be possible unmapped surface ruptures from the 1954 Fairview Peak event. These features trend more towards the east and are southwest of the ruptures associated with the 1954 sequence (Figure 1). The faults appear to have experienced only normal slip; no dextral motion was detected on these faults. Further field investigations will be required to determine whether or not these faults represent historic surface rupture and whether the cross-cutting fault relations play a structural role in the resource potential on the LMF.

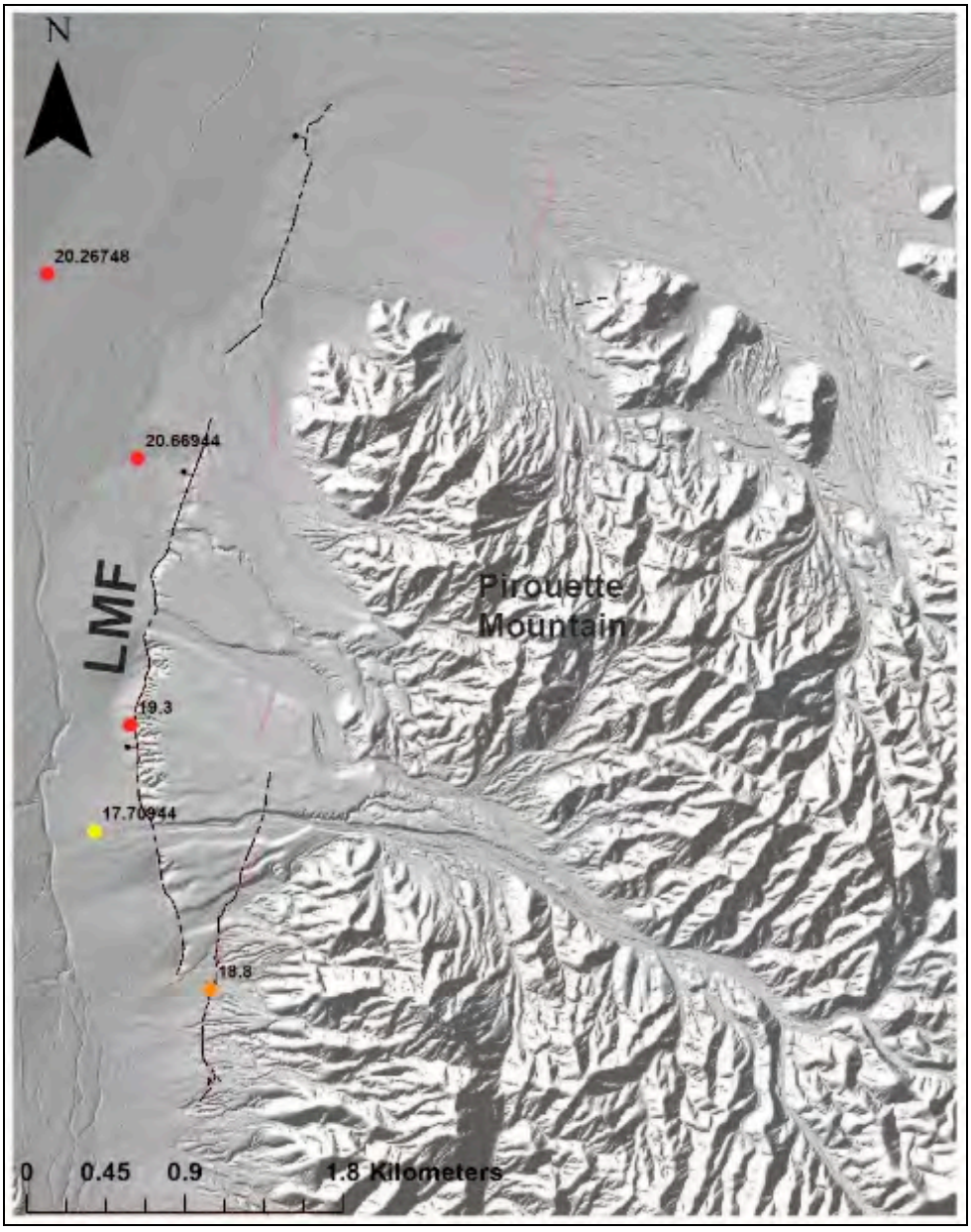

Figure 2. LiDAR image of the Pirouette Mountain area, at the north end of the Louderback Mountains fault (LMF). Bar and ball on downthrown side of fault. Red, orange, and yellow points indicate places where shallow 2-meter temperature surveys were performed (Skord et al., 2011). Temperatures in degrees Celsius are next to the points, rounded to the 5th significant figure. Background 2-meter shallow temperature: ~17°C. See Figure 1 for location.

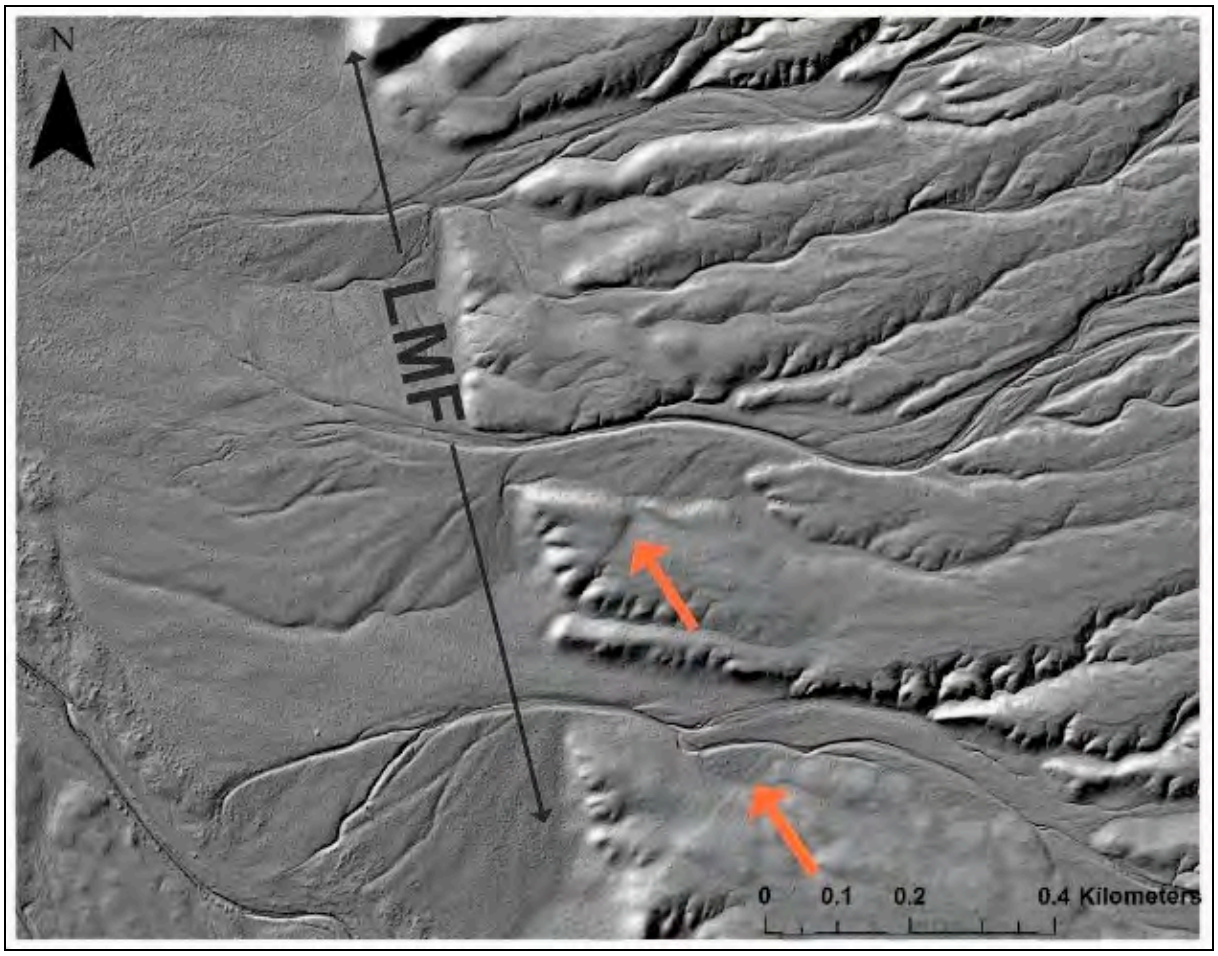

Figure 3. LiDAR image of the southern end of the Louderback Mountains fault (LMF). Orange arrows are pointing to NE trending faults which cross-cut the more prominent N-S trending fault. See Figure 1 for location.

La Plata Canyon Fault Zone

The LPCFZ is located in the southern Stillwater Range, at the mouth of La Plata Canyon (Figure 4). The faults at the mouth of La Plata Canyon trend approximately NNE and are down-to-the-east. The faults that are approximately 2 km to the WSW of the mouth of the canyon also trend NNE, but are down-to-the-west. These two fault sets appear to form graben-in-graben structures at the mouth of La Plata Canyon. Previous trench studies across a fault segment in La Plata Canyon indicated that the Quaternary motion along these faults has likely been only dip-slip, and that the most recent slip occurred during late Holocene time (Bell et al., 2004).

The LPCFZ is located approximately 6 km south-southwest of the Elevenmile Canyon geothermal anomaly. A 2-meter temperature survey was performed in La Plata Canyon during

the same time as the survey in the Pirouette Mountain area (Figure 2). No 2-meter temperature anomalies were anticipated in this area prior to survey, but a low-temperature anomaly was recorded (Figure 4). Further temperature surveys in the LPCFZ will be performed summer in 2011, closer to the faults to see if hotter shallow temperatures occur. If hotter temperatures do occur, further field work will be required to determine whether this is related to the geothermal anomaly to the north, or a new, previously unidentified system that may separately be related to the La Plata Canyon faults.

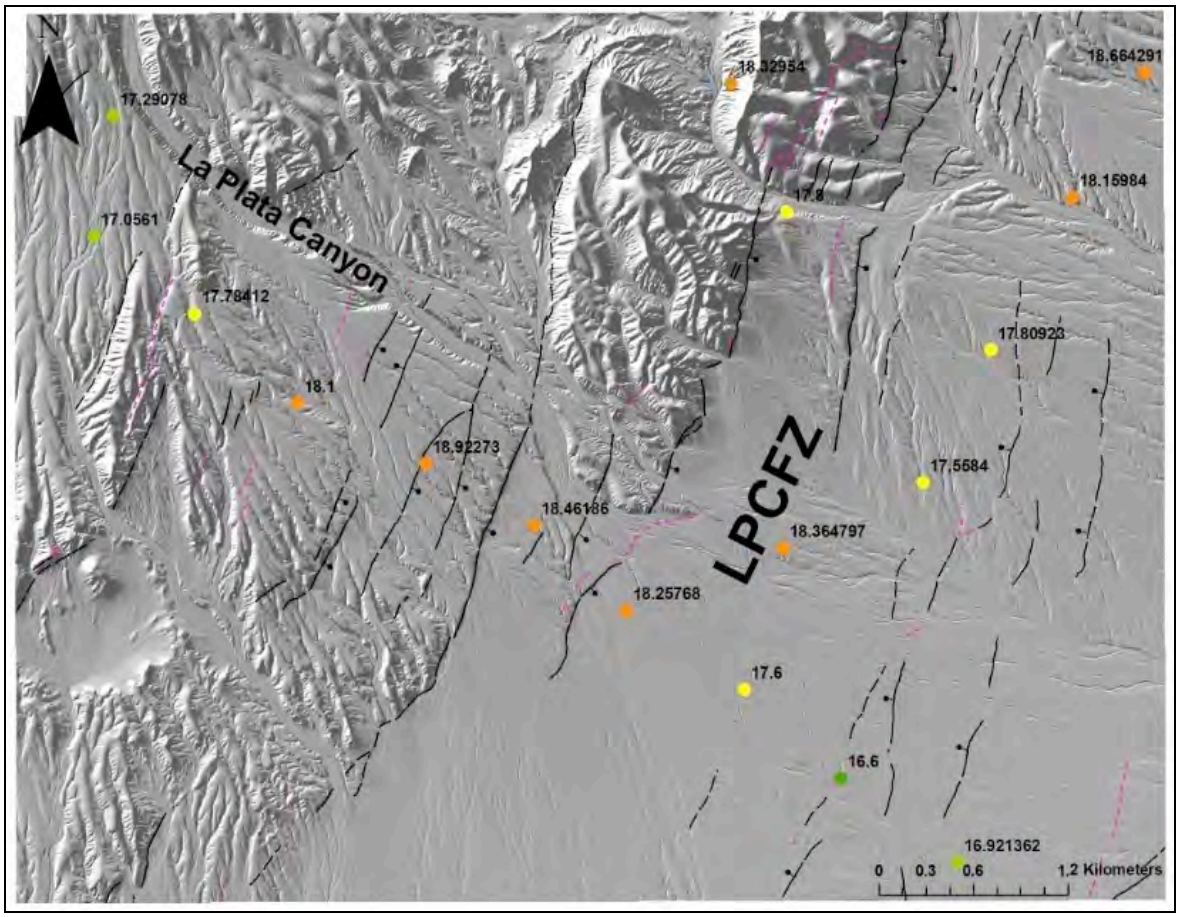

Figure 4. LiDAR image of NNE trending faults within the La Plata Canyon Fault Zone (LPCFZ). Bar and ball on downthrown side of fault. Red, orange, and yellow points indicate places where shallow 2-meter temperature surveys were performed (Skord et al., 2011). Temperatures in degrees Celsius are next to the points, rounded to the 5th significant figure. Background 2-meter shallow temperature: ~17°C. See Figure 1 for location.

Mid-Valley Fault Zone

The faults in the MVFZ were mostly undetected prior to the LiDAR acquisition (Figure 5). These mid-valley structures trend approximately N45E, oblique to the general northerly trend of the Stillwater, Sand Springs, and Louderback Mountains faults. Upon preliminary analysis using only the LiDAR, the faults appear to exhibit only normal motion, with either NW or SE dip directions. Based on apparent dip direction inferred from the LiDAR, these structures appear to form a series of complex nested graben. The faults are oriented approximately perpendicular to the ~N60W Basin and Range extension direction (Hammond and Thatcher, 2007); although this is a favorable orientation for fault extension, the shallow 2-m temperatures are not significantly elevated (Figure 5). Based on this relationship, these faults could be some of the youngest prehistorical structures in the study area. Based on fault orientation alone, these faults do not appear to fall into the Sand Springs, Stillwater, or Louderback fault systems, but they may be kinematically linked and further field analysis is underway to determine this.

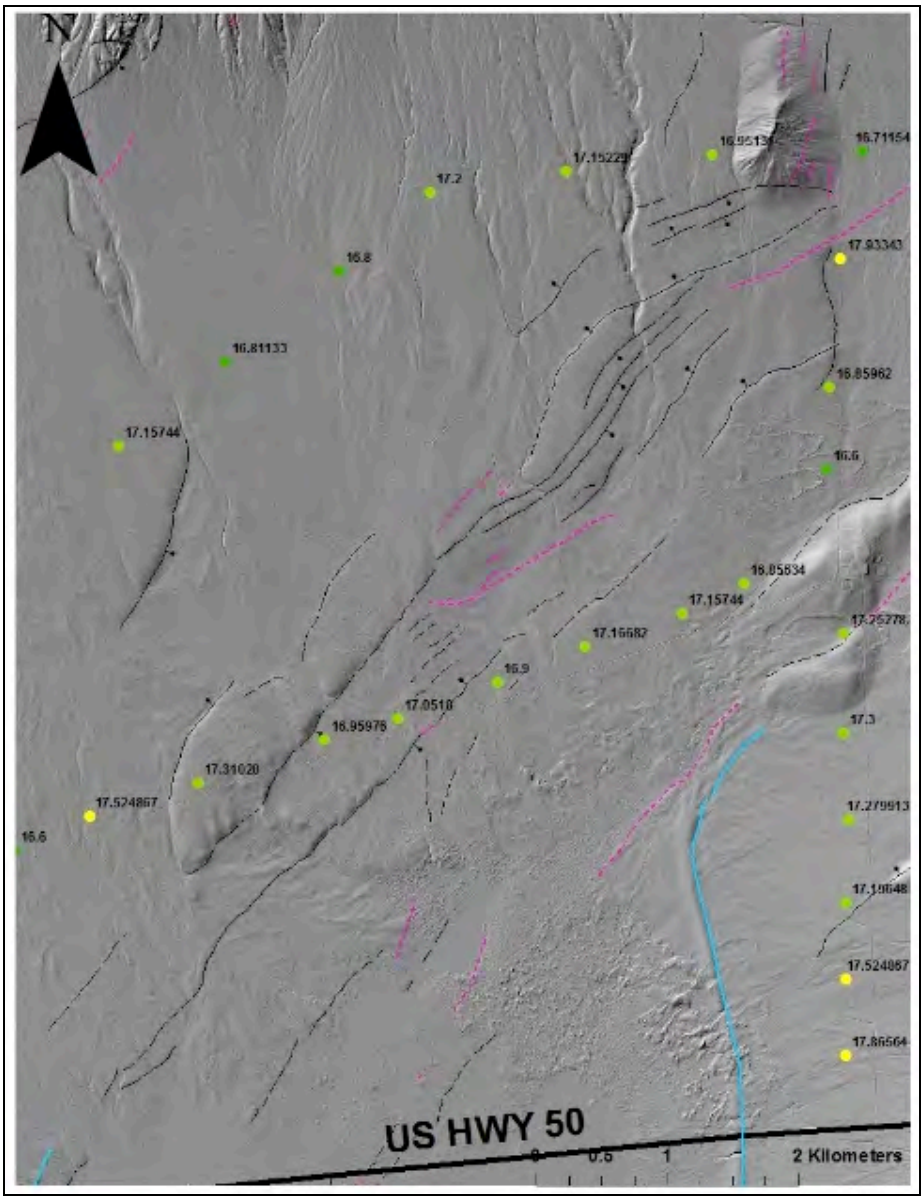

Figure 5. LiDAR image of NE-trending faults in the Mid-Valley Fault Zone (MVFZ). Blue line represents a possible shoreline. Bar and ball on downthrown side of fault. Red, orange, and yellow points indicate places where shallow 2-meter temperature surveys were performed (Skord et al., 2011). Temperatures in degrees Celsius are next to the points, rounded to the 5th significant figure. Background 2-meter shallow temperature: ~17°C. See Figure 1 for location.

Preliminary Structural Models

Pathways for upward migration of geothermal fluids are largely dependent upon the slip and dilation tendencies of the faults, with dilation being considered one of the most important factors

(Moeck et al., 2010). Slip and dilation tendencies are dependent upon fault orientation and geometry within the present stress field. Understanding the structural kinematic motion of these faults is key to developing a conceptual exploration model. Some previous studies have shown that geothermal systems in the Basin and Range often occur at fault terminations or in fault step-over (releasing bend) zones (Faulds et al., 2006). This is likely due to the enhanced permeability created by these structural features. While one or both of these models may apply to the two anomalies within the project area, it is important to note that there are multiple kinematic models which could create fault dilation. The structural zones in southern Dixie Valley may be linked, meaning that movement on one fault, or within one fault zone, may create dilation on another set of adjacent faults.

The Pirouette Mountain geothermal anomaly appears to occur near the termination of the LMF. LiDAR and LSA photo analysis shows no other faults in the area of the Pirouette Mountain anomaly, only the N-S trending, down-to-the-west fault trace seen in Figure 2. However, it is possible that a continuation of the LMF is concealed beneath alluvium to the north. It is poorly understood why the Pirouette Mountain anomaly, if it is related to the N-S trending LMF, occurs where it does, because the LMF is not optimally oriented for dilation in the current N60W stress regime.

The faults in La Plata Canyon may comprise a structural step-over between the Sand Springs and Stillwater range front fault systems. Based on the Faulds and Varga (1998) model, the Sand Springs and Stillwater range front faults may be connected by a right-stepping accommodation (releasing bend) zone within the La Plata Canyon area. At the same time, the La Plata Canyon faults in the step-over strike north towards the Elevenmile Canyon thermal anomaly, suggesting that the anomaly may also be related to the La Plata Canyon fault. However, these structural relations are presently being studied, and it is not clear whether or not the LPCFZ and the Elevenmile Canyon anomaly are genetically related.

As noted, faults within the MVFZ are preferentially oriented for dilation, as they are roughly perpendicular to the N60W Basin and Range extension direction (Hammond and Thatcher, 2007), but no shallow temperature anomalies have been recorded (Skord et al., 2011). Preliminary analysis of this fault zone suggests that it contains numerous young (Holocene-age) faults that may structurally link the northern end of the Sand Springs fault zone with the Louderback Mountain fault zone. This includes some possible 1954 rupture traces that lie near

the northern end of the Sand Springs Range and also cross-cut the Louderback Mountains fault (Figure 3). Such complex structural relations may play an overall role in the occurrence of geothermal potential in southern Dixie Valley and will be the basis for the development of a conceptual exploration model.

References

Bell, J.W., Caskey, S.J., Ramelli, A.R., and Guerrieri, L., 2004, Pattern and Rates of Faulting in the Central Nevada Seismic Belt, and Paleoseismic Evidence for Prior Beltlike Behavior: *Bulletin of the Seismological Society of America*, v. 94, no. 4, pp. 1229-1254.

Bell, J.W., and Ramelli, A.R., 2009, Active Fault Controls at High Temperature Geothermal Sites: Prospecting for New Faults: *Geothermal Resources Council Transactions*, v. 33, pp. 425-429.

Blackwell, D.D., Smith, R.P., Waibel, A., Richard, M.C., and Stepp, P., 2009, Why Basin and Range Systems are Hard to Find II: Structural Model of the Producing Geothermal System in Dixie Valley, NV: *Geothermal Resources Council Transactions*, v. 33, pp. 441-446.

Caskey, J.S., 1996, Surface faulting, static stress changes, and earthquake triggering during the 1954 Fairview Peak (M_s 7.2) and Dixie Valley (M_s 6.8) earthquakes, central Nevada: Ph.D. Dissertation, Plates 1A-C, University of Nevada, Reno.

Caskey, J.S., Wesnousky, S.G., Zhang, P., and Slemmons, D.B., 1996, Surface Faulting of the 1954 Fairview Peak (M_s 7.2) and Dixie Valley (M_s 6.8) Earthquakes, Central Nevada: *Bulletin of the Seismological Society of America*, v. 86, no. 3, pp. 761-787.

Faulds, J.E., and Varga, R.J., 1998, The role of accommodation zones and transfer zones in the regional segmentation of extended terranes: Geological Society of America Special Paper 323, 45 p.

Faulds, J.E., Coolbaugh, M.F., Vice, G.S., and Edwards, M.L., 2006, Characterizing Structural Controls of Geothermal Fields in the Northwestern Great Basin: A Progress Report: *Geothermal Resources Council Transactions*, v. 30, pp. 69-76.

Hammond, W.C., and Thatcher, W., 2007, Crustal deformation across the Sierra Nevada, northern Walker Lane, Basin and Range transition, western United States measured with GPS, 2000-2004: *Journal of Geophysical Research*, v. 112, B05411, doi:10.1029/2006JB004625.

John, D.A., 1993, Geologic map of the Job Peak quadrangle, Churchill County, Nevada: Nevada Bureau of Mines and Geology Field Studies Map 5, scale 1:24,000, 8 p. interpretative pamphlet.

John, D.A., 1995, Geologic map of the Pirouette Mountain quadrangle, Churchill County, Nevada: Nevada Bureau of Mines and Geology Field Studies Map 9, scale 1:24,000, 6 p. interpretative pamphlet.

John, D.A., 1997, Geologic map of the Wonder Mountain 7-1/2-minute quadrangle, Churchill County, Nevada: Nevada Bureau of Mines and Geology Map 109, scale 1:24,000, 16 page interpretative pamphlet.

John, D.A., and Silberling, N.J., 1994, Geologic map of the La Plata Canyon quadrangle, Churchill County, Nevada: U.S. Geological Survey Geologic Quadrangle Map GQ-1710, scale 1:24,000, 8 p. interpretative pamphlet.

Mankhemthong, N., Oppliger, G.L., and Aslett, Z., 2008, Structural Localization of Two Low Temperature Geothermal Systems Within the Gravity Defined Linkage Between Dixie Valley and Fairview Valley, Nevada, USA: *Geothermal Resources Council Transactions*, v. 32, pp. 291-295.

Moeck, I., Hinz, N., Faulds, J., Bell, J., Kell-Hills, A., and Louis, J., 2010, 3D Geological Mapping as a New Methods in Geothermal Exploration: A Case Study from Central Nevada: *Geothermal Resources Council Transactions*, v. 34, pp. 807-811.

Okaya, D.A. and G.A. Thompson, 1985, Geometry of Cenozoic Extensional Faulting: Dixie Valley, Nevada: *Tectonics*, v. 4, no. 1, pp. 107-125.

Skord, J., Sladek, C., Coolbaugh, M., Cashman, P.H., Lazaro, M., and Kratt, C., 2011, Two Meter Temperature Surveys for Geothermal Exploration Project at NAS Fallon: *Geothermal Resources Council Transactions* (in press).

GEOTHERMAL EXPLORATION USING HYPERSPECTRAL ANALYSIS OVER DIXIE AND FAIRVIEW VALLEYS, NEVADA

[1]Amie Lamb, [2]Chris Kratt, and [1]Wendy Calvin

[1]Geological Sciences, and the Great Basin Center for Geothermal Research
University of Nevada-Reno, MS 172
Reno, NV 89557 USA
[2]Desert Research Institute, Reno, NV
Email: amiekl@gmail.com

Keywords: Hyperspectral, HyMap, ASD spectrometer, x-ray diffraction, remote sensing, hydrothermal mineralogy, geothermal system, Elevenmile Canyon, Dixie Meadows, Pirouette Mountain, FairDixie Valley, Fairview Valley, kaolinite, opal-chalcedony, alunite, borate

Abstract

Two HyMap hyperspectral data sets were acquired over Dixie Valley and several other smaller adjacent basins that totaled more than 1700 km^2 of coverage. Hyperspectral analysis permits rapid identification of geothermal indicators such as hydrothermal alteration minerals and evaporite deposits over large surface areas. The hyperspectral data were acquired at 3m spatial resolution with 125 c hannels across the visible-near infrared and short-wave infrared wavelength regions. Data was collected over the northern portion of the valley in 2002 as part of a program sponsored by Lawrence Livermore National Lab. Our analysis of the 2002 data focuses on areas that have not been previously mapped. The second data set was funded by the Department of the Navy Geothermal Program Office, and acquired in September of 2010. Mineral maps were provided by the data vendor for the area covered in 2010 and augmented by our own analysis.

The study area spans the southern portion Dixie Valley and northern Fairview Valley, located in Churchill County, Nevada approximately 60 air kilometers northeast of Fallon. Eleven geothermal fields have been identified along the entire extent of Dixie Valley. The Dixie Valley Geothermal System is the hottest known system in Nevada with temperatures above 285°C at 3 km depth and a 63 MW power plant in the northern part of the valley that has been operational

for over 30 years. Furthermore, the Stillwater and Salt Wells geothermal plants are also within close proximity to our study areas.

Comparing the hyperspectral data with known areas of high heat flow and analysis from other data sets (shallow-temperature surveys and LiDAR) we identified three regions for initial detailed examination, 11-Mile Canyon, Pirouette Mountain and Fairview Peak. We will explore the mineral diversity in these areas coupled with other analyses acquired as part of our group effort supported by the Navy Geothermal Program office.

Introduction

In 2010, the Navy Geothermal Program Office (NGPO) funded several exploration data sets that include: airborne hyperspectral remote sensing, LiDAR, shallow 2-m temperature probe surveys, and shallow temperature gradient drilling in southern Dixie Valley and Fairview Valley (DVFV). High temperatures in thermal gradient wells drilled in the early 1980s helped motivate NGPO to fund a phased, project scale exploration approach to DVFV. The geothermal systems are poorly understood.

Numerous authors describe the use of hyperspectral remote sensing data sets for the identification of acid-sulfate mineral assemblages and chemical precipitates associated with both active and fossil geothermal systems (e.g. Kruse et al, 1999; Vaughan et al., 2005; Kratt et al., 2006 and 2010; and Littlefield et al., 2010). Regional to project scale areas can be quickly surveyed and analyzed to produce geothermal-indicator mineral maps that are associated with thermal fluid movement along structural features.

Hyperspectral mineral mapping results from the 2002 and 2010 data will be validated with laboratory spectral measurements and selected X-ray diffraction analysis for more than 50 field samples. In addition, field spectra will be acquired along several transects. Our goals were

to 1) recommend favorable areas for shallow temperature measurements; 2) combine our results with the LiDAR data for a more robust interpretation of favorable areas for gradient drilling. Results for the LiDAR, temperature survey and drilling can be found, respectively, in Helton et al, Skord et al and Navy et al, this issue.

Background

Local Geothermal Setting

The Dixie Valley geothermal reservoir results from deep circulation in the highly fractured upper crust; magmatic thermal input is minor (Blackwell, 2007). During the past several decades workers have conducted dozens of studies, including geophysical, chemical, spectral, hydrological, and geological, to characterize the Dixie Valley Power Plant system located in the northern portion of Dixie Valley. Data suggests that deeply circulating geothermal fluids hosted within Dixie Valley may generate all eleven recognized geothermal systems spread along the extent of Dixie Valley (Blackwell, 2007). However, geologic maps and well data are particularly limited in DVFV due to difficulty accessing Navy bombing ranges.

Geological Setting

Dixie Valley (DV) lies within an asymmetrical north-northeast trending alluvial-filled half-graben that dips to the west. DV is bound on the west by the Stillwater Range, and to the east by the Clan Alpine Range and Louderback Mountains (fig. 1). South of DV is Fairview Valley, which lies between Sand Springs Mountain in the west and Fairview Mountains in the east. Jurassic metamorphic sediments and volcanic units underlie Oligocene-Miocene volcanics, and are intruded by gabbroic to granitic intrusives (Willden and Speed, 1974). Southern Dixie

and Fairview Valleys are aligned roughly north-south. South of Dixie Meadows, the strike of the Stillwater Mountains transitions from north-south to north-northeast at a feature descriptively named The Bend (Bell et al., 2004). Recent to Pleistocene faulting occurs on the east side of the mountain ranges in the study area. Faulting is normal in the Stillwater Mountains, and strike-slip in the Fairview Mountains. A left step in a complex, poorly understood transitional accommodation zone occurs between southern Dixie Valley and northern Fairview Valley (Caskey, 1996, Mankhemthong et al., 2008).

Remote Sensing

Hydrothermal identifiers include sinter (siliceous precipitate from geothermal chloride fluids, tufa (carbonate) and minerals including opal, clays, hydrates, hydroxides, and iron oxides (Rowan et al., 2000). It can be impossible to visually discern between some important temperature-variant hydrothermal alteration minerals or sulfate and borate-rich evaporite minerals in the field, but we can readily identify many such minerals on the basis of intrinsically unique spectral signatures (Hunt, 1977), many of which occur at wavelengths the human eye is not sensitive to. The parameters in spectra such as absorption feature wavelength, width, asymmetry, and depth help to distinguish between minerals (van der Meer, 2004).

The visible and near infrared (VNIR) and shortwave infrared (SWIR) spectral ranges that span 0.4-2.5 µm are where many diagnostic spectral features are found for mineral groups such as smectites, kaolinites, alunite, carbonates, sulfates, hydroxyls, and hydrates. Hyperspectral sensors have hundreds of narrowly spaced contiguous channels, designed to sample and discriminate among these minerals from aircraft or satellite platforms.

Data

Two HyMap hyperspectral data sets were acquired in Dixie Valley by the HyVista Corp. and provide the basis for our analysis. The HyMap airborne sensor measures solar reflected radiation with 125 bands between 0.44 – 2.48 μm. In September of 2010, approximately 1300 km^2 in 12 flightlines, or scenes, were acquired over Fairview and Dixie Valleys. In September 2002, ~400 km^2 of hyperspectral data acquisition occurred in 18 flightlines centered over Dixie Meadows. Atmospherically and geometrically corrected radiance and reflectance data with spatial resolution of ~3m were supplied by HyVista. HyVista also provided preliminary mineral maps for 13 minerals for the 2010 Fairview –Dixie Valley data set.

Methods

We analyzed atmospherically corrected reflectance data using statistically-based and feature-based methods in ENVI image analysis software. First, vegetation, shadows, and water bodies were masked from the data. In the statistical approach, the Minimum Noise Fraction (Boardman et al., 1995) (MNF) is a double principle component transform that separates noise from data. The reduced data was input into Pixel Purity Index algorithm, which identifies unique endmembers in the scene. Endmembers of interest were extracted using the n-Dimensional Visualizer tool, which projects the spectral endmembers in an n-dimensional data cloud in which pixels on the margins of the cloud are most unique. Endmembers are selected from this process to be mapped later, in conjunction with endmembers selected from the feature-based methods below.

Feature-based methods also used to identify spectra with characteristic features in each scene. Decorrelation stretches (DCS) remove correlation from three input bands and generate a highly saturated color map (Gillespie et al., 1986). Absorption band depth (ABD) (Crowley,

1989) were generated to identify pixels with diagnostic absorption features. To produce the ABD image, several bands around the absorption feature shoulder are summed and divided by summed bands surrounding the minimum as a relative gauge of band strength.

To generate mineral abundance maps, the Mixture Tuned Matched Filter (MTMF) algorithm was used with endmembers identified in both the statistical and analyst-driven methods described above. The MTMF statistically maps similar spectra in an unknown background (Boardman et al., 1995). User-defined thresholds generate spectral maps over regions of interest. High thresholds results in high confidence picks. The mineral maps were geocorrected and exported to a geodatabase.

In the field and lab, a portable Analytical Spectral Device (ASD) Field Spec Pro field spectrometer was used to measure high resolution data in 2151 channels over the spectral range 0.35-2.5 µm. Spectral transects in the field and individual sample measurements were acquired. The USGS spectral library was used to compare field and lab spectra to known standards and identify minerals in our samples. We performed X-ray diffraction analysis on several hand samples to corroborate selected mineral compositions.

Results

HyMap-derived mineral maps for two data sets that cover more than 1700 km^2inDixie Valley and Fairview Valley, Nevada were generated to indicate hydrothermal-related minerals. Kaolinite, alunite, eugsterite, goethite, and opal were mapped in several locations (fig. 2). In most cases the remote sensing results were supported by the analysis performed on the field samples and where this was not the case mineral maps were then revised.

In southwestern quadrant of Fairview Mountains, widespread illite/smectite, and discrete locations of alunite, gypsum and opal-chalcedony, were mapped remotely. This is less than a kilometer west of the Nevada Fairview Mine where small amounts of silver and gold were mined in the 1930s (Willden and Speed, 1974). The deposit is associated with dacite intruding into silicic tuff (Henry, 1996). In the field we confirmed our mapping results, and also found abundant gypsum, eugsterite, banded chalcedony, and realgar (fig. 3). Many fault damage zones and slickensides were observed in the area, and a small ($<3m^2$) outcrop of gypsum appears to be forming by the evaporation of groundwater from a seep.

Some of the hydrothermal indicator mineral spectra are not uniquely related to geothermal activity, and can occur in several geological environments. For example, we found that opal-chalcedony was remotely mapped in several locations. The opal described at the location in the previous paragraphis related to hydrothermal alteration, and several other hydrothermal indicator minerals help support this assertion. In La Plata Canyon, our mapping results for opal-chalcedony were associated with silicified Pleistocene diatomaceous earth mapped by Wilden and Speed (1974.) Opal-chalcedony also was confirmed in the non-welded zone of Tertiary volcanic tuffs in Sand Springs Mountains. A north-northeast striking lineation on the southeast side of Fairview Mountain was a meters-wide white silicic dike that spectrally mapped as an opal-chalcedony false-positive as a result of spectral ambiguity. Field visits to these locations quickly determined context of the geological environment, and relevance to hydrothermal mineral mapping.

In the Dixie Meadows area, previous hyperspectral mineral mapping was confirmed both by spectral analysis and field verification. Additionally, borates and kaolinite were mapped in the

Dixie Lake area in the valley floor. Kainite, a b orate, was field verified with the ASD spectrometer, south of Dixie Meadows (fig. 2). Kaolinite and borates were spectrally mapped in east of Dixie Lake over a 12 km^2 area.

Spectrally derived maps of micas were not good indicators of hydrothermal alteration. The spectrally-derived mapped areas were frequently found to be weathering volcanic deposits (e.g. in the Piroutte Mountain area) or related to intrusives (e.g. in the 11-Mile Canyon). Our results suggest the best potential for further exploration is in the Dixie Meadows area and along the southwest side of Fairview Peak.

Field checking the spectra helped to discern false positives. In all cases, the spectral analysis pointed to areas of alteration and interest. Additional field work and sampling will occur in summer 2011 and we will report on the final mapped mineralogy at the meeting in October.

References

Bennett, R. A., B. P. Wernicke, N. A. Niemi, A. M. Friedrich, and J. L. Davis, 2003, Contemporary Strain Rates in the Northern Basin and Range Province from GPS Data: Tectonics, v. 22, p. 31.

Bell, J. W., S. J. Caskey, A. R. Ramelli, and L. Guerrieri, 2004, Pattern and rates of faulting in the Central Nevada Seismic Belt, and paleoseismic evidence for prior beltlike behavior: Bulletin of the Seismological Society of America, v. 94, p. 1229-1254.

Blackwell, D. D., R. P. Smith, and M. C. Richards, 2007, Exploration and development at Dixie Valley, Nevada: summary of DOE studies, 32nd Workshop on Geothermal Reservoir Engineering, Stanford University, Stanford, California.

Boardman, J.W., Kruse, F.A., Green, R.O., 1995. Mapping target signatures via partial unmixing of AVIRIS data, Proceedings of the Fifth JPL Airborne Earth Science Workshop. JPL Publication, pp. 23-26.

Caskey, S. J., S. G. Wesnousky, P. Shang, and D. B. Slemmons, 1996, Surface faulting of the 1954 Fairview Peak (Ms 7.2) and Dixie Valley (Ms 6.8) earthquakes, Central Nevada: Bulletin of the Seismological Society of America, v. 80, p. 761-787.

Crowley, J.K., Brickey, D.W., Rowan, L.C., 1989. Airborne Imaging Spectrometer Data of the Ruby Mountains, Montana: Mineral Discrimination Using Relative Absorption Band-depth Images. Remote Sensing of the Environment 29, 121-134.

Faulds, J. E., M. F. Coolbaugh, G. S. Vice, and M. E. Edwards, 2006, Characterizing Structural Controls of Geothermal Fields in the Northwestern Great Basin: A Progress Report, v. 30, p. 8.

Gillespie, A. R., Kahle, A. B., and Walker, R. E., (1986). Color Enhancement of HighlyCorrelated Images. I. Decorrelation and HIS Contrast Stretches. Remote Sensing of Environment, v. 20; p. 209-235.

Hammond, W. C., C. Kreemer, and G. Blewitt, 2009, Geodetic constraints on contemporary deformation in the northern Walker lane: 3. Central Nevada seismic belt postseismic relaxation: The Geological Society of America, v. Special Paper 447, p. 33-54.

Henry, C.D., 1996. Geologic Map of the Bell Mountain Quadrangle, western Nevada, Nevada Bureau of Mines and Geology Field Studies Map 12c.

Hunt, G. R., 1977, Spectral signatures of particulate minerals in the visible and near infrared: Geophysics, v. 42, p. 501-513.

Kratt, C., W. Calvin, and M. Coolbaugh, 2006, Geothermal Exploration with Hymap hyperspectral data at Brady-Desert Peak, Nevada: Remote Sensing of the Environment, v. 104, p. 313-324.

Kruse, F. A., J. W. Boardman, and J. F. Huntington, 1999, Fifteen Years of Hyperspectral Data: northern Grapevine Mountains, Nevada: 8th JPL Airborne Earth Science Workshop, p. 247-258.

Mankhemthong, N., Oppliger, G.L., Aslett, Z., 2008. Structural localization of two low temperature geothermal systems within the gravity defined linkage between Dixie Valley and Fairview Valley, Nevada, USA. GRC Transactions 32, 250-254.

Rowan, L.C., Hook, S.J., Abrams, M.J., and J.C. Mars, 1998. Mapping hydrothermally altered rocks at Cuprite, Nevada, using the Advanced Spaceborne Thermal Emission and Reflection Radiometer (ASTER), a new satellite-imagining system. Economic Geology, v. 98, p. 1019-1027.

van der Meer, F., 2004. Analysis of spectral absorption features in hyperspectral imagery. International Journal of Applied Earth Observation 5, 55-68.

Vaughan, G. R., S. J. Hook, W. M. Calvin, and J. V. Taranik, 2005, Surface mineral mapping at Steamboat Springs, Nevada, U.S.A., with multiwavelength thermal infrared images: Remote Sensing of Environment, v. 99, p. 140-158.

Willden, R., Speed, R.C., 1974. Geology and Minerals Deposits of the Churchill County, Bulletin 83. Nevada Bureau of Mines and Geology.

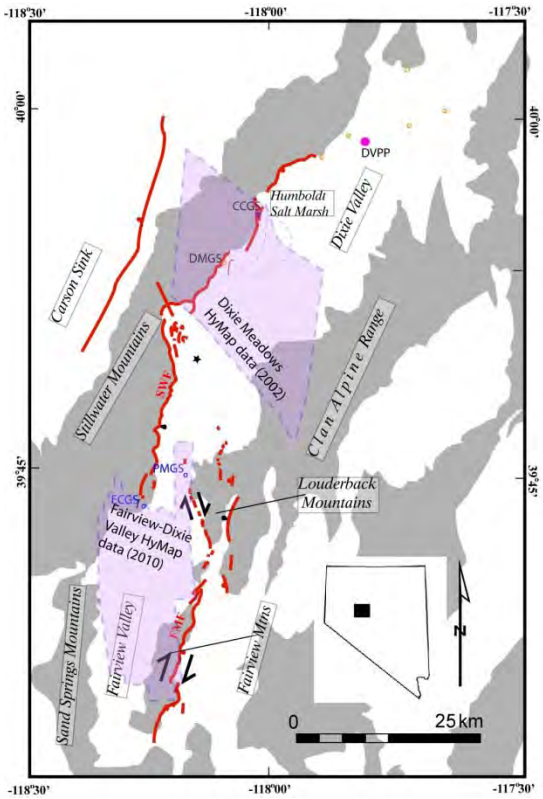

FIGURE 1 Study area with major features mapped. 1954 fault ruptures in red. Orange circles are hot springs, star is Dixie Town Center.Abbreviations: Geothermal systems (GS): CCGS – Coyote Canyon GS, DMGS – Dixie Meadows GS, DVPP –Dixie Valley Power Plant, ECGS - Elevenmile Canyon GS, PMGS – Pirouette Mtn GS. Faults: FMF – Fairview Mountain Fault (oblique dextral normal); SWF – Stillwater Fault (normal).

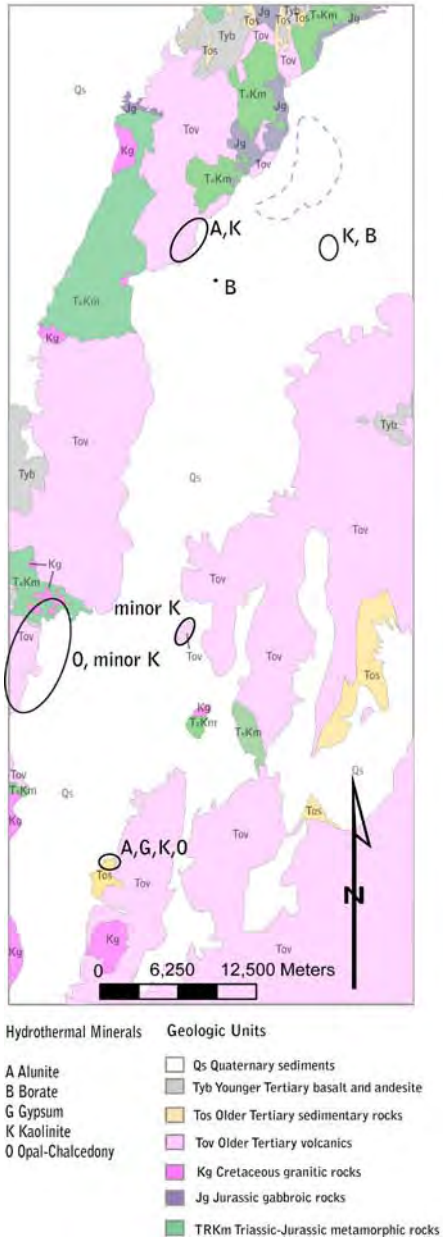

Figure 2 Regional map of remotely sensed hydrothermal minerals in the Fairview Peak-Dixie meadows area. Geological map after Wilden and Speed (1974).

Figure 3. Gypsum mound mapped remotely in southwest Fairview Peak. A thick vein (~5 cm) of banded chalcedony abutted it, and may have been fault controlled.

Two-Meter Temperature Surveys for Geothermal Exploration Project at NAS Fallon

Justin Skord[1,2], Chris Sladek[1,2], Mark Coolbaugh[1,2], Patricia H. Cashman[1,2], Michael Lazaro[3], Chris Kratt[4]

[1]Department of Geological Sciences and Engineering University of Nevada, Reno, [2]Great Basin Center for Geothermal Energy, [3]Department of the Navy Geothermal Program Office, [4]Desert Research Institute

Abstract

The two-meter temperature survey method is a fast and inexpensive method of geothermal exploration but its main limitation is the need to consider possible surface effects on temperature data. In recent years the Great Basin Center for Geothermal Energy has made progress toward developing methods and corrections aimed at eliminating these effects. Seasonal drift, albedo, slope-aspect, and thermal diffusivity are among the surface-effects being considered in this project. Initial results from two-meter temperature surveys on Navy managed land near Fallon, Nevada indicate the presence of several temperature anomalies. At least one of the anomalous areas seems to be geothermal-related. The others are more subtle and may be related to surface effects. The most significant shallow temperature anomaly was found at the Pirouette Mountain area. This area was previously identified from drilling. A more recent gradient hole, drilled by the Navy Geothermal Program, found a temperature of ~77°C at a depth of ~150m. No shallow temperature surveys have previously been conducted in the Pirouette Mountain area. The two-meter anomaly found here is characterized by temperatures 3-4°C above background, and covers a north-south trending area 3-5km long.

Introduction

This study is part of a large interdisciplinary geothermal exploration project on Navy managed lands near Fallon, Nevada. Much of the study area is located within close proximity to other known geothermal resources. The most notable near-by geothermal resource is the Dixie Valley power plant, which is the largest single geothermal power plant in Nevada. Previous geothermal exploration activity on these lands is fragmented. Gradient-hole drilling on a small portion of the area has identified some geothermal anomalies, but they have not been comprehensively studied. The areas outside of the previous gradient hole drilling, for the most part, remain unexplored. The objectives of this project include developing a more comprehensive understanding of the identified geothermal anomalies and exploring the remainder of these lands for geothermal potential.

The Great Basin Center for Geothermal Energy at the University of Nevada Reno is conducting several exploration activities including light detection and ranging (LiDAR) imagery analysis, hyper-spectral mineral mapping, and shallow temperature surveys. This paper discusses initial results of the two-meter shallow temperature surveys.

Survey Areas

The project consists of two survey areas, both of which are on Navy managed land associated with the Fallon Naval Air Station (NAS Fallon). One of the survey areas is along the perimeter of Bombing Range 17 (BR 17) which is a large area that covers parts of Southern Dixie Valley and Fairview Valley in Churchill County Nevada; this survey area will hereby be referred to in this paper as Survey Area 1 (Figure 1). The other survey was conducted along the eastern section of Bombing Range 19 (BR 19) which covers part of the western flank of the Cocoon Mountains in Churchill County, Nevada; this survey area is hereby referred to in this paper as Survey Area 2 (Figure 1).

Geologic Setting

Survey Area 1 covers portions of Southern Dixie Valley and Fairview Valley in Churchill County, Nevada (Figure 1). These valleys are the result of Basin and Range tectonics characterized by northwest extension generating large northeast trending valley and range topography (e.g. Dickinson, 2002). The area is also known for its active fault systems including ground ruptures from a 1954 earthquake swarm (e.g. Caskey and others, 2004). Many of these recent ruptures are near the Dixie Valley-Fairview Valley Transition Zone. This area has been characterized by complex fault systems associated with the termination of Dixie Valley (Mankhemthong and others, 2008). The two previously identified geothermal anomalies on Survey Area 1, Pirouette Mountain and Eleven-Mile Canyon, are located along this transition zone (e.g. Blackwell and others, 2007; Mankhemthong and others, 2008; Figure 1). Refer to Helton and others (2011) for more detailed structural maps and interpretations of Eleven Mile Canyon and Pirouette Mountain.

Survey Area 2 is along part of the western flank of the Cocoon Mountains in Churchill County, Nevada (Figure 1). Geologically, this area is associated with Walker Lane-type tectonics, which is characterized by the combination of northwest extension and right lateral movement. This combination of stresses generates complex fault networks (e.g. Stewart, 1988). Detailed geologic studies have not been done in this area beyond the work of Morrison (1964), who mapped faults within the tertiary volcanic units that make up the Cocoon Mountains. This area is located near two better studied areas with known geothermal resources: Salt Wells Basin and Lee Allen Springs (Figure 1).

Figure 1. Map showing Location of Survey Area 1, Survey Area 2, and other important features. Survey Area 1 is a large area covering southern Dixie Valley and Fairview Valley. There are two known geothermal anomalies: Pirouette Mountain and Eleven Mile Canyon, both of which are located along the Dixie Valley-Fairview Valley transition zone(e.g. Mankhemthong, 2008). Survey Area 2 is a smaller area to the southwest and has no known geothermal anomalies but is located within close proximity to Lee Allen Springs and Salt Wells Basin geothermal areas.

Two-Meter Temperature Survey Method

The techniques and equipment used for these surveys have incorporated the most recent modifications to the long-standing shallow temperature survey method. The fieldwork is conducted primarily from an ATV (All-Terrain-Vehicle) allowing for maximized mobility in rugged terrain and rapid access to equipment (Coolbaugh, 2006). Temperature probes made from ¼" steel pipe with tungsten carbide tips are driven into the ground with an impact hammer. This makes ground penetration relatively easier and permits shorter equilibration times than previous shallow temperature methods. Temperature is measured from a Resistance Temperature Device (RTD) that is lowered into the hollow probe. The temperature is taken to a tenth of a degree at 2, 1.5, and 1 meter depths in the probe. Measuring these three depths allows analysis of two-meter temperature gradients in addition to the two meter bottom-temperature. Typically ten to fifteen temperature probes can be emplaced and temperatures measured during one field day.

Surface-effects can be responsible for fluctuation in two-meter temperatures. The most common surface effects on two-meter temperatures are seasonal drift, albedo, slope aspect, elevation, and thermal conductivity. Corrections and consideration of these effects has utilized the most recent advances of ongoing research in this area (Sladek and others, 2009). Daily temperature variations do not affect temperatures at two-meter depth but the seasonal temperature variations do. Generally if a survey lasts longer than a week, a noticeable temperature change will occur, depending on the time of year. This can be corrected for by measuring base stations regularly and normalizing all new stations using the base station readings (figure 2). The impact of solar radiation on two-meter temperatures varies depending on surface-albedo and slope aspect. Albedo (reflectance) controls how much heat is absorbed, so higher

albedo areas will have lower temperatures while low albedo areas will have higher temperatures. Albedo can be estimated from remote sensing imagery and then plotted vs. temperature for analysis of anomalies (figure 3). The slope aspect of an area effects the angle the sun hits the surface and this effect is particularly evident between north and south-facing slopes. This can be adjusted for in the field by surveying on flat ground. Thermal diffusivity controls the rate of heat transfer which is a function of the ground composition and water saturation. Typically this effect typically does not account for much variation in temperature unless the morphology or climate of a survey area is particularly heterogeneous.

Results

Survey Area 1

The Survey Area 1 temperature survey was conducted from November 2010 to January 2011. A large seasonal drift in two-meter temperatures occurred over this relatively long time period. In order to correct for this, three base stations were consistently measured throughout the survey. All three of the base stations show a consistent seasonal drift of roughly five degrees Celsius over the span of the survey (figure 2). The correction was applied by adding decreases in base station temperature to new stations measured on the same day. Once this correction was made the data could be analyzed for any possible anomalies.

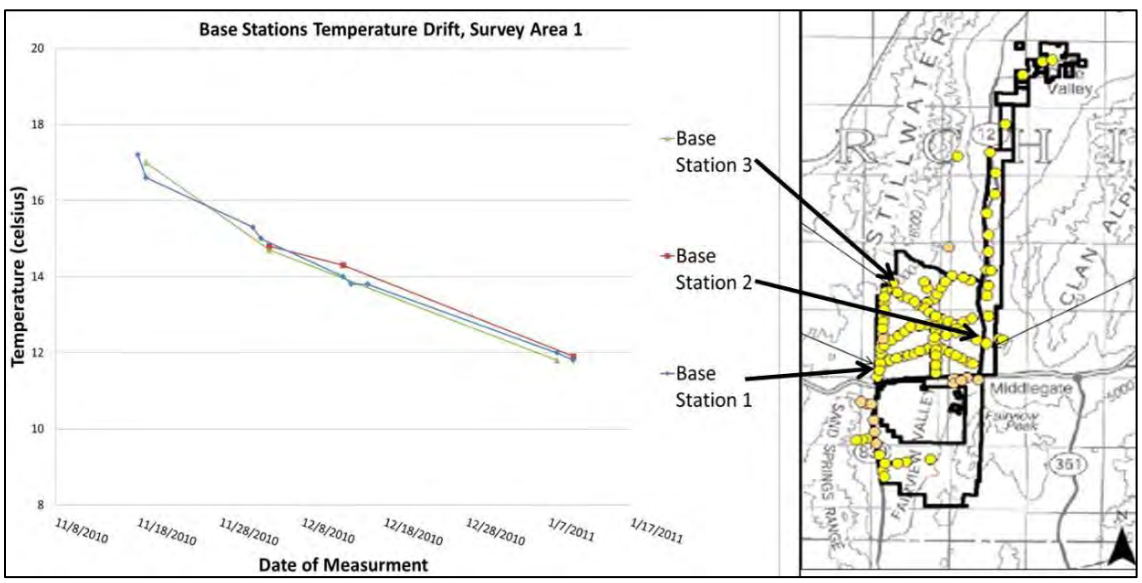

Figure 2. Graph (left) showing seasonal drift of three base stations. The picture (right) shows their general locations. Base stations were chosen to get a good geographic representation of the survey area.

There are four thermal anomalies at Survey Area 1 after seasonal drift corrections (figure 3). The Pirouette Mountain anomaly is the strongest, with temperatures 3-4°C above background. The Fairview Valley Northwest, Fairview Valley East, and Fairview Valley Southwest anomalies are more subtle with temperatures 1.5°C to 2.5°C above background.

A plot of albedo vs. temperature for Survey Area 1 stations provides insight into possible albedo effects on the results (figure 4). A best-fit line through the data shows the expected decrease in temperature with increase in albedo. All of the Pirouette Mountain anomalies (shown in red) are outliers in this plot, which indicates that the high temperatures are not due to albedo. One of the stations from the Fairview Valley Southwest anomaly (shown in yellow) is also clearly an outlier. The other two anomalies, Fairview Valley Northwest (in green) and Fairview Valley East (in pink) plot near the best-fit line, indicating they may be related to albedo rather than geothermal heat.

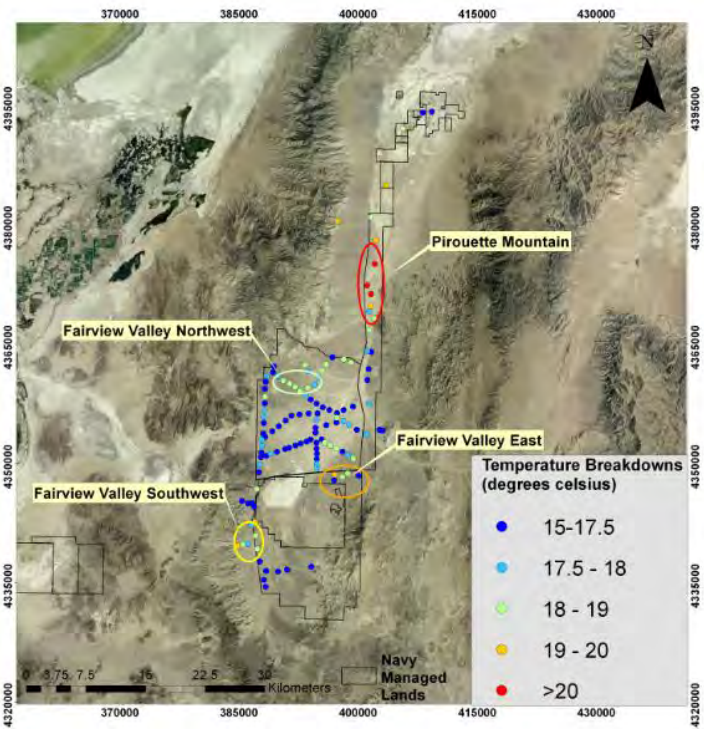

Figure 3. Map showing temperature distribution at Survey Area 1 after correction for seasonal drift. The map shows four anomalies: Pirouette Mountain, Fairview Valley Northwest, Fairview Valley East, and Fairview Southwest

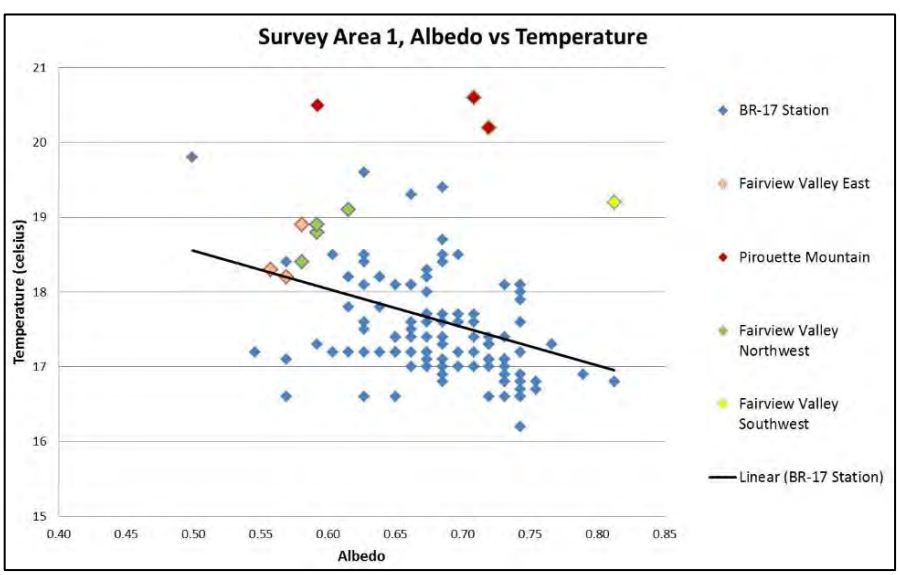

Figure 4. Albedo vs. temperature plot showing the four anomalies found from Survey Area 1. When plotted against albedo, two of the anomalies are outliers (Pirouette Mountain and Fairview Valley Southwest) and the other two plot near the best fit line (Fairview Valley Northwest and Fairview Valley East).

Survey Area 2

The temperature survey of Survey Area 2 was conducted within the time-span of roughly one week. Seasonal drift was a very small factor in correcting the data; base stations changed by less than one degree Celsius. After making this very small seasonal drift correction the the coolest stations measured ~11°C while the warmest were slightly above 13°C. This is a much smaller range in temperature compared to Survey Area 1. The highest temperature stations are shown in yellow in Figure 5 and are located along the eastern portion of the survey area. These subtle anomalies have a relatively low albedo which suggests that there may be an albedo effect involved (Figure 6). If these stations are related to geothermal activity they may be reflecting outflow of warm water within drainages at the eastern portion of the survey area. Further analysis of other possible surface effects at Survey Area 2 are needed to test these interpretations.

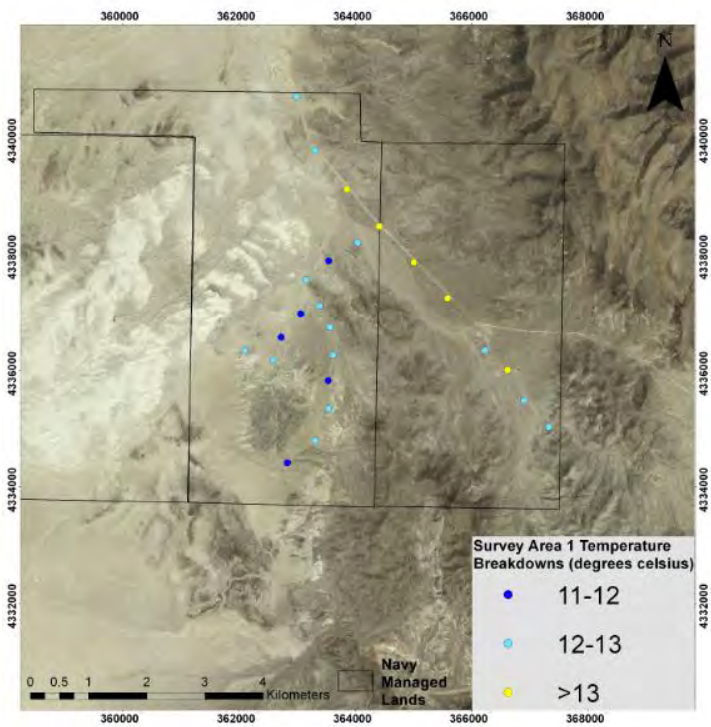

Figure 5. Map showing temperature distribution at Survey Area 2. The range of temperatures here is small but the highest temperatures were found along the eastern portion of the survey area.

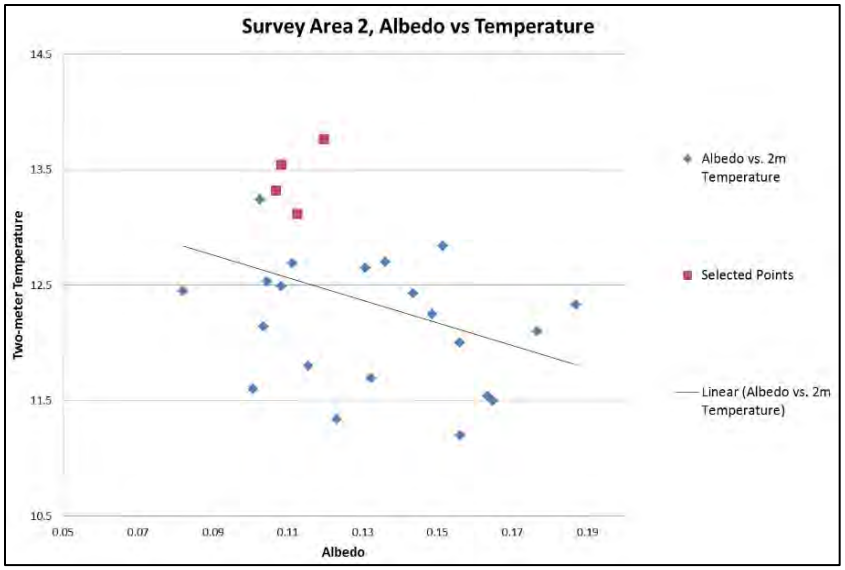

Figure 6. Albedo vs. temperature plot for stations at Survey Area 2. The highest recorded temperatures are highlighted in red. These stations have a relatively high albedo which may account for their increased two-meter temperatures.

Other Possible Surface Effects and Follow-up Work

The remaining surface-effects are: slope aspect, elevation, and thermal conductivity. Slope aspect was controlled for in both surveys by placing the majority of base stations on flat ground. Elevation was controlled for by measuring base stations at different elevations. Since the base stations changed consistently, no elevation correction is necessary for either survey area. There is currently no practical method to correct for thermal conductivity but ongoing research is focused on devising new methods. However, it is unlikely that any of the temperatures in either of the survey areas are drastically affected by thermal conductivity, due to the relatively homogeneous composition and vegetation cover indicates a relatively consistent saturation level of the surveyed alluvial fans.

Follow-up work will be conducted during June 2011. The Pirouette Mountain and Eleven-Mile Canyon geothermal anomalies will be mapped in detail. Their shape and extent may have implications for structural controls and resource potential. The work will also investigate the more subtle anomalies to better determine whether they are geothermal or related to surface effects. Additional work will be guided by hyper-spectral mineral mapping and LiDAR structural interpretations (e.g. Helton and others, 2011).

Conclusions

Initial two-meter temperature surveys have been completed as part of a large multidisciplinary geothermal exploration project on Navy managed lands near Fallon, Nevada. The surveys were conducted with the most up-to-date modifications to the shallow temperature survey method.

Four two-meter temperature anomalies were found at the Dixie Valley – Fairview Valley area (Survey Area 1). After correcting for seasonal drift and analyzing albedo, several interpretations on these anomalies can be made. At least one of the anomalies (Pirouette Mountain) is likely geothermal-related. Drill-hole data provide independent evidence for this anomaly; the shallow temperature survey provides new information about its location and extent. Ongoing fault mapping and interpretations from LiDAR imagery indicate that this anomaly may be associated with a quaternary fault scarp that projects northward from Pirouette Mountain (refer to Helton and others, 2011). The other anomaly that stands out is Fairview Valley Southwest. The two-meter temperature in this area is only ~ 2°C above background levels but it plots as a clear outlier on the albedo vs. temperature plot (figure 4). The other two anomalies are more subtle (Fairview Valley Northwest and Fairview Valley East) and seem to plot near the best-fit line from the albedo vs. temperature plot. Follow-up work could help determine whether they are the result of surface-effects or are geothermal related.

The results from the second survey near the Cocoon Mountains (Survey Area 2) showed a smaller range in temperatures than at the Dixie –Valley Fairview Valley area (Survey Area 1). The highest temperatures were clustered along the eastern section of the survey area. Follow-up work is planned for June 2011 and will focus on the Dixie Valley – Fairview Valley area, where the more significant anomalies were found.

Acknowledgements

This work was funded by the Navy Geothermal Program Office. Wendy Calvin and John Bell provided valuable guidance as the principal investigators. Craig Desbrow and Jonathyn Payne assisted with fieldwork.

References

Blackwell, D., Smith, R. Richards, M., 2007. Exploration and Development at Dixie Valley, Nevada: Summary of DOE Studies: Proceedings, 32nd Workshop on Geothermal Reservoir Engineering, Stanford University, CA, Jan. 22-24, 16 pages.

Caskey, S.J, Bell, J.W., Ramelli, A.R., and Wesnousky, S.G., 2004, Historic Surface Faulting and Paleoseismicity in the 1954 Rainbow Mountain-Stillwater Earthquake Sequence, Central Nevada: Bull. Seis. Soc. Amer., v. 94, p. 1255-1275.

Coolbaugh, M.F., Sladek, C., Faulds, J.E., Zehner, R.E., and Oppliger, G.L., 2007a. Use of rapid temperature measurements at a 2-meter depth to augment deeper temperature gradient drilling: Proceedings, 32nd Workshop on Geothermal Reservoir Engineering, Stanford University, Stanford, CA, Jan. 22-24, 2007, p. 109-116.

Dickinson, W. R., 2002, The Basin and Range Province as a Composite Extensional Domain. International Geology Review, v 22, p. 1-38.

Helton, E.L., Bell, J.W., Cashman, P.H., Lazaro, M., and Alm, S., 2011, Structural analysis of southern Dixie Valley using LiDAR and low-sun-angle aerial photography, NAS Fallon Geothermal Exploration Project, Dixie Valley, Nevada: Geothermal Resources Council Transactions (in press)

Kratt, C., Coolbaugh, M. F., Peppin, B., and Sladek, S., 2009, Identification of a new blind geothermal system with hyperspectral remote sensing and shallow temperature measurements at Columbus Salt Marsh, Esmeralda County, Nevada: Geothermal Resources Council Transactions, v. 33, p. 481-485.

Mankhemthong N., Oppliger G. L., Aslett Z., 2008, Structural Localization of Two Low Temperature Geothermal Systems Within the Gravity Defined Linkage Between Dixie Valley and Fairview Valley, Nevada, USA: Geothermal Resources Council Transactions, v. 32, p. 291-295.

Sladek, C., Coolbaugh, M., and Kratt, C., 2009, Improvements in shallow (two-meter) temperature measurements and data interpretation: Geothermal Resources Council Transactions, v. 33, p. 535-541

Stewart, J.H. 1988, Tectonics of the Walker Lane belt western Great Basin - Mesozoic and Cenozoic Deformation in a Zone of Shear. Prentice Hall, New Jersey, p. 683–713.